Investigations of *in vitro* Test Systems for the Detection of Glucocorticoid-induced Skin Atrophy as a Tool in Drug Discovery

Dissertation

zur Erlangung des akademischen Grades
doctor rerum naturalium
(Dr. rer. nat.)
im Fach Biologie

eingereicht an der
Mathematisch-Naturwissenschaftlichen Fakultät I

der Humboldt-Universität zu Berlin
von

Dipl. Biol. Stefanie Schoepe
geboren am 12.08.1979 in Berlin

Präsident der Humboldt-Universität zu Berlin
Prof. Dr. Dr. h.c. Christoph Markschies

Dekan der Mathematisch-Naturwissenschaftlichen Fakultät I
Prof. Dr. Lutz-Helmut Schön

Gutachter: 1. Prof. Dr. med. Hans-Dieter Volk
2. Prof. Dr. med. Khusru Asadullah
3. Prof. Dr. Dr.-Ing. Jürgen Lademann

Tag der mündlichen Prüfung: 16.07.2009

When you want something, all the universe conspires in helping you to achieve it.

Paulo Coelho, The Alchimist

Meinen Großeltern Irmgard und Erich Schoepe

und

Den Labortieren

Zusammenfassung

Topische Glukokortikoide (GCs) sind sehr wirksam bei der Therapie von entzündlichen Hauterkrankungen. Durch ihr hohes Nebenwirkungspotential, welches sich besonders in der Induktion von Hautatrophie zeigt, ist ihr Einsatz jedoch deutlich limitiert. Für die Entwicklung von Medikamenten ist die Bestimmung des atrophogenen Potenzials neuartiger Verbindungen daher von großer Bedeutung. Derzeit stehen diesbezüglich keine prädiktiven *in vitro* Modelle zur Verfügung. Aus diesem Grund war das Ziel dieser Arbeit die Etablierung von Atrophie-Testsystemen, bestehend aus Zellsystem und Messparameter.

Es wurden fünf murine und humane kutane Zelltypen bzw. Zelllinien, die in einschichtiger Zellkultur wachsen (3T3 Mausfibroblasten, primären Rattenfibroblasten, HaCaT-Zellen, normalen humane epidermale Keratinozyten [NHEK] und dermale Fibroblasten) und zwei humane Vollhautäquivalente (AST-2000 von CellSystems und FTSM von Phenion) untersucht. Bekannte und nahe liegende Atrophie-Marker, die Proliferation, Kollagen-Metabolismus und epidermale Dicke betreffend, wurden auf mRNA-, Protein- bzw. zellulärer Ebene gemessen. Darüber hinaus wurden mittels Genexpressionsanalysen von GC-behandelter Nagerhaut acht neue potenzielle Marker identifiziert, deren Regulation *in vitro* jedoch nicht bestätigt werden konnte. Insgesamt wurden Kombinationen aus sieben verschiedenen Zellsystemen mit jeweils bis zu 20 Messparametern untersucht.

In Pilotexperimenten wurden diese Testsysteme mit einem hochdosierten klassischen GC behandelt und auf eine reproduzierbare Regulation der Messparameter von mehr als 2-fach als Vorraussetzung für weitere Evaluierungsexperimente hin geprüft. Folgende Testsysteme erfüllten diese Anforderungen: 1). *MMP1*, *-2, -3* und *-9* mRNA-Expression in NHEK, 2). *COL1A1* und *COL3A1* mRNA-Expression in 3T3 Mausfibroblasten, 3.) Epidermisdicke, Kollagen- und MMP-Synthese in FTSM. Diese drei Systeme wurden weiterhin mit vier bis fünf Referenz-GCs behandelt. Die Messparameter der drei Testsysteme erwiesen sich als dosis-abhängig reguliert und korrelierten mit dem atrophogenen Potenzial der GCs. Daher wurden diese Testsysteme als potenziell geeignete Atrophie-Modelle betrachtet. Schließlich wurde die Prädiktabilität der drei empfohlenen *in vitro* Testsysteme für die *in vivo* Situation im Nager analysiert. In allen drei *in vitro* Systemen induzierte die Behandlung mit einem neuartigen selektiven GC Rezeptor Agonisten (SEGRA) weniger atrophogene Effekte als das Referenz-GC Clobetasol. Ähnliche Ergebnisse wurden auch *in vivo* im OFA *hr/hr* Ratten-Hautatrophie Modell gefunden.

Zusammenfassend wird eine Kaskade von drei *in vitro* Modellen auf der Grundlage von NHEK, 3T3 Fibroblasten und FTSM empfohlen, um das atrophogene Potential von GC-Rezeptor-Liganden zu bestimmen. Der tatsächliche prädiktive Wert für die klinische Situation sollte in weiteren Studien untersucht werden.

Schlagworte: Hautatrophie, Glukokortikoid, in vitro Testsystem, humane Keratinozyten, 3T3 Mausfibroblasten, Vollhautmodell

Abstract

Topical Glucocorticoids (GCs) are highly effective for the therapy of inflammatory skin diseases. However, their use is limited by their side effect potential, with skin atrophy being the most prominent one. Thus, determining the atrophogenic potential of novel compounds is of importance for drug development. Currently, there are no according predictive *in vitro* models available. The aim of the present study was to establish atrophy test systems consisting of cellular assay and read out parameter.

Five rodent and human cutaneous cell types / cell lines grown in monolayer culture (3T3 mouse fibroblasts, primary rat fibroblasts, HaCaT cells, normal human skin keratinocytes [NHEK] and fibroblasts) and two human full-thickness skin equivalents (AST-2000 from CellSystems and FTSM from Phenion) were investigated. Known and suspected atrophy markers related to proliferation, collagen metabolism and epidermal thickness were measured on mRNA, protein and cellular level, respectively. Additionally, by gene expression profiling of GC-treated rodent skin eight novel potential markers were identified, but subsequently not confirmed *in vitro*. Altogether, combination of seven different cellular assays with up to 20 read out parameters each were investigated.

To pre-screen the test systems, a high-dosed classical GC was applied and a reproducible regulation more than 2-fold of the read out parameter was defined as a precondition of further evaluation. This was fulfilled by: 1.) *MMP1, -2, -3* and *-9* mRNA expression in NHEK, 2.) *COL1A1* and *COL3A1* mRNA expression in 3T3 mouse fibroblasts, 3.) number of keratinocyte cell layers as well as dermal collagen and epidermal *MMP1* mRNA expression and the protein secretion of C-terminal propeptide of collagen type I, MMP-1 and MMP-3 into the medium of FTSM. These three test systems were further treated with a panel of four to five GCs, used as tool compounds. The read out parameters of all three test systems turned out to be regulated dose-dependently and correlated with the atrophogenic potential of the GCs. Thus, the test systems were considered as potentially suitable atrophy models. Finally, the predictability of the three recommended *in vitro* test system for the rodent *in vivo* situation was analyzed. In all three *in vitro* test systems, the treatment with a novel selective GC receptor agonist (SEGRA) induced less atrophogenic effects than the reference GC clobetasol. Indeed, similar results were found in the OFA *hr/hr* rat skin atrophy model.

In summary, a cascade of three *in vitro* models based on NHEK, 3T3 fibroblasts and FTSM is recommended to be applied for the characterization of the atrophogenicity of GC receptor ligands. Further experiments are necessary to eventually demonstrate the true predictability of these models for the clinical situation.

Keywords: skin atrophy, glucocorticoid, in vitro test system, human keratinocytes, 3T3 mouse fibroblasts, full-thickness skin model

Table of Contents

1 Introduction

1.1 Clinical Aspects of GC-induced Skin Atrophy

Glucocorticoids (GCs) belong to the most widely used and most powerful anti-inflammatory drugs at all. The first systemic treatment with GCs was performed by Hench and co-workers in patients with rheumatoid arthritis in 1949 (Hench et al., 1949). The introduction of topical hydrocortisone in the early 1950s provided great advantages over previously available therapies. Triamcinolone acetonide was the first halogenated corticosteroid, which began a revolution that cumulated in the appearance of potent and superpotent GCs. Such highly effective GCs have on the one side great advantages in certain indications, localizations and types of disease; on the other side, they may have undesired effects when used over longer periods or when applied improperly. The enthusiasm for these highly effective agents was at its peak during the 1960s and 1970s and more potent GCs were often used inappropriately and indiscriminately. Adverse effects became apparent and the subsequent backlash of opinion against topical GCs created confusion (Maibach and Wester, 1992). However, topical GCs are successfully used in the treatment of several common cutaneous diseases but their major limitation, their side effect potential, is still remaining. Topical GCs might have pleiotropic systemic effects potentially causing several adverse reactions such as suppression of pituitary adrenal axis, diabetes mellitus, muscle atrophy, growth retardation and others, in particular after high-dose and long-term application (Mills and Marks, 1993; Schoepe et al., 2006).

Skin atrophy is the most important cutaneous side effect of GC therapy (Sterry and Asadullah, 2002), where a major function of the skin, the formation of a permeability barrier between the external milieu and the organism, is compromised (Kao et al., 2003). This barrier disruption is characterized by a profound increase in transparency of skin, a cigarette-paper-like consistency, an increased fragility, skin thinning and the occurrence of a telangiectatic surface (Booth et al., 1982; Kimura and Doi, 1999; Mills and Marks, 1993) (**Fig. 1**). The first original description of the phenomenon was published in 1963 (Epstein et al., 1963) reporting five patients with atrophic striae in the groins, who had topically received a triamcinolone acetonide containing cream. Histopathologically, flat dermal-epidermal junctions (Kimura and Doi, 1999), reduced thickness of the epidermis (Mills and Marks, 1993), decreased size of keratinocytes (Kolbe et al., 2001), reduced number of fibroblasts (Kolbe et al., 2001; Saarni and Hopsu-Havu, 1978), and rearrangement of the geometry of the dermal fibrous network (Lehmann et al., 1983) are found in GC-induced skin atrophy.

Fig. 1: GC-induced skin atrophy. Chronic topical steroid use has led to marked thinning of the skin. (Image kindly provided by Charles Goldberg and Jan Thompson, University of California, San Diego)

Both topical and systemic GC therapy can induce cutaneous atrophy. Factors that affect the atrophogenic potential of a given topical GC are its dose, potency, duration of therapy, frequency of application (Garbe and Wolf, 2005), and further unknown factors. Different formulations may also markedly affect both the clinical efficacy of a GC as well as its atrophogenic potential, simply because of the differing potential of the vehicle to release the drug into the stratum corneum (Smith et al., 2002).

The classification of topical GCs is based on their anti-inflammatory potencies after Niedner **(Tab. 1 A)**. Thus, class I GCs like hydrocortisone (HC) have weak effects (regarding both desired anti-inflammatory effects and side effects) whereas class IV GCs like clobetasol-17-propionate (CB) have very strong effects (Niedner, 1996). More recently, in addition to classification on potency, the therapeutic index (TIX) has been introduced for topical GCs (Luger et al., 2004). The TIX indicates the ratio of beneficial (potency in atopic dermatitis, vasoconstriction) and adverse (atrophogenicity, pituitary adrenal axis suppression and allergic potential) effects of several GCs and thus integrates its advantages and limitations. The concept of the benefit/risk ratio evaluation with topical GCs is based on both, *in vitro* and *in vivo* data, concerning efficacy and safety (Korting et al., 1992; Schackert et al., 2000; Schäfer-Korting et al., 1993). Atrophy of the skin is the most prevalent side effect of topical administered GCs, therefore, the atrophogenic potential **(Tab. 1 B)** is weighted more than other side effects for calculating the TIX. Since a TIX of $1 \leq 2$ is defined as an equal relation of beneficial and adverse effects, a TIX of $2 - 3$ indicates a GC with improved benefit/risk ratio. For example hydrocortisone, a class I GC with a TIX of 1 has a balanced benefit/risk ratio, while mometasone furoate, a class III GC with a TIX of 2 has stronger desired effects than side effects.

Tab. 1: Classification of GCs based on potency [A], therapeutic indices and their potential to induce skin atrophy [B]. Class: I = mild, IV = super potent. TIX = Therapeutic Index: 1≤2 relation between desired and adverse effect is equal, 2-3 means GC with improved benefit/risk ratio. Skin atrophy: 1 = GC induces little skin atrophy, 3 = GC induces much skin atrophy. (Modified after Luger et al. 2004, Garbe & Wolf 2005)

A

Class	Effects	Examples
I	weak	hydrocortisone, hydrocortisone acetate, prednisolone
II	moderate	dexamethasone, prednicarbate
III	strong	betamethasone-17-valerate, mometasone furoate
IV	very strong	clobetasol-17-propionate

B

TIX	Skin atrophy	Class	Glucocorticoid
1	1	I	hydrocortisone
1,2	2	III	betamethasone-17-valerate
1,5	2	IV	clobetasol-17-propionate
2	1	II	prednicarbate
2	1	II	methylprednisolone aceponate
2	1	III	mometasone furoate

1.2 Cellular Mechanisms of GC-induced Skin Atrophy

GCs have profound effects on both anatomically distinct layers of the skin, the epidermis and the dermis that is connected by the basement membrane. The epidermis is constituted mainly by keratinocytes. Keratinocytes originate from basal proliferating cells attached to the basement membrane, whose daughter cells migrate into the upper layer of the epidermis undergoing a differentiation process. As keratinocytes die they produce a cornified external membrane, the stratum corneum. The stratum corneum provides mechanical resistance and is embedded in a lipid-enriched extracellular matrix (ECM), which is responsible for the permeability barrier. The dermis is mainly composed of fibroblasts. Their major function is production and delivery of components of connective tissue, like proteins of the dermal ECM. The basement membrane contains specialized structures, called anchoring complex, which ensure stability of connection and communication between these two tissue compartments. Keratinocytes and fibroblasts are known target cells of GC-effects in skin (Schoepe et al., 2006).

1.2.1 Keratinocytes Effects

GC treatment can lead to epidermal thinning (=epidermal atrophy). This epidermal atrophy might be due to decreased size (Delforno et al., 1978; Kolbe et al., 2001) and suppressed proliferation of keratinocytes (Lange et al., 2000). Reasons for decreased cell size are not exactly known, but it is assumed that reduced biosynthesis of macromolecules of these cells might play an important role (De Paiva et al., 2006; Marks et al., 1971). The anti-proliferative effect of GCs has been reported to be

associated with reduced mitotic rates of GC-treated keratinocytes (Fischer and Maibach, 1971; Zendegui et al., 1988). However, accelerated keratinocyte maturation results in thinning of the living epidermis due to the shorter epidermal cell life (Delforno et al., 1978; Laurence and Christophers, 1976; Woodbury and Kligman, 1992). It has been shown that topical GCs inhibit the terminal epidermal differentiation (Sheu et al., 1991). The GC-induced epidermal thinning and especially the thinning of the stratum corneum are accompanied by an increased permeability and an increased transepidermal water loss (Kolbe et al., 2001), which generally indicates disrupted barrier function of the skin (Kao et al., 2003; Sheu et al., 1989).

1.2.2 Fibroblasts Effects

GCs also inhibit the proliferation of dermal fibroblasts (Hein et al., 1994; Lange et al., 2000; Ponec et al., 1977) by reducing their mitotic rate (Hein et al., 1994). Apoptosis appears not to be the reason for reduced numbers of fibroblasts as shown by Hammer and colleagues. They demonstrated protective activity of dexamethasone (DEX) in primary human fibroblasts against TNF-α-, UV- or ceramide-induced apoptosis (Hammer et al., 2004). The cellular effects of GCs on fibroblasts result in the thinning of the dermis. Moreover, fibroblasts play an important role in the synthesis of ECM proteins whose production is significantly interfered by GCs, as shown below.

1.3 Molecular Mechanisms of GC-induced Skin Atrophy

1.3.1 Glucocorticoid Action

GCs mediate their effects via many and diverse genomic and non-genomic mechanisms (for review see Schäcke et al. 2007). After diffusion into the cell they bind to the intracellular GC receptor (GR). Binding of ligands induces a conformational change in the GR molecule resulting in translocation of the activated GR into the nucleus (Oakley and Cidlowski, 2001). There, the GR is able to affect gene expression either positively (transactivation) or negatively (transrepression). The positive regulation of target genes is mediated by a specific binding of the activated GR as a homodimer to GC response elements (GREs) in the promoter or enhancer region of responsive genes (Beato et al., 1989), followed by an induction of gene transcription. Three types of GREs, which require slightly different GR conformations, are described: simple, composite, and tethering GREs. The activated GR binds as a sole sequence-specific DNA binding protein, i.e. without recruitment of co-factors, to simple GREs. GR-binding to composite GREs needs one or more non-receptor factors. For binding to tethering GREs, the GR is recruited through protein-protein interaction to another DNA-bound factor (Lefstin and Yamamoto, 1998). Transrepression effects of the receptor are mechanistically as variable as described for the transactivation effects. First, activated GR can bind to negative GREs (nGRE), leading to repression of gene transcription (Sakai et al., 1988). Second, the GR binds to sequences that overlap the recognition sites of other essential transcription factors and interferes with their binding (Stromstedt et al., 1991). Third, the GR interacts via protein-protein interaction with other

transcription factors, e.g. activator protein-1, nuclear factor-κB, or Smad3, preventing an activation of transcription by these factors (De Bosscher et al., 2000; Schüle et al., 1990; Tuckermann et al., 1999).

1.3.2 Extracellular Matrix Protein Effects

The effects of GCs are ubiquitous. In the skin, keratinocytes and fibroblasts are known target cells of GC action. Fibroblasts synthesize ECM proteins that give tensile strength and elasticity to the skin. An impaired synthesis and degradation of ECM proteins by GC treatment decreases these skin properties (Oikarinen and Autio, 1991; Saarni and Hopsu-Havu, 1978). ECM proteins include collagens, proteoglycans, and elastin. Alterations of the dermis mainly result from effects of GCs on collagen turnover (Cutroneo et al., 1981; Nuutinen et al., 2001). Collagens are the major components of ECM and constitute a highly specialized family of glycoproteins with at least 27 members. They distribute tensile strength to the skin. Type I collagen, the major skin collagen fibril, is forming ~80 % of the skin collagen. The minor components are type III collagen forming 10-15 %, type IV collagen forming the basement membrane, and type V collagen forming 5 % of the skin collagen (Schäcke et al., 2002a). Type I collagen is a heterodimer composed of two α1(I) chains and one α2(I) chain, which are encoded by *COL1A1* and *COL1A2* genes (Vuorio and de Crombrugghe, 1990). These chains are synthesized in a 2:1 ratio, and they undergo extensive post-translational modifications before assembling in a characteristic triple helix (review in Prockop & Kivirikko 1995). In the extracellular space, procollagen molecules are trimmed of their C propeptide and N propeptide, and they assemble into quarter-staggered fibrils and then into fibres. GCs decrease the rates of type I collagen protein synthesis in human skin (Autio et al., 1994), human skin fibroblasts (Ponec et al., 1979b), rat skin (Shull and Cutroneo, 1983) and rat skin fibroblasts (Raghow et al., 1986). Additionally, GC-induced decreases at the mRNA levels of *COL1A1* have been reported in the skin of humans and rats (Oikarinen et al., 1998; Oishi et al., 2002) and in skin fibroblasts of humans and rats (Raghow et al., 1986; Russell et al., 1989). In contrast to collagen type I, type III is synthesized as a homotrimeric procollagen comprising three identical α1(III) chains. The assembly to fibres is similar to that of collagen type I. GCs display inhibitory effects on type III collagen at the protein level in rat and human skin (Nuutinen et al., 2003; Oishi et al., 2002) as well as at the mRNA level in rat skin (Oishi et al., 2002) and in human skin fibroblasts (Russell et al., 1989).

GCs may affect the collagen synthesis also indirectly by reducing prolyl 4-hydroxylase (P4h) activity (Cutroneo et al., 1975; Oikarinen and Hannuksela, 1980). P4h catalyzes hydroxylation of proline residues in peptide linkages, and therefore stabilizes the triple-helical structure of collagen.

Molecules participating in the collagen turn over, like matrix metalloproteinases (MMP), might also be affected by GCs. MMPs belong to a family of at least 25 highly homologous Zn^{++}-endopeptidases that collectively cleave the constituents of the ECM (Birkedal-Hansen et al., 1993; Woessner, 1994). The collagenase MMP-1 has the capacity (shared with MMP-13) to cleave the triple helix of type I and III collagen by hydrolysis, allowing the chains to unwind and become susceptible to further degradation (Shapiro, 1998). Murine MMP-13 is the rodent counterpart of human interstitial collagenase MMP-1

(Balbin et al., 2001). MMP-3, also called stromelysin 1, degrades in general denatured collagens (= gelatine) and proteoglycans and activates MMP-1 (Krane, 1994). Besides final degradation of fibrillar collagens, MMP-2 and MMP-9 (gelatinase A and B) also degrade collagen type IV and remove unfolded or abnormal folded collagens (Kähäri and Saarialho-Kere, 1997). Their production is transcriptionally regulated and requires an additional stepwise activation from inactive precursors (proMMP) to active enzyme (Nagase and Woessner, 1999). Activity of MMPs further depends on interactions with ECM components and binding to endogenous inhibitors such as tissue inhibitor of metalloproteinases (TIMP) (Vincenti, 2001). As such, these mechanisms allow a fast activation or deactivation of MMPs and thus, the adaptation to changes in the cutaneous environment.

In skin, keratinocytes and fibroblasts are capable of producing MMPs. Although there is a constitutive expression in the skin to ensure homeostasis, most of the MMPs can also be regulated in response to exogenous signals, e.g. MMP-1 is temporarily induced by various growth factors or cell-matrix interactions (Heino, 1996; Vaalamo et al., 1997), and altered cell-cell contacts (Lacraz et al., 1994). In normal skin, MMP levels are balanced. Excessive and restrained levels of MMPs can impair the structural integrity of the epidermis and the dermis and result in the remodelling of the skin. Thus, MMPs play an important role in various aspects of skin biology and pathology, e.g. in wound repair (Xue et al., 2006), tumor cell invasion (Deryugina and Quigley, 2006), photoaging (Dong et al., 2008), as well as in GC-induced skin atrophy. GC treatment of human skin was found to repress MMP-1 and MMP-2 mRNA expression (Oikarinen et al., 1998). In rat skin, application of DEX decreases both active and latent forms of collagenase as well as its mRNA levels (Oishi et al., 2002). MMP-1 and MMP-3 mRNA expression is repressed by the activated GR via protein-protein interaction with activator protein-1 (reviewed in Frisch & Ruley 1987, Vincenti et al. 1996). The decreased production of *MMP1* and *MMP2* mRNA as well as MMP-2 and MMP-9 protein by DEX treatment in human gingival fibroblasts was demonstrated Kylmaniemi and co-workers (Kylmaniemi et al., 1996).

1.4 Determination of the Atrophogenic Potential of GCs

1.4.1 Clinical Assessment

In clinical studies, to asses a GR ligand's effect on skin thickness, the ultimate atrophogenic potential of GCs is determined for compound development. Since atrophy is potentially irreversible and obtaining skin biopsies represents an invasive method with certain risks (scars, infection) it is aimed to limit such investigations or at least to apply compounds to very small areas and to use non-invasive methods. There are many non-invasive methods to clinically investigate the atrophogenic potential of GCs by measuring the thinning of the skin directly, e.g. micrometer screw gauge, confocal laser microscopy, optical coherence tomography and ultrasound (Gans et al., 2008; Josse et al., 2009; Kolbe et al., 2001; Newton et al., 1984). For both, research purposes and clinical evaluation, measurement of GC-induced skin barrier impairment is frequently used, e.g. evaporimetry is used to demonstrate transepidermal water loss (Kolbe et al., 2001).

1.4.2 Preclinical *in vivo* Test Systems for GC-induced Skin Atrophy

To estimate the relative risk of a topical GC to induce skin atrophy, preclinical test systems are important. There are some animal models available allowing the determination of the atrophogenic potential of GCs (**Tab. 2**). The atrophogenicity of GCs has been evaluated in mice (Kirby and Munro, 1976; Sheu et al., 1998), rats (Schäcke et al., 2004; Smith et al., 1976), pigs (Lavker et al., 1991; Winter and Wilson, 1976), and dogs (Kimura and Doi, 1999). In the past, for atrophy assessment, rats were shaved and skin thickness was determined (Smith et al., 1976; Young et al., 1977). Repeated shavings for multiple topical applications increased the risk of to skin irritation and caused a high variability in results (Marks, 1976; Young et al., 1978). The currently preferred standard model for GC-induced skin atrophy in basic and pharmaceutical research is the model of hairless OFA *hr/hr* rats (Schäcke et al., 2004). As a major overall read out parameter skin thickness is determined over time until the end of the treatment period. The thickness of skin folds (two thicknesses of the skin) is measured with a special gauge (Kirby and Munro, 1976; Schäcke et al., 2004). The skin thickness is also be determined by counting the cell layers in skin biopsies (Woodbury and Kligman, 1992). The transepidermal water loss in intact skin (Ahn et al., 2006) or in skin biopsies (Sheu et al., 1998) and the skin-breaking strength of skin biopsies are used as additional parameters for skin atrophy (Mirshahpanah et al., 2007; Schäcke et al., 2004). Although these models are of certain predictability for the human situation they display some limitations. The major and most important disadvantage is their non-human character. Additionally, *in vivo* models require high labor, time and compound amount and are not favorable experimental models due to ethical reasons.

Tab. 2: Overview of preclinical rodent *in vivo* models used to determine the atrophogenic potential of GCs. (Modified after Schoepe et al. 2006)

Model	Reported findings	Reference
Mouse ear	Daily treatment over 11 days. Thinning of mouse ear used to asses the atrophogenic potential of GCs. Well suited for measurement with a ratchet control micrometer; low standard errors, reproducible; reliable, non-invasive, safe.	Kirby et al. 1976
Dorsal skin of hairless mouse	Daily treatment over 18 days. Loss of volume of all cutaneous compartments used to asses the atrophogenic potential of nine GCs. GC-induced atrophy is similar to that in human. Volume reduction of sebocytes, cysts; thickness reduction of dermal and muscle. Caliper measurement of skin thickness is relative insensitive.	Woodbury et al. 1992
Mouse tail	Daily treatment over 3 weeks. Epidermal thinning of mouse tail used to asses the atrophogenic potential of five GCs. All tested GCs caused significant epidermal thinning. Ranking similar to that in human. Difficult to quantify epidermal atrophy.	Woodbury et al. 1992
Flank skin of shaved Sprague-Dawley rat	Daily treatment over 12 days. The degree of atrophy determined by comparing the weights of skin plugs taken from GC-treated areas with contra laterally paired control areas. Potencies in dermal atrophy assay directly comparable with topical anti-inflammatory potencies in the rat.	Young et al. 1977
Dorsal skin of hairless rat	Daily treatment over 19 days. Skin thickness and skin breaking strength was used to asses the atrophogenic potential of a classic GC compared with selective GR agonists. Well suited to measure skin thickness with a special gauge; sensitive; low standard errors, reproducible; reliable, non-invasive, safe.	Schäcke et al. 2004

1.4.3 Preclinical *in vitro* Test Systems for GC-induced Skin Atrophy

The beauty of *in vitro* test systems in general is that they are fast, inexpensive, and feasible with limited amounts of compounds. They are, therefore, highly attractive for pharmaceutical companies, especially in early drug discovery projects. They also allow medium or even high throughput compound screening. However, there are just a few approaches that might to some extent allow to determine the atrophogenic potential of GCs *in vitro* (**Tab. 3**). Classically, those tests assess proliferation of keratinocytes and fibroblasts. Dependent on the experimental model, GCs might either favour or inhibit division of fibroblasts, depending on the working-group (reviewed in Durant et al. 1986). An explanation for the differences observed among *in vitro* experiments is that GCs also indirectly affect fibroblast proliferation by controlling the synthesis or actions of various factors produced by other cell types. Yet, more recent studies show anti-proliferative effects of GCs on primary human fibroblasts (Görmar et al., 1990; Hein et al., 1994; Lange et al., 2000; Wach et al., 1998) and HaCaT cells, a human keratinocyte cell line (Wach et al., 1998). Similarly, effects of GCs on collagen synthesis in fibroblasts vary from stimulating (Görmar et al., 1990) to inhibiting (Ponec et al., 1979a). However, the limitation of *in vitro* models is that the isolated cells are kept under non-physiological conditions, that comprised 1. difference between growth medium and tissue fluid, 2. presence of the cells in a „monolayer“ and bathing in a large excess of growth medium, 3. absence of inter-tissue interactions, and 4. absence of many humoral factors acting *in vivo* (Hein et al., 1994; Lange et al., 2000; Ponec et al., 1977). So far, no suitable *in vitro* test system exists that allows the

prediction of skin atrophy. Much research remains to be done to establish reliable *in vitro* models to determine GC-induced atrophy.

In vitro test systems using monolayer cell culture systems are beneficial, as they allow high compound throughput in an appropriate time and are cost saving in comparison to animal experiments. Of course, they can not reflect all aspects of an tissue or organ system sufficiently such as the missing cell-cell interactions. Recently, the development of human organotypic full-thickness 3D skin models marked a major step for research. These models represent a link between limited *in vitro* cultures and the situation *in vivo*. These 3D *in vitro* models are increasingly used to measure the skin-irritant effects of compounds. In principle, they consist of epidermal cell layers supported by a dermis equivalent, and therefore, are able to reflect the complex interactions of fibroblasts and keratinocytes. A number of different 3D models have been established in dependency on the goal. For example, the AST-2000 (CellSystems, St. Katharinen, Germany) was developed as a tool for pharmaceutical and chemical compound testing. It is used to test toxic or irritating effects of compounds by multiple end-point analysis including viability and cytokine release (Heisler et al., 2002). Another 3D skin equivalent named full-thickness skin model (FTSM, Phenion, Düsseldorf, Germany) was very recently shown to be suitable to investigate some parameter of skin atrophy (Zöller et al., 2008). Different GCs applied to FTSM induced epidermal and dermal atrophy monitored by counting epidermal cell layers and by measuring type I collagen synthesis. Results obtained by Zöller and co-workers supported the aim of the present study to further evaluate and qualify the suitability of skin equivalents as test systems for the atrophogenic potential of compounds.

For the characterization of novel compounds in pharmaceutical research and development, *in vitro* models with high predictability for atrophogenicity of compounds would be favorable as they are less time-consuming, cost saving and requiring fewer amounts of compounds compared to *in vivo* experiments. However, no appropriate, sufficiently characterized *in vitro* test system for determination of GCs atrophogenic potential has been described so far.

Tab. 3: Overview of potential *in vitro* models to test the atrophogenic potential of GCs.

Model	Reported findings	Reference
Proliferation of NHDF	Inhibition or induction by GCs	reviewed in Durant el al. 1986, Lange et al. 2000
Proliferation of HaCaT	Dose-dependent inhibition by different GCs	Wach et al. 1998
Collagen synthesis of NHDF	Inhibition by different GCs	Ponec et al. 1977, Ponec et al. 1979
Epidermal thickness and collagen synthesis in FTSM	Epidermal and dermal atrophy was induced by topical treatment with GC of different classes.	Zöller et al. 2008

1.5 Strategies to Reduce the Side Effect / Atrophogenic Potential of GR Ligands

Topical GCs are very efficient in treatment of chronic inflammatory skin diseases, but their use is limited due to their side effect profile. Thus, the need for GR ligands with an improved benefit/risk ratio still remains. Progress in early, sensitive and predictive determination of the atrophogenic potential will have impact on the identification and development of novel drugs. The atrophogenic potential of existing topical GCs varies to some degree, however, the atrophogenic potential of a conventional GC generally correlates with its anti-inflammatory potency (Brazzini and Pimpinelli, 2002). To selectively address both issues, inflammation and atrophy, one may consider strategies based on pharmacokinetics, i.e. temporal, histological and spatial aspects, optimized and adjusted drug delivery, or strategies that involve pharmacodynamics, i.e. mechanistic aspects and modes of action that result from intrinsic pharmacological properties of a compound. Both types of approaches should ultimately favor suppressive effects on immunocytes over those on keratinocytes and fibroblasts (Schoepe et al., 2006). Such mechanisms obviously do not obey clear-cut mechanisms since GR ligands may activate and suppress gene activation in several different ways. The recently identified selective GR agonists (SEGRA) are non-steroidal GR ligands with dissociated properties (Schäcke et al., 2002b; Schäcke and Rehwinkel, 2004; Schäcke et al., 2004). These SEGRA compounds are equipotent regarding immuno-suppression but show reduced side effects in comparison with GCs. Rats topically treated with a SEGRA compound showed significantly reduced skin atrophy compared to animals treated with the reference GC prednisolone (Schäcke et al., 2004).

2 Objectives and Project Strategy

The goal of this study was the identification of an *in vitro* test system, applicable in preclinical screening of substances to predict the atrophogenic potential of new compounds. The desired test system had to be efficient and economical and at the same time lead to reliable and reproducible results. It had to require lower amounts of compound compared to *in vivo* test systems and to allow a high throughput when screening new compounds, particularly of a new compound class selective GR agonists (SEGRA), which hypothetically exhibits less atrophogenic but similar anti-inflammatory potential compared to classical GCs.

A suitable test system consist of two parts, an *in vitro* assay and read out parameters predictive of atrophogenicity. To focus on economical and highly efficient assays, the study aimed at analyzing i) rodent and ii) human cutaneous cells grown in monolayer culture and iii) human cutaneous cells grown as human full-thickness skin equivalents. For analyzing these assays, known atrophy markers or hypothetical markers not yet known as atrophy markers ought to be used. Additionally the study aimed at identifying new markers highly predictive for atrophogenic potential using a hypothesis-free driven approach, i.e. analysis of the gene expression profile of GC-treated rodent skin. In a broad approach, multiple combination of cellular assays and read out parameters should be investigated.

To pre-screen the numerous test systems, a classical GC should be applied and a reproducible regulation of the read out parameter by GC treatment was defined as inclusion criteria for further evaluation. It is known that the risk to develop skin atrophy increases with increasing concentrations of the applied GC. The class of GC indicates both the anti-inflammatory potency and the atrophogenic risk: strong GCs induce more atrophy than weak GCs. Furthermore, an unfavorable therapeutic index (TIX) indicates a higher risk to induce atrophy than another GCs from the same class. Thus a promising test system should comply with the following requirements: 1.) Dose-dependent regulation by GC 2.) Correlation with GC classification, i.e. weak (class I) GCs– hydrocortisone (HC), moderate (class II) – prednicarbate (PC), strong (class III – mometasone furoate (MF), and very strong class IV – clobetasol-17-propionate (CB) show different effects 3.) Correlation with TIX, i.e. betametasone-17-valerate (BMV) with a low TIX shows more atrophogenicity than MF with a high TIX. Test systems fulfilling at least two of these requirement should be additionally characterized. In a further approach, the recommended systems should be applied with the new compound class SEGRA. To evaluate the predictive potential of the test system, the resulting regulation of the read out parameters should be compared with the skin thinning potential of the novel compound in the *hr/hr* rat skin atrophy model.

3 Material and Methods

3.1 Cell Culture

3.1.1 Monolayer Cell Culture

3.1.1.1 Cultivation of Adherent Cell Lines

3T3 mouse fibroblasts (ECACC, Taufkirchen) and HaCaT keratinocytes were maintained in DMEM (Gibco, Eggenstein, Germany) supplemented with 10 % heat-inactivated FCS (Gibco) in 165 cm² tissue culture flasks (Corning-Costar, Bodenheim, Germany) and passaged (1/10 or 1/20) twice a week at 70 – 80 % confluence. For all passaging cells were washed with PBS w/o Ca^{2+} and Mg^{2+} (Gibco) and detached with TrypLExpress (Gibco). Cells were grown in a moist atmosphere in at 37°C and 7.5 % CO_2.

3.1.1.2 Cultivation of Human Primary Fibroblasts and Keratinocytes

Normal human dermal fibroblasts (NHDF) and normal human epidermal keratinocytes (NHEK) from female adult donors were purchased from Provitro (Berlin, Germany). Cells of passages 3 – 7 were used for the experiments. In brief, cells were maintained in fibroblast growth medium supplemented with 10 % heat-inactivated FCS (Provitro) or in serum-free keratinocyte growth medium (Provitro), respectively. Additionally, both media were supplemented with penicillin (100 U/ml), streptomycin (100 mg/ml) (Provitro). NHDF and NHEK were washed with PBS w/o Ca^{2+} and Mg^{2+}, detached with TrypLExpress at 70 – 80 % confluence and 4000 cells / cm² and were seeded in new flasks with fresh medium. Cells were grown in a moist atmosphere in at 37°C and 5 % CO_2.

3.1.1.3 Cultivation of Human Monocyte Cell Line THP-1

THP-1 suspension cells were maintained in VLE RPMI 1640 (Seromed, Vienna, Austria) supplemented with 10 % heat-inactivated FCS, 50 U/ml penicillin, 50 µg/ml streptomycin and 50 µMl β-mercaptoethanol in 165 cm² tissue culture flasks and passaged (1/10) twice a week. Cells were adjusted to 50000 cells / ml, and were grown in a moist atmosphere in at 37°C and 5 % CO_2.

3.1.1.4 Isolation and Cultivation of Primary Rat Fibroblasts

Ears of adult *hr/hr* rats were disinfected with 70 % ethanol and washed in 4 % antibiotic-antimycotic solution (400 U/ml penicillin, 400 µg/ml streptomycin and 1 µg/ml amphotericin, Gibco). The front and back side of ears were separated under aseptic conditions with forceps and the dermis side carefully laid flat in a sterile cell culture plate. Ear sheets were incubated overnight at 4°C in PBS w/o Ca^{2+} and Mg^{2+} with 2.4 U dispase II (Roche, Mannheim. Germany) / ml to separate epidermis from dermis. The dermis was separated from epidermis using forceps and incubated with sterile filtered 0.2 % collagenase type IA (Sigma, Deisenhofen, Germany) in PBS w/o Ca^{2+} and Mg^{2+} for 1 hour at 37°C with constant shaking until the solution became opaque. After filtration through a 100 µm cell strainer (BD Biosciences, Heidelberg, Germany) cells were centrifuged, cell pellet was washed two

times with fibroblast growth medium (Provitro) containing 10 % FCS and cells were seeded in cell culture flasks (3-8x10^4 cells / cm²). Medium was changed every second day.

3.1.1.5 Cryoconservation and Thawing of Cells

Growing cells (70 – 80 % confluence) were suspended in 0.5 ml ice-cold freezing medium (10 % v/v DMSO in FCS), frozen at –70°C and stored in liquid nitrogen. Frozen cells were thawed at 37°C in a water bath, resuspended in prewarmed medium and washed twice before culturing.

3.1.1.6 Tests with Adherent Monolayer Cells

To determine the effect of GCs on mRNA and protein expression and proliferation of fibroblasts and keratinocytes, cells were washed with PBS w/o Ca^{2+} and Mg^{2+}, detached from culture flask with TrypLExpress and counted in a Neubauer cell counting chamber (Brand, Berlin, Germany) by diluting cell suspension 1:2 with 0.4 % Trypan blue (Serva, Heidelberg, Germany). Fibroblasts were seeded at a density of 2.1x10^4 cells/cm², whereas the smaller keratinocytes were seeded at 5.2x10^4 cells/cm² in cell culture plates (Corning-Costar). Test media for 3T3, NHDF and HaCaT was supplemented with 5 % charcoal-treated serum (CCS) instead of FCS. Test medium for NHEK was hydrocortisone-free. After 24 hour adhesion time, cells were treated with 0.1 % DMSO with or without different GR agonists. After 4, 24 or 48 hours treatment time, supernatants were collected for measurement of protein secretion (see **3.5.3**) and cells were lysed in RNA lyses buffer (see **3.4**) or in protein lyses buffer (see **3.5.1**). To compare the effects of GR ligands, potencies [%] in relation to DEX and efficacies were calculated. Thereby, IC_{50} [µM] indicates the half maximal (50 %) inhibitory concentration (IC) of a substance.

3.1.1.7 Tests with THP-1 Cells

Inhibition of pro-inflammatory cytokines or chemokines is well known as a major molecular mechanism of anti-inflammatory activity of GCs. IL-8 is a major chemokine for neutrophil attraction strongly overexpressed in inflammatory dermatoses including atopic dermatitis. *In vitro* release of IL-8 can be stimulated by LPS in monocytes. The human monocytic cell line THP-1 was treated with 10 µg/ml LPS in the absence or presence of DEX or other GR ligands for 18 hours. IL-8 concentration was determined in the supernatant by an IL-8-specific ELISA (MesoScale Discovery, Gaithersburg, MD, USA). DEX was used as reference and its maximum effect was set to 100 % inhibition.

3.1.2 Human 3D Skin Models

In the present study, two multi-layered human full-thickness skin equivalents consisting of a fully stratified epidermis and a dermis rich in extracellular matrix (ECM) were compared. The skin equivalents consisted of fibroblasts and keratinocytes isolated from human foreskin tissue. The fibroblasts were seeded in a rat collagen solution (AST-2000, CellSystems, St. Katharinen, Germany) or in a lyophilized bovine collagen matrix (FTSM, Phenion, Düsseldorf, Germany). Keratinocytes were seeded on top of the fibroblasts. After a cultivation period under submersed conditions the skin

models were cultivated at the air-liquid interface (ALI) for another cultivation period. The skin models grew in hydrocortisone free media from day 7 after airlift, and the experiment started on day 15 after airlift.

3.1.2.1 Advanced Skin Test (AST-2000)

After arrival, 0.63 cm² inserts with advanced skin test-2000 (AST-2000, CellSystems) were placed in 1 ml hydrocortisone free AST medium (CellSystems) in a 6-well plate and adapted to cell culture conditions (37°C, 5 % CO_2, max. humidity). Test substances were dissolved in AST medium (final concentration 0.01 % DMSO with or without 1 µM test compound) and applied topically onto the dry *stratum corneum* in a volume of 15 µl / 0.63 cm² or systemically in AST medium (final concentration 0.01 % DMSO with or without 0.1 µM test compound). The medium was replaced daily by fresh and prewarmed medium. AST-2000 were exposed to the compounds for 4 hours (minimum) up to 12 days (maximum). After exposure, reconstructed skin models were washed twice with PBS w/o Ca^{2+} and Mg^{2+} and are prepared for histological analysis. For molecular analysis like measurement of mRNA and protein expression the epidermis was detached from the dermis mechanically with a pair of tweezers and analyzed separately.

3.1.2.2 Full-thickness Skin Model (FTSM)

After arrival, the 1 cm² FTSM (Phenion) were placed on filter papers on top of pre-placed metal support in 5 ml hydrocortisone-free FTSM medium in a 6-well plate and adapted to cell culture conditions (37°C, 5 % CO_2, max. humidity). Test compounds were dissolved in FTSM medium (final concentration 0.01 % DMSO with or without test compounds) and applied systemically. To compare the atrophogenic activity in skin equivalents, equieffective concentrations of GR ligands were defined in previous experiment with THP-1 cells. The IC_{50} of LPS-induced IL-8 secretion in these cells was calculated for every tested GR ligand and was for CB 0.06 µM (data not shown). It was necessary for the experiment with skin equivalents, that the chosen treatment concentrations would surely induce atrophy. The previous FTSM experiment showed, that 0.1 µM CB lead to the maximum reduction of epidermal thickness. To compare the atrophogenic activity in skin equivalents, the use of equipotent concentrations of different GR ligands is necessary. Therefore, a constant factor derived from the IC_{50} and the minimum dose to induce maximal epidermal atrophy in FTSM was calculated and used in a further experiment, i.e. 0.1 x 0.06 = 0.0006. Additionally, a ten times lower concentration was used to test dose dependency. The conditioned medium was replaced daily by fresh and prewarmed medium. FTSM were exposed to the compounds for 24 hours (minimum) up to 12 days (maximum). After compound exposure, reconstructed skin models were washed twice with PBS w/o Ca^{2+} and Mg^{2+} and were prepared for histological analysis. For compartment separation, FTSM were washed twice with PBS with Ca^{2+}, Mg^{2+}, incubated in thermolysin solution (0.5 mg / ml thermolysin in 33 mM KCl, 50 mM NaCl, 5 mM $CaCl_2$, 0.01 M HEPES) for 2 hours at 4°C the epidermis separated from the dermis by using forceps. For molecular analysis, mRNA and protein expression of epidermis and dermis were analyzed separately.

3.2 Animal Models

SKH1 hairless mice weighing 24-26 g were purchased from Charles River (Berlin, Germany). OFA hr/hr rats weighing 70-90 g were purchased from Charles River (Berlin, Germany) or Bayer (Wuppertal, Germany). All animal studies were approved by the competent authority for labor protection, occupational health, and technical safety for the state and city of Berlin, Germany, and were performed in accordance with the ethical guidelines of Bayer Schering Pharma AG.

3.2.1 Skin Atrophy in Rodents

To investigate induction of skin atrophy *in vivo*, different GR agonists (clobetasol-17-propionate, mometason-17-valerate, SEGRA) were applied (75 µl on a marked area of 9 cm^2 in 95 % ethanol / 5 % isopropyl myristate) daily for several times (0 d, 1 d, 3 d, 8 d, 10 d, 19 or 26 d) to dorsal skin of female hairless rats (strain *hr-hr*, 120–140 g) or of female hairless mice (strain SKH1, 24–26 g, Charles-River).

Skin thickness was determined every third day by using a specifically designed dial thickness gauge (Schering, Berlin, Germany). Animals were sacrificed at the end of the experiment. To determine effects on body weight, animals were weighed before and after completion of treatment.

3.2.2 Irritant Contact Dermatitis in Rats

Test compounds or vehicle were topically co-applied with the Croton oil solution (6 %) in ethanol/isopropylmyristate (95:5 v/v) to both ears of Wistar rats (Schäcke et al., 2004). After 24 hours, rats were sacrificed and then weight of 10 mm ear punch biopsies was determined as an overall read-out of inflammation. Peroxidase activity as parameter for granulocyte infiltration was analyzed in ear homogenates. The effects of SEGRA compound A were compared to clobetasol-17-propionate.

3.3 Proliferation Tests

To investigate the effects of GCs on proliferation 3T3, HaCaT, NHDF and NHEK were seeded at several cell densities in 96-well plates (Corning-Costar). After 24 hours of adhesion, cells were treated for 24 hours until 7 days with GCs or with menadione (Sigma) as positive control for proliferation inhibition. Medium was changed every second day.

3.3.1 [^{3}H]-Thymidine Incorporation

During the last 24 hours cells were incubated with 25 µCi [^{3}H]-thymidine (Amersham, Mainz, Germany). Cells were transferred onto filter plates using a cell harvester (Packard, Dreieich). Filter plates were dried at 60°C in warm case, and scintillator (Wallack, Heidelberg, Germany) was added. [^{3}H]-thymidine incorporation was measured by a β-counter (Wallack, Freiburg, Germany).

3.3.2 Alamar Blue Fluorometry

Alamar Blue (BioSource, Ratingen, Germany) is a commercial preparation of the dye resaruzin (O'Brien et al., 2000), which is used to quantify viability, cytotoxicity, and cell proliferation. Cells

incorporate Alamar Blue by endocytosis, the dye is reduced, its color changes and the cell releases the dye via exocytosis. Viable metabolizing cells can be quantified by this method. Cell proliferation rate was also quantified by incubation of cells with 10 % [v/v] Alamar Blue during the last 24 hours and optical density detected at 590 nm with a microtiter plate spectrofluorometer (Molecular Devices, Ismaning, Germany).

3.4 Measurement of mRNA Expression

3.4.1 Isolation and Quantification of Total RNA

3.4.1.1 Column Preparation

Cells

Effects of GCs on mRNA expression in cutaneous cells were determined with TaqMan®-RT-PCR $2x10^5$ fibroblasts (NHDF or 3T3) per well or $5x10^5$ keratinocytes (NHEK or HaCaT) per well were seeded in 6-well plates (Costar). After 24 hour adhesion time, cells were treated with different GR agonists for 4 and 24 hours.

Total RNA was extracted using an ABI Prism 6100 Nucleic Acid PrepStation (Applied Biosystems, Darmstadt, Germany). All chemicals for the ABI 6100 were purchased from Applied Biosystems. The yield (4 – 15 µg total RNA) from 2 x 10^5 fibroblasts or 5 x 10^5 keratinocytes was collected in a volume of 80 µl and quantified using an Agilent 2100 BioAnalyzer (Applied Biosystems) and the RNA 6000 Nano Assay kit (Ambion Biotechnology, Cambridgeshire, UK). Total RNA was stored at -80°C.

Tissue

Total RNA was isolated from rat whole skin (5 mm punch biopsies) and separated epidermis and dermis from human skin equivalents using the Qiagen RNeasy protocol to analyze the gene expression patterns with TaqMan®-RT-PCR. Initially, samples were placed in 300 µl RLT buffer including 1 % β-mercaptoethanol and homogenized using the Ultra-Turrax (IKA, Staufen, Germany) for 1-2 min. Samples were then processed using the Qiagen RNeasy protocol. Briefly, after efficient homogenization, samples were centrifuged at 13000 rpm for 3 min. The supernatants were transferred into fresh tubes, 590 µl RNase-free water (Gibco) and 10 µl proteinase K (Qiagen, Hilden, Germany) were added, incubated at 55°C for 10 min and centrifuged at 13000 rpm for 30 sec. The supernatants were transferred into fresh tubes and half a volume of $ethanol_{abs}$ was added to the cleared lysate. The contents of each tube were then mixed and applied to an RNeasy minicolumn followed by a series of centrifugation steps and washes. In addition, the on-column DNase digestion was performed using the RNase-free DNase set (Qiagen). RNA was finally eluted in 50 µl of RNase-free water and quantified using an Agilent 2100 BioAnalyzer (Applied Biosystems). Total RNA was stored at -80°C.

3.4.1.2 Chloroform / Phenol Preparation

For microarray study, total RNA of GC-treated skin biopsies (5 mm) form *hr/hr* rats and SKH1 mice was extracted with the Invisorb RNA Kit II (Invitek, Berlin, Germany) using the manufacturer's

protocol. Briefly, frozen samples were homogenized with an Ultra-Turrax in 700 µl of Invisorb RNA Kit II lyses solution and incubated for 1 hour with 4 mg/ml proteinase K (BD Biosciences) at room temperature. 50 µl Adsorbin was added for DNA binding. After 5 min incubation on ice, samples were centrifuged (1 min, 14000 rpm, 4°C) and the supernatant was transferred into a new tube. 500 µl DEPC-water saturated phenol (Roth, Karlsruhe, Germany), 50 µl buffer A (Invisorb RNA Kit II) and 100 µl chloroform were added and 15 s vigorously mixed and incubated on ice for 5 min. After centrifugation upper phase containing RNA was transferred into a new tube, 2 µl glycogen and isopropanol (the same volume as the upper phase) were applied and RNA precipitated over 45 – 60 min at -20°C. Following centrifugation, supernatant was rejected and 1 ml of 75 % EtOH was added to the pellet and centrifuged. The last procedure was repeated; the pellet was dried at 60°C for 2 min and dissolved in 30 µl RNase free water. The obtained total RNA was quantified using an Agilent 2100 BioAnalyzer and used for gene expression analysis. Total RNA was stored at -80°C.

3.4.2 Reverse Transcription

Total RNA was transcribed to complementary DNA (cDNA) using reverse transcriptase. Reverse transcription was performed using 250 ng of total RNA dissolved in 38.5 µl RNase-free water (Gibco). The TaqMan® Reverse Transcription Reagents Kit (Applied Biosystems) was used according to the manufacturer's protocol. RNA was preincubated at 70°C for 2 min. 61.5 µl reaction mixture, containing 1× RT buffer, 5.5 mM $MgCl_2$, 2.5 µM random hexamer primers, 0.4 U/L RNase Inhibitor, 2 mM each NTP (dNTPs mixture) and 1.25 U/L MultiScribe™ reverse transcriptase (TaqMan® Reverse Transcription Reagents, Applied Biosystems), was added and samples incubated in a PCR System 9700 Thermocycler (Applied Biosystems) using the following cycling parameters: 25°C for 10 min, 48°C for 30 min, 95°C for 5 min (inactivation), and 4°C hold. The obtained cDNA product was stored at -20°C.

3.4.3 Quantitative Real Time Polymerase Chain Reaction (qRT-PCR)

Quantitative RT-PCR was performed in triplicates or quadruplicates in 384-well plates using the ABI Prism® 7900HT sequence detection system (Applied Biosystems, Darmstadt, Germany). PCRs contained 0.5 µl of cDNA template, 6.25 µl qPCR Mastermix Plus w/o UNG (Eurogentec, Cologne, Germany), 5.15 µl RNase-free water (Gibco) and 0.62 µl Assay-on-Demand™ (AoD, Applied Biosystems) for specific gene (**Tab. 4**). Hypoxanthine-guanine phosphoribosyltransferase (*HPRT*) was used as endogenous reference gene. The reactions were carried out at 50°C for 2 minutes, 95°C for 10 minutes, and then 95°C for 15 seconds and 60°C for 1 minute for 40 cycles. Standard curves (log of template dilution versus Ct value) for each gene-specific primer set were used to determine relative mRNA content for each target gene. Triplicate / quadruplicate values obtained from each gene-specific PCR were used to determine a relative baseline for each of the experimental groups. Gene expression was repressed if the ratio between treatment with 1 µM GC vs. 0.1 % DMSO was smaller or equal to 0.5x in every experiment ($n \geq 3$), expression was induced if the ratio was greater or equal to 2x,

expression was not regulated if ratio was between 0.5x and 2x. The ratio between GC-treated and control was also called fold regulation.

Tab. 4: Assays on DemandTM (AoD, Applied Biosystems, Darmstadt, Germany) used for TaqMan real time PCR.

Gene	Name	AoD human	AoD rat	AoD mouse
HPRT	Hypoxanthine guanine phosphoribosyl transferase	Hs99999909_m1	Rn01527840_m1	Mm00446968_m1
COL1A1	Collagen type I, alpha 1	Hs00164004_m1	Rn00801649_g1	Mm00801666_g1
COL3A1	Collagen type III, alpha 1	Hs00164103_m1	Rn01437683_m1	Mm00802331_m1
COL4A1	Collagen type IV, alpha 1	Hs00266237_m1		Mm00802372_m1
COL5A1	Collagen type V, alpha 1		Rn00593170_m1	Mm00489342_m1
COL7A1	Collagen type VII, alpha 1	Hs00164310_m1		Mm00483818_m1
COL11A1	Collagen type XI, alpha 1	Hs00266273_m1		Mm00483387_m1
COL14A1	Collagen type XIV, alpha 1	Hs00385388_m1		Mm00805269_m1
COL17A1	Collagen type XVII, alpha 1	Hs00166711_m1		
FGFBP1	Fibroblast growth factor binding protein 1	Hs00183226_m1	Rn00575070_s1	Mm01219609_m1
FMOD	Fibromodulin	Hs00157619_m1	Rn00589918_m1	Mm00491215_m1
IL1B	Interleukin 1 beta	Hs00174097_m1		
IL6	Interleukin 6	Hs00985639_m1		Mm00446190_m1
IL8	Interleukin 8	Hs99999034_m1		
LCN2	Lipocalin 2	Hs00194353_m1		Mm01324470_m1
MMP1	Matrix metalloproteinase 1	Hs00233958_m1	Rn01486634_m1	
MMP2	Matrix metalloproteinase 2	Hs00234422_m1	Rn02532334_s1	Mm00439508_m1
MMP3	Matrix metalloproteinase 3	Hs00233962_m1	Rn00591740_m1	Mm00440295_m1
MMP9	Matrix metalloproteinase 9	Hs00234579_m1	Rn00579162_m1	
MMP13	Matrix metalloproteinase 13	Hs00233992_m1	Rn01448197_m1	Mm00439491_m1
P4HA1	Prolyl-4-Hydroxylase, alpha 1	Hs00168575_m1	Rn00597082_m1	Mm00803137_m1
P4HB	Prolyl-4-Hydroxylase, beta	Hs00168586_m1	Rn00564459_m1	
PRG4	Proteoglycan 4	Hs00195140_m1		Mm00502413_m1
TNMD	Tenomodulin	Hs00223332_m1		Mm00491594_m1

3.4.4 Microarray Analysis

Chloroform / phenol extracted mRNA samples from GC-treated *hr/hr* rat and SKH1 mosue skin were kindly processed by colleagues from Target Research I for DNA microarray analysis.

3.4.4.1 *In vitro* RNA Transcription and Hybridization to Affymetrix GeneChips

The „One-Cycle Eukaryotic Target Labeling Kit" from Affymetrix (PN 900493, Santa Clara, CA, USA) was used according to the manufacturer's instructions. Briefly, 2 µg of high quality total RNA was reverse transcribed using T7 tagged oligo-dT primer for the first-strand cDNA synthesis reaction. After RNase H-mediated second-strand cDNA synthesis, the double-stranded cDNA was purified and served as template for the subsequent *in vitro* transcription reaction which generates biotin-labeled complementary RNA (cRNA). Biotinylated cRNA was then cleaned up, fragmented and hybridized to GeneChip Rat Genome 230 2.0 or Mouse Genome 430 2.0 expression arrays respectively (Affymetrix). GeneChips were washed and stained with streptavidin-phycoerythrin on a GeneChip Fluidics Station 450 (Affymetrix). After washing, the arrays were scanned on an Affymetrix®

GeneChip 3000 scanner (Affymetrix) with autoloader and barcode reader. HGU133Plus2.0 arrays were processed.

3.4.4.2 Data Analysis

Quality of hybridized arrays was analyzed with Expressionist Pro 4.0 Refiner software (GeneData, Basel, CH). Here, based on raw intensities of individual oligonucleotide features (probes), the following analyses were performed: experiments were grouped according to similarity and potential outlier experiments were removed (or selected for re-hybridization and/or re-fragmentation), the quality of a particular experiment was compared with a virtual reference experiment, which was computed as average of all feature intensities of all arrays in that group. Moreover, defects on the arrays were masked. Here, for each array, the spatial signal distribution was compared with the reference experiment of the experiment group it belonged to. Regions with sharp boundaries which have consistently higher or lower feature intensities compared to the reference experiment were flagged as defects and excluded from further analysis. In addition, a signal correction (distortion and gradient) was performed, the control gene statistics were calculated, and an overall classification of the quality of the experiments was provided.

Probe intensities on each array were summarized with the MAS5.0 summarization algorithm and refined and summarized data were loaded into the CoBi database (GeneData). Analysis of the probe set's specific signal intensities was performed with Expressionist Pro 4.0 Analyst software (GeneData). Data set was Lowess normalized. Genes were found to be repressed, if the ratio of GC-treated vs. vehicle treated was ≤ 0.5, and to be induced if ratio was ≥ 2.

3.5 Protein Expression

3.5.1 Western Blot

3.5.1.1 Cell and Tissue Lyses

To determine the effect of GCs on protein expression of cutaneous cells, $2x10^5$ fibroblasts (NHDF or 3T3) or $5x10^5$ keratinocytes (NHEK or HaCaT) were seeded per well in 6-well plates (Costar). After 24 hours of adhesion, cells were treated with different GR agonists for 24 or 48 hours, washed twice with ice cold PBS (5 ml) and lysed in 500 µl freshly prepared lyses buffer (50 mM Tris, pH 7.5, 150 mM NaCl, 2 mM EGTA, 1 mM NaF, 1 % Triton X-100, 1 mM sodium orthovanadate) in the presence of protease inhibitor cocktail (Roche) for 10 min with agitation. 5 mm punch biopsies of GC-treated rat skin or separated epidermal and dermal layers of GC-treated skin equivalents were homogenized with an Ultra Turrax (IKA) in 500 µl lyses buffer. All lyses steps were performed on ice, in ice cold tubes with cooled centrifuge. Thereafter, lysate was transferred into a 1 ml Eppendorf tube (Merck, Berlin, Germany), mixed vigorously twice for 30 sec, centrifuged at 4°C and 14000 rpm for 20 min, and the protein supernatants were transferred into 1 ml Eppendorf tubes.

3.5.1.2 Centrifugal Concentration of Cell Supernatant

Cell supernatants of GC-treated cells were collected and proteins larger than 30 kDa were concentrated by centrifugal concentration using Vivaspin 2 (Sartorius, Göttingen, Germany).

3.5.1.3 Measurement of Protein Concentration

In order to compare the protein expression under different experimental conditions, total protein concentrations were measured with BCA Protein Assay Reagent kit (Pierce, Berlin, Germany) and, before Western blot adjusted to the same protein concentration.

Protein quantification was performed according to the manufacturer's protocol (Pierce) in 96-well plates with 5 µl sample volume. Protein amount was quantified using Spectra Max 340 microplate reader (Molecular Devices).

3.5.1.4 Electrophoresis

For electrophoresis, 18 µl sample in sample buffer (100 mM Tris, pH 6.8, 3 % SDS, 10 % sucrose, 0.03 % Bromphenol Blue, 50 mM DTT) was denatured for 5 min at 95°C in an Eppendorf Thermomixer (Merck), cooled on ice, mixed and then 15 µl (minimum 5 µg protein) were loaded to pre-cast gels (Tris-HCl buffered polyacrylamide gel without SDS) with an acrylamide concentration of 4-20 % (Biorad, Munich, Germany). Rainbow Marker (Amersham) was used, and the electrophoresis was performed in 1x running buffer (77 mM Tris, pH 8.3, 100 mM HEPES, 0.1 % SDS) for 90 min at 110 V with Mini-PROTEAN II Electrophoresis Cell (Biorad). The expected molecular weight for the protein marker ranged from 10 to 250 kDa.

3.5.1.5 Protein Transfer

After electrophoresis, proteins were transferred onto pre-cut nitrocellulose membranes (activated in transfer buffer) surrounded by filter papers and pads. Protein transfer was performed with transfer buffer (37 mM Tris, pH 8.3, 39 mM glycine, 0.038 % SDS, 20 % methanol) for 1:30 hour at 75 V in Mini Trans-Blot Electrophoretic Transfer Cell (Biorad). Thereafter, nitrocellulose membrane was washed for 5 min in 0.1 % TBS-T buffer (100 mM Tris, pH 7.5, 150 mM NaCl, 0.1 % Tween 20).

3.5.1.6 Protein Detection

After blocking unspecific binding with 20 ml 5 % BSE (in 0.1 % TBS-T) over 1 hour, and washing (5 x 5 min in 0.1 % TBS-T buffer) the membrane was incubated over night at 4°C with the appropriate primary antibody diluted in 5 ml 0.1 % TBS-T. Unbound fraction of primary antibody was removed by washing (5 x 5 min in TBS-T buffer). Thereafter, peroxidase-conjugated secondary antibody diluted in 5 ml in 0.1 % TBS-T (**Tab. 5**) was added for 40 min at room temperature. After washing (5 x 5 min in 0.1 % TBS-T buffer), peroxidase activity was detected with chemoluminescent ECL reagent (enhanced chemoluminescence) in a lightproof cassette and exposition to photosensitive Hyperfilm ECL (Amersham Biosciences). The film was developed with Curix 60 (Agfa, Berlin, Germany).

Tab. 5: Antibodies and dilutions used for Western blot.

Primary antibody specific for	Size (kDa)	Dilution	Secondary antibody	Dilution
βActin (A1978, Sigma)	42	1:5000	anti-mouse	1:10000
Col1a1 (R1038, Acris, Hiddenhausen, Germany)	95-138	1:10000	anti-rabbit	1:10000
Col3a1 (ab23746, Abcam, Cambridgeshire, UK)	95-138	1:5000	anti-rabbit	1:10000
MMP-1 (IM35, Calbiochem, Darmstadt)	55 / 60	1:1000	anti-mouse	1:10000
MMP-2 (ab2462, Abcam)	66 / 72	1:500	anti-mouse	1:10000
MMP-3 (MAB513, R&D Systems, Wiesbaden, Germany)	55 / 60	1:1000	anti-mouse	1:10000
P4hα1 (NB100-57852, Acris)	64	1:1000	anti-goat	1:10000
P4hα2 (NB110-40494, Acris)	64	1:1000	anti-rabbit	1:10000
P4hβ (AF0910-1, Acris)	57	1:1000	anti-mouse	1:10000

3.5.2 Histology and Immunohistochemistry

3.5.2.1 Embedding

Rats were sacrificed at the end of the experiment and punch biopsies (10 mm) taken from the GC-treated area. GC-treated AST-2000 samples were washed in PBS for 2 x 30 min. Samples were frozen at -80°C for a minimum of 24 hours. Frozen punch biopsies and AST-2000 samples were cut in halves and embedded in tissue freezing medium (Jung, Nussloch, Germany) over liquid nitrogen steam. Six micrometer frozen serial sections (Cryostat Leica CM3050S, Leica, Munich, Germany) were transferred onto object slide (Superfrost plus, Menzel, Wiesbaden, Germany) were dried (2-24 hours).

At the end of the experiment, human skin equivalents were washed twice in PBS and fixed for 24 hours in 4 % formalin. Afterwards, samples were embedded in paraffin. Six micrometer sections were transferred onto object slide (Superfrost plus) and dried at least 24 hours.

3.5.2.2 Hematoxylin-Eosin Stain

In order to analyze the tissue structure and epidermal size in vehicle treated (control) and in GC-treated rat skin / skin equivalent, Hematoxylin-Eosin (HE) stain was performed according to Lillie Mayer. Briefly, nuclei from cryosections were stained with the alcohol soluble hematoxylin (1:2 dilution in drinking water) for 150 sec, and rinsed under water. Thereafter, staining with 1 % eosin (Dako, Hamburg, Germany) was performed for 120 sec. After a short wash in distilled water, the sections were covered with Faramount (watery medium, Dako, Hamburg, Germany) and cover slips and were analyzed 24 hours later at 10- to 20-fold extension under the microscope (Zeiss Axioplan, Jena, Germany) with MetaVue program (Visitron, Puchheim, Germany).

3.5.2.3 Immunohistology for Expression of Extracellular Matrix Proteins

Cryo sections were fixed for 2 min in ice-cold 100 % acetone, dried for 2 hour at RT and washed with PBS (pH 7.2) to remove tissue freezing medium (storage at -20° C possible).

Paraffin sections were deparaffinized with xylene and re-hydrated with descending alcohol concentrations and bidest. water. Tissue sections were demasked with Target Retrieval 1x Solution

(Dako) for 20 min in a steamer (95-99° C) and cooled down to room temperature in TBS for another 20 min.

Skin sections were washed 3 x 2 min with PBS and subsequently incubated for 5 min at room temperature with control serum of the secondary antibody host. After flow down (not washing), PBS-diluted primary antibody (**Tab. 6**) was added for 30 min, sections washed for 3x2 min with PBS and thereafter incubated with biotinylated secondary antibody for 15 min. Following further wash steps (3x2 min with PBS) streptavidin-HRP (Pharmingen, Heidelberg) was added for 10 min, then sections were washed (3x2 min PBS) and stained by oxidation of the alcohol soluble AEC (3-amino-9-Ethylcarbacol) chromogenic substrate diluted 1:200 in water (Pharmingen, Heidelberg, Germany). After 5 min of incubation and three times rinsing with distilled water, nuclei were counterstained for 1 min with hematoxylin diluted 1:2 in drinking water (Dako, Hamburg) after Mayer and 10 min incubated under running water for precipitation of blue color. After rinsing with distilled water, sections were covered with Faramount (Dako) and cover slip and analyzed 24 hours later at 10- to 20-fold extension under the microscope (Zeiss Axioplan) with Meta Vue program (Visitron, Puchheim, Germany).

Tab. 6: Antibodies used for immunohistological investigations.

Primary antibody	Dilution	Secondary antibody	Dilution
Col1a1	1:400	anti-rabbit	1:200
Col3a1	1:100	anti-rabbit	1:200
Ki-67	Ready-to-use	anti-rabbit	
P4hβ	1:100	anti-mouse	1:200
P4hα1	1:1000	anti-goat	1:200
P4hα2	1:1000	anti-rabbit	1:200
Perp	1:500	anti-rabbit	1:200

3.5.3 Enzyme-linked Immunosorbent Assay (ELISA)

ELISA is an immunological detection method for antigenic determination in fluids, e.g. homogenates, cell lysates and supernatants. Following ELISAs were used: MMP-1 ELISA (Calbiochem, Darmstadt), Metra CICP EIA Kit (Quidel, Marburg, Germany), MS6000 Human MMP 3-Plex Ultra-Sensitive Kit for detection of MMP-1, MMP-3 and MMP-9 (Meso Scale Discovery), MA6000 Human IL-8 Base Kit (Meso Scale Discovery) and Human Proinflammatory II 4-Plex Kit for detection of IL-1β, IL-6, IL-8 and TNF-α (Meso Scale Discovery). Supernatants of GC-treated cutaneous cells or skin equivalents were collected and prepared for detection according to manufacturer's protocol.

3.6 Statisical Analysis

For all monolayer *in vitro* models, statistical analysis was performed using the paired t-test after Wilcoxon (SigmaStat 3.0, SPSS GmbH, Munich, Germany). First, the repression of mRNA expression was assessed, and the concentration of drug needed to reduce mRNA expression by 50 % (IC_{50}) was calculated for each GC treatment with sigmoidal curve regression (4 parameter fit) from SigmaPlot

2002 (SPSS GmbH). Differences between GCs were assessed by comparison of the IC_{50} of different GC treatment groups among each other. Values with $p \leq 0.05$ were considered as statistically significant.

For GR ligand induced epidermal atrophy in Phenion® FTSM, one of the 3D *in vitro* models, differences between several groups were assessed by calculating the Fieller's confidence interval (Zerbe, 1978) based on recommendation of Dr. Hannes-Friedrich Ulbrich (Global Drug Discovery Statistics, Bayer Schering Pharma AG, Berlin, Germany). For that it was to be assumed that Gaussian distributions with equal variances are a reasonable model for the original scale of measurement. Literature search revealed that no alternative models have been proposed so far for the situation under investigation. Keratinocyte layers were counted in 5 areas of 3 non-consecutive sections per single FTSM. By event replication more information was obtained: a.) Level 1 contains two independent events, as the experimental group size contained two independent FTSM (n=2). b.) Level 2 contains six dependent subreplicates (3 sections per sample, 2 samples per group). c.) Level 3 consists of 30 dependent subreplicates (5 areas counted per section, 3 sections per sample, 2 samples per group). To calculate the Fieller's confidence interval the mean inhibition was estimated with the lower and upper 0.95 confidence limit. The confidence intervals were calculated at all three levels. The inhibition between the compared groups is statistically significant, if a.) the values for mean inhibition, lower and upper confidence limit are all negative and b.) these values are negative at all three tested levels. The inhibition between the compared groups tends to be statistically significant, if a.) the values for mean inhibition, lower and upper confidence limit are all negative and b.) these values are negative in two at the three tested levels. First, DMSO treated groups was compared with all GR ligand treated groups. Second, the compound treated groups were compared among each other: a.) HC vs. PC, MF, CB, b.) PC vs. MF, CB, c.) MF vs. CB, and d.) SEGRA vs. CB. The confidence intervals are not globally calculated over all comparisons, but were specifically calculated with 95 % probability for every (multiple-) group comparison. A multiplicity correction between the comparisons was not implemented.

Differences between several groups in the *in vivo* experiments were assessed with the Mann-Whitney U test (SigmaStat 3.0, SPSS GmbH, Munich, Germany). Outliers were determined according to Dixon's r_{10} outlier test (Dixon, 1953) using the formula [$r_{10} = d_{max} / r$]where r_{10} is the critical value that depends on sample size and a-level (e.g. $r = 0.468$ for $a = 0.90$ and n = 8), r is the range and d_{max} is the maximal difference between two lowest or two highest values. Figures show mean values ± SD if not mentioned otherwise. Values with $p \leq 0.05$ were considered as statistically significant.

4 Results

4.1 Selection of Cellular Assays

Cellular systems were selected that are either pre-published or expected to be suitable for prediction of the atrophogenic potential of GCs. GC-induced skin atrophy is caused by GC effects on keratinocytes and fibroblasts. These cells can be grown in monolayer culture systems as well as in organotypic 3D culture systems. Full-thickness 3D *in vitro* skin equivalents represent a link between *in vitro* monolayer cell culture and *in vivo* systems with the advantage that fibroblasts and keratinocytes can communicate with each other. In skin equivalents, not only molecular markers from both fibroblasts and keratinocytes in one system are detectable, but also the investigation of epidermal thinning is possible.

Pre-published cellular systems for skin atrophy. The anti-proliferative activity of GCs on the immortalized human keratinocyte cell line **HaCaT** and on normal human dermal fibroblasts (**NHDF**) was shown by Wach and colleagues (Wach et al., 1998). In NHDF as well as in primary rat skin fibroblasts (**rFib**) an inhibition of the collagen synthesis after GC treatment was obtained (Raghow et al., 1986; Russell et al., 1989). The 3D skin equivalent named full-thickness skin model (**FTSM**) from Phenion® (Düsseldorf, Germany) has been recently reported to be suitable for investigation of several parameter of skin atrophy (Zöller et al., 2008).

→ *HaCaT cells, NHDF, rFib and FTSM were selected after literature search and were used as cellular assays.*

Obvious cellular systems for skin atrophy. Normal human epidermal keratinocytes (**NHEK***)* were found to be described as suitable cells for detection of anti-inflammatory activity of GCs (Lange et al., 1997; Stein et al., 1997). Therefore, it was interesting to learn whether these cells are also appropriate to detect atrophogenic potential of GCs. Similarly, the mouse embryonic fibroblast cell line **3T3** was also not found to be described in context with atrophogenic potential of GCs, yet. Additionally, another skin equivalent system was selected to investigate its suitability as models for GC-induced skin atrophy. The advanced skin test **AST-2000** (CellSystems®, St. Katharinen, Germany) was developed as a tool for pharmaceutical and chemical compound testing. Usually, it was used in-house to test toxic or irritating effects of compounds by multiple end-point analysis including viability and cytokine release (Heisler et al., 2002).

→ *NHEK and 3T3 mouse fibroblasts were used as monolayer cell cultures, while AST-2000 was used as 3D cell culture systems to investigate various read out parameters for GC-induced skin atrophy.*

4.2 Identification of Potential Read Out Parameters

Read out parameters were selected in three ways: 1.) Based on pre-published data: marker for GC-induced skin atrophy described in the literature. 2.) Hypothesis-driven: obvious marker derived from pre-published data were chosen 3.) Hypothesis-free: search for new read out parameters by analyzing the gene expression profile of GC treated rodent skin.

4.2.1 Pre-published Read Out Parameters

Collagens represent the major ECM component of the skin with 70 % of skin dry weight. Many studies have shown, that collagens are strongly negatively affected by GC treatment, leading to decreased skin thickness and elasticity (reviewed in Oikarinen & Autio 1991, and Schoepe et al. 2006). Collagen type I and III α1 subunit (***COL1A1*** and ***COL3A1)*** mRNA expression are decreased in human skin by hydrocortisone treatment (Nuutinen et al., 2003). A GC-decreased collagen turn over was also demonstrated. Oikarinen and co-workers detected negative effects of GCs on ***MMP1*** and ***MMP2*** mRNA expression in GC-treated human skin (Oikarinen et al., 1998).

→ *Based on these published data, the synthesis of collagen type I and III, MMP-1 and MMP-2 after GC treatment was investigated in the present study at the mRNA and partly at the protein level.*

4.2.2 Identification of Hypothesis-driven Parameters

As the inhibition of collagen type I and III synthesis by GCs seems to be a prominent event in development of skin atrophy, it was obvious to also analyze the GC-dependent expression of other collagens synthesized in the skin.

Type IV collagen is exclusively found in basement membranes where it provides structural support for this matrix. *COL4A1* mRNA expression is decreased by DEX treatment of basement-membrane-forming fibrosarcoma cells (Oikarinen et al., 1987). In addition, MMP-2 is a collagen type IV degrading enzyme and it is repressed by GCs (Oikarinen et al., 1998). Thus, the expression patterns of its substrate after GC-treatment was investigated in the present study.

Type V collagen is mixed with collagen types I and III to form heterotypic fibrils (Berthod et al., 1997). **Type VII collagen** forms the anchoring fibril that attaches the basement membrane to the underlying dermis (Gras et al., 2001). It was investigated in the present study, whether *COL5A1* and *COL7A1* mRNA expression are affected by GCs and might serve is marker for GC-induced skin atrophy.

GCs may affect the collagen synthesis also indirectly by reducing prolyl 4-hydroxylase (**P4h**) activity (Oikarinen and Hannuksela, 1980). A GC-dependent regulation of the mRNA of P4h subunits was not found to be described in literature. Thus, the mRNA expression of the two α and one β subunits *P4Ha1*, *P4HA2* and *P4HB* was investigated in the present study for their suitability as atrophy markers.

In addition to MMP-1 and MMP-2 more MMPs are involved in the collagen turn over. **MMP-3**, also called stromelysin 1, degrades in general gelatine like MMP-2 (gelatinase A) and activates MMP-1 (Krane, 1994). **MMP-9** (gelatinase B) is beside the above mentioned MMP-2 the second member of the gelatinase family. Thus, the MMP-3 and MMP-9 was obviously investigated for atrophy prediction.

→ *Taken together, the synthesis of Col4a1, Col5a1, Col7a1, P4ha1, P4ha2, P4hb, MMP-3 and MMP-9 was investigated in the present study for their suitability as predictive markers for GC-induced skin atrophy.*

4.2.3 Identification of Hypothesis-free Parameters

GeneChip analysis was used to search for potential new genes as read out parameters for GC-induced skin atrophy. Two approaches were performed to identify GC-regulated genes in skin of topically treated hairless rodents: 1.) SKH1 mice were treated daily for 14 days with 0.01 % clobetasol-17-propionate (CB; n=9) or 0.01 % momentasone-furoate (MF; n=9). 2.) OFA *hr/hr* rats were treated for 0, 6 and 24 hours on the first day and then daily for 2, 4 and 8 days with 0.01 % CB (n=3). As control for the induction of skin atrophy, skin thinning was determined every day in both rodent models (**Fig. 2**). Animals were sacrificed at the end of the experiment and gene expression profile of the skin was analyzed by DNA microarray analysis.

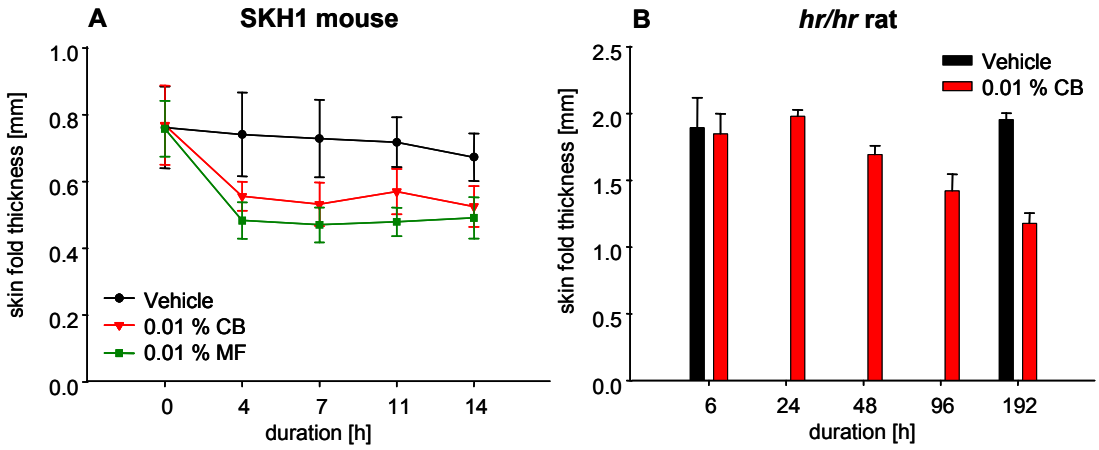

Fig. 2: Reduction of skin thickness of GC-treated rodent skin. Dorsal skin was daily treated with vehicle or 0.01 % GCs. SKH1 mice (A) were treated for 14 days, *hr/hr* OFA rats (B) for 6, 24, 48, 96 or 192 hours. Vehicle groups were used for the start and end point of the experiment. At the end of the experiments skin biopsies were taken and samples were prepared for microarray as described in Material and Methods. Skin fold thickness was measured with a specifically designed dial thickness gauge. In mice, this parameter was monitored over time. In rats, skin fold thickness was measured at the end points for each group. CB – clobetasol-17-propionate, MF – mometasone furoate

SKH1 mouse study. In atrophic mouse skin, 90 genes were found to be induced more than 2-fold and 228 genes to be repressed more than 0.5-fold by GC treatment relative to vehicle treatment. Genes involved in immune regulation and a marker gene known to be regulated by GCs were selected to proof the validity and quality of the test system. FK506 binding protein 5 (*FKBP5*), a marker for GC-mediated activation of gene expression (U et al., 2004), displayed a 2.7-fold increased expression in CB-treated compared to vehicle-treated skin. Furthermore, chemokine (C-X-C-motif) ligand 5 and 9 and chemokine (C-C-motif) ligand 8 and 27 were shown to be repressed in GC-treated mouse skin (e.g. *CXCL9* was 0.04-fold repressed by CB). Surprisingly, expression of the atrophy marker genes *COL1A1* and *COL3A1* was not found to be affected in GC-treated mouse skin after 14 days CB treatment. However, regulated and annotated genes were classified as follows: ECM component, protease, protease inhibitor / activator or growth factor. Therefrom, the eight genes with the highest fold-regulation were selected regarding their potential involvement in skin atrophy development for further characterization: lipocalin 2 (*LCN2*), proteoglycan 4 (*PRG4*), cathepsin E (*CTSE*), FGF-binding protein 1 (*FGFBP1*), fibromodulin (*FMOD*), *COL11A1*, *COL14A1* and tenomodulin (*TNMD*). The function and the biological processes of these selected eleven genes are summarized in **Tab. 7**. The regulation of these genes were further investigated by RT-PCR.

hr/hr rat study. For the rat, many genes were not as well annotated as for the mouse. The expression of the marker gene for GC activity *FKBP5* was 2.9-fold induced, while the expression of genes involved in inflammation like *CXCL5* and *CXCL9* was slightly repressed to 0.52-fold and 0.72-fold, respectively after 6 hour CB treatment. Similar to SKH1 mice, the expected GC-dependent gene regulation of *COL1A1* and *COL3A1* was not detected in rat skin by microarray analysis. Due to high intra-assay variability it was not possible to certainly detect time-dependent GC effects. Similar to the results obtained in atrophic mouse skin, in rat skin *LCN2* gene expression was induced, whereas expression of *CTSE*, *FMOD* and *TNMD* was repressed after GC treatment. In the rat study, it was not possible to identify more novel potential genes that might be relevant for GC-induced skin atrophy.

Tab. 7: Selection of GC regulated genes as potential read out parameters for GC-induced skin atrophy. SKH1 mice were daily treated with 0.01% CB. After 14 days, gene expression of skin biopsies was analyzed by microarray. Genes were selected according to their strength of regulation and to their possible importance in skin atrophy induced by GC treatment. Detected fold-regulation is given as ratio between CB-treated : vehicle-treated. Fib = fibroblasts, Ker = keratinocytes

Gene	Function / biological process	Expressed by	Regulation
COL11A1: Procollagene type XIα1	Cell adhesion; cellular sensing and response; osteogenesis; ECM component	Fib (Yates and Glowacki, 2003)	0.41x repressed
COL14A1: Procollagene type XIVα1	Cell adhesion; osteogenesis; ECM component	Fib (Berthod et al., 1997)	0.49x repressed
CTSE: Cathepsin E	Proteolytic degradation; protease inhibitor	Fib (Finley and Kornfeld, 1994)	0.36x repressed
FGFBP1: FGF binding protein 1	Fibroblasts growth factor-receptor signaling pathway; ECM component; protein binding	Ker (Abuharbeid et al., 2006)	2.0x induced
FMOD: Fibromodulin	ECM component; fibrous connective tissue	Fib (Westergren-Thorsson et al., 1991)	0.47x repressed
LCN2: Neutrophil gelatinase-associated lipocalin	Transporter activity; dysregulated epidermal differentiation marker	Ker (Mallbris et al., 2002)	2.0x induced
PRG4: Proteoglycan 4	Proteolytic degradation; extracellular / secretion proteins; enzyme activator	Fib (Jay et al., 2000)	2.4x induced
TNMD: Tenomodulin	ECM forming cell (fibrocyte, chondrocyte, osteocyte)	Fib (Mendias et al., 2008)	0.32x repressed

Further investigation of genes identified from hypothesis-free approach.

Surprisingly, in GeneChip analyses the pre-published atrophy marker genes *COL1A1* and *COL3A1* were not found to be repressed. Therefore, it was investigated whether a regulation of these markers could be detected by RT-PCR. The SKH1 mouse experiment analyzed by microarray was repeated with similar conditions: the skin of SKH1 mice was treated for 14 days with 0.01 % CB. Subsequently, the mRNA expression was determined by RT-PCR i.) in samples used for microarray analyses from the first mouse study and ii.) in samples of the additional experiment. In both experiments, RT-PCR analyses showed a repression of -59 % of *COL1A1* mRNA in CB-treated mouse skin compared to vehicle treated skin. *COL3A1* mRNA expression was found to be repressed about -63 %. The microarray results of the eight selected genes (**Tab. 7**) were additionally checked by RT-PCR in samples of both experiments. The CB-induced repression detected by microarray analysis of *COL14A1, CTSE* and *FMOD* was not found by RT-PCR neither in the samples used for microarray nor in the samples from the second experiment. Similar results were obtained for *LCN2* mRNA expression. The microarray study indicated an induction of *LCN2* mRNA expression, while no regulation was determined by RT-PCR in CB-treated mouse skin samples. In accordance with the microarray results, the CB-induced regulation of the following four genes was confirmed by RT-PCR: the mRNA expression of *COL11A1* was reduced about -61 % and of *TNMD* about -94 % in CB-treated compared to vehicle-treated skin, while the mRNA expression of *FGFBP1* was induced about +70 % and of *PRG4* about +224 %. Taken together, for four of eight genes, the regulation pattern in CB-treated mouse skin detected by microarray could be confirmed by RT-PCR.

In a next step, the four *in vivo* regulated genes should be tested whether they are also regulated by GCs *in vitro*. mRNA expression of *COL11A1, FGFBP1, PRG4* and *TNMD* was investigated in different *in vitro* cell systems. Therefore, cells grown in monolayer culture were treated with 1 µM DEX for 4 and 24 hours. The skin equivalents AST-2000 and FTSM were treated daily with 0.1 µM CB for 1, 3 and 12 days. mRNA expression was determined by RT-PCR. The expression patterns of selected genes after GC treatment of *in vitro* models is listed in **Appendix Tab. 20**.

Col11a1 is synthesized by fibroblasts (Yates and Glowacki, 2003) and its mRNA expression was found to be repressed in CB-treated mouse skin. In contrast to the microarray results, *COL11A1* mRNA expression was induced in 3T3 mouse fibroblasts about +171 % and in primary human fibroblasts NHDF about +2250 % after DEX treatment for 24 hours relative to vehicle control.

FGFbp1 is secreted by keratinocytes (Abuharbeid et al., 2006). *In vivo* FGFB1 was induced by GCs. In NHEK, *FGFBP1* mRNA expression was slightly repressed about -47 % after 24 hours of DEX treatment compared to vehicle treated cells. It was not found to be regulated in epidermal samples of AST-2000 and FTSM treated with CB for 1, 3, and 12 days.

Prg4 is expressed by fibroblasts (Jay et al., 2000) and was found to be induced in mouse skin after CB treatment. In accordance to the microarray results, *PRG4* mRNA expression was induced about +3500 % in 3T3 mouse fibroblasts after 24 hours of DEX treatment. In human samples (NHDF, dermal compartment of AST-2000 and FTSM), *PRG4* mRNA was not detectable.

Tnmd is described to be expressed by fibroblasts (Mendias et al., 2008). In *in vitro* systems, *TNMD* mRNA was not detectable neither in 3T3 cells, in NHDF nor in dermal samples of AST-2000 and FTSM.

Summarizing the data obtained from the hypothesis-free approach to identify novel read out parameters, four genes were found to be regulated in GC-treated mouse skin. Their expression patterns, however, could not be confirmed in different human and rodent *in vitro* monolayer cell culture systems (3T3 cells, NHDF, NHEK) with one exception (*PRG4*) and human *in vitro* 3D skin models (AST-2000, FTSM). Compared with the *in vivo* results, the selected genes were either not expressed *in vitro*, like *PRG4* or *TNMD* mRNA in human assays (NHDF, FTSM), or their regulation was different in the *in vitro* assays. *COL11A1* mRNA expression was repressed in CB-treated mouse skin, while it was induced in DEX-treated NHDF and 3T3 cells.

→ *Therefore, with the hypothesis-free approach, it was not possible to identify reliable novel parameters for GC-induced skin atrophy that might be used* in vitro.

The selected cellular assays (chapter **4.1**) and identified read out parameters are summed up in **table 8**.

Tab. 8: Investigated assays and read out parameters.

Assay		**Read out**
in vitro monolayer	• HaCaT – immortalized human keratinocyte cell line • NHEK – primary normal human epidermal keratinocytes • 3T3 – mouse embryonic fibroblast cell line • rFib – primary rat dermal fibroblasts • NHDF – primary normal human dermal fibroblasts	• proliferation • mRNA expression of *COL1A1, COL3A1, COL4A1, COL5A1, COL7A1, P4HA1, P4HA2, P4HB, MMP1 / MMP13, MMP2, MMP3, MMP9* • protein secretion of human CICP, MMP-1, MMP-2, MMP-3, MMP-9 • epidermal thickness
in vitro 3D	• AST-2000 – advanced skin test • FTSM – full-thickness skin model	

4.3 Investigations of Test Systems Based on Monolayer Cell Cultures

HaCaT cells, NHEK, 3T3 mouse fibroblasts, rFib and NHDF were used as rodent and human cutaneous cellular assays. As read out parameters proliferation, mRNA and protein synthesis of collagen metabolism (collagens, P4h, MMPs) were analyzed (**Tab. 8**). In keratinocytes, the expression of MMPs was analyzed, while in fibroblasts additionally the expression of collagens and P4h subunits was studied. The test systems were screened with 1 µM DEX for a reproducible ($n \geq 3$) regulation more than 2-fold. As soon as the screening criteria were fulfilled, the test system was further characterized for 1.) dose-dependent gene regulation, 2.) correlation with topical GCs of known classification (tested with HC, PC, MF, CB), and 3.) correlation with distinct atrophogenic potentials of GCs of the same class but with a different TIX (tested with MF, BMV). Thus, the cells were incubated with ascending concentrations of the selected GCs. Afterwards, statistical analyzes were performed using the paired t-test after Wilcoxon. If at least two of these three criteria were met by a test system, it was a defined as suitable test system for GC-induced skin atrophy.

DEX effects on the proliferation of 3T3 fibroblasts, NHDF, HaCaT cells and NHEK was determined by [^{3}H]-thymidine incorporation and Alamar Blue fluorometry. Menadione, a chemotherapeutic and cytostatic agent was used as positive control. Test systems were initially optimized regarding culture conditions, such as cell number, duration of cell adhesion, cell passage, serum concentration, cell culture medium, duration of treatment, detection methods and medium change with or without washing with PBS.

GC effects on mRNA expression were measured by RT-PCR. HaCaT cells, NHEK, 3T3 mouse fibroblasts, rFib and NHDF were treated for 2, 4, 6 and 24 hours with DEX. The regulation of mRNA expression after 2, 4 and 6 hours of DEX treatment was under the defined threshold of 2-fold (data not shown). Only after 24 hours treatment time, the regulation became evident as the expression level after GC application was less than -50 % compared to DMSO-treated control (0 %). Thus, in subsequent experiments gene expression analysis was performed after a 24-hour period of DEX treatment in all monolayer cell systems tested (see also **Appendix Tab. 20**).

4.3.1 HaCaT Cells

4.3.1.1 Proliferation

After optimization the culture conditions regarding the above mentioned aspects (see above), the maximum inhibiting effect of DEX were found in 1000 seeded cells / cm² treated for 7 days with medium change and compound application every other day. At the end of the experiment the proliferation was measured with [^{3}H]-thymidine incorporation. But the maximum effect obtained with 10 µM DEX was very low with -13 ± 7 % (n=5) relative to vehicle treatment and difficult to confirm. In comparison to the positive control menadione at an equimolar concentration resulted in -86 ± 8 % (n=5) change relative to vehicle treatment.

→ *This test system was not further characterized as there were no reproducible DEX effects measurable under the defined conditions.*

4.3.1.2 mRNA Expression

In the keratinocyte cell line HaCaT, *MMP2* and *MMP9* mRNA expression were investigated. DEX treatment resulted in a change of -41 % for *MMP2* mRNA and -35 % *MMP9* mRNA expression compared to vehicle treatment (**Tab. 9**). This change is below the defined threshold of a 2-fold regulation. Thus, no DEX-induced regulation of *MMP2* and *MMP9* mRNA expression was detected in HaCaT cells.

→ *No further characterizations were performed with HaCaT cells as the tested mRNA expression was not found to be regulated by DEX.*

Tab. 9: DEX-dependent regulation of mRNA expression in HaCaT cells. Keratinocytes were treated for 24 hours with 0.1 % DMSO and with or without 1 µM dexamethasone. Relative regulation compared to DMSO [%] is given as mean ± SD (n=3), DMSO control equates 0 %. n.t. = not tested.

Gene	Change [%]
MMP1	n.t.
MMP2	-41 ± 7
MMP3	n.t.
MMP9	-35 ± 14

4.3.2 Normal Human Epidermal Keratinocytes (NHEK)

4.3.2.1 Proliferation

The proliferation experiments with primary normal human epidermal keratinocytes were performed under similar conditions as the proliferation experiments with the HaCaT cells. A cell number of 1000 cells / cm² was seeded and after a 7-day cultivation period with 10 µM DEX treatment every other day the proliferation was measured by [^{3}H]-thymidine incorporation. The DEX-treated cells proliferated -3 ± 1 % (n=3) less compared to vehicle treated cells.

→ *With NHEK it was not possible to establish a reliable proliferation inhibition test system for characterization of test compounds.*

4.3.2.2 mRNA / Protein Expression

MMP1, *-2*, *-3* and *-9* mRNA expression were investigated in NHEK treated for 24 hours with DEX. A strong DEX-dependent repression of about -76 to -65 % of all investigated MMP mRNAs was detected (**Tab. 10**). Additionally, the protein secretion of MMP-1 into medium was measured after 24 and 48 hours of 1 µM DEX incubation (data not shown). The change of MMP-1 was less pronounced compared to the effects at the mRNA level (-20 ± 7 % reduced after 24 hour-DEX treatment, n=5).

Tab. 10: DEX-dependent regulation of mRNA expression in NHEK. Primary keratinocytes were treated for 24 hours with 0.1 % DMSO and with or without 1 µM dexamethasone. Relative regulation compared to DMSO [%] is given as mean ± SD (n=3), DMSO control equates 0 %. n.t. = not tested.

Gene	Change [%]
MMP1	–76 ± 3
MMP2	–66 ± 3
MMP3	–75 ± 8
MMP9	–65 ± 3

As the mRNA expression of *MMP1*, *MMP2*, *MMP3* and *MMP9* was strongly and reproducibly repressed in DEX-treated NHEK, this test system was further characterized for its predictability for GC-induced skin atrophy.

Further Investigations with GC Panel

Dose-dependency. NHEK were treated for 24 hours with increasing concentrations of CB and *MMP1*, *-2*, *-3* and *-9* mRNA expression were determined. In the following, as the regulation pattern of *MMP1* mRNA expression was similar to those of *MMP2*, *-3* and *-9*, only *MMP1* is described representatively (**Fig. 3**). 0.1 nM CB had no effect on *MMP1* mRNA expression, while increasing concentrations of this GC resulted in an increased inhibition of *MMP1* mRNA expression (**Fig. 3**). The maximum inhibitory effect of -54 % was detected after treatment with 10 nM CB.

Correlation with GC classification. The classical GCs HC (weak GC), PC (moderate GC), MF (strong GC) and CB (very strong GC) inhibited *MMP1* mRNA expression in NHEK with distinct potencies of 19, 12, 4.4 and 0.7 nM, respectively (**Fig. 3**). The IC_{50} of these four GCs were significant distinguishable from each other according to GC classes (**Tab. 11**). The expression of *MMP2*, *-3* and *-9* mRNAs was GC-repressed like *MMP1* mRNA.

Correlation with TIX. Cells were treated with two class III GCs (MF, BMV), which different atrophogenic potentials are indicated by different TIX. So, BMV is known to show a higher atrophy potential than MF in human skin. *MMP1* mRNA expression was inhibited by BMV with an IC_{50} of 2.3 nM. BMV was about 2-fold more potent than MF (4.4 nM) in inhibiting *MMP1* mRNA expression (**Fig. 3**). Although these differences were not statistically significant (**Tab. 11**), it suggests that differentiation of GCs from the same class with different atrophogenicity may be possible. *MMP2*, *-3* and *-9* mRNA expression were repressed like *MMP1* mRNA expression by BMV and MF.

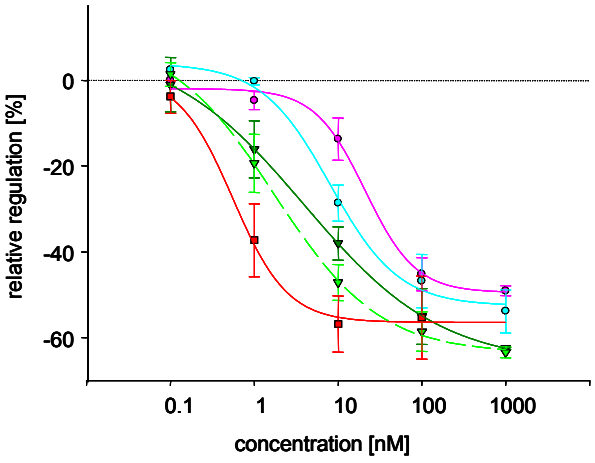

IC_{50} [nM]	*MMP1*	*MMP2*	*MMP3*	*MMP9*
HC	19 ± 6	23 ± 6	25 ± 5.	83 ± 8
PC	12 ± 5	8.8 ± 1.9	8.8 ± 0.9	9.9 ± 2.4
MF	4.4 ± 2.8	4.7 ± 1.9	3.7 ± 2.6	4.1 ± 2.8
BMV	2.3 ± 0.8	2.7 ± 0.5	2.1 ± 1.4	3.3 ± 2.5
CB	0.7 ± 0.2	0.7 ± 0.6	0.3 ± 0.02	0.6 ± 0.1

Fig. 3: Dose-dependent and compound-specific repression of MMP mRNA expression in NHEK after GC treatment. After adhesion over night cells were treated with ascending concentration of classical GCs for 24 hours and mRNA expression of *MMP1*, *-2*, *-3* and *-9* was determined by RT-PCR as described in Material and Methods. Regulation of *MMP1* mRNA expression is representative for *MMP2*, *-3* and *-9* mRNA expression. The regulation relative to DMSO control is given in % and the resultant IC_{50} of GC-treated vs. DMSO-treated cells is given in the table as mean ± SD (n=5). Dotted line indicates DMSO control. HC – hydrocortisone, PC – prednicarbate, MF – mometasone furoate, BMV - betamethasone-17-valerate, CB – clobetasol-17-propionate.

Tab. 11: Results of statistical analysis of MMP mRNA expression in NHEK. Cells were treated once for 24 hours with classical GCs at ascending concentrations (5 experiments). MMP mRNA expression was analyzed by RT-PCR and resulted IC50 for every GC. Results of the paired t-Test to estimate variations of GC treatment among each other are given as p-values (* ≤ 0.5, ** p ≤ 0.01, *** p ≤ 0.001)

MMP1	PC	MF	BMV	CB
HC	*	*	**	**
PC		*	*	**
MF			0.114	*
BMV				0.063

MMP2	PC	MF	BMV	CB
HC	*	**	**	**
PC		**	**	**
MF			0.091	*
BMV				*

MMP3	PC	MF	BMV	CB
HC	**	***	***	***
PC		*	***	***
MF			0.060	*
BMV				0.059

MMP9	PC	MF	BMV	CB
HC	***	***	***	***
PC		*	*	***
MF			**	*
BMV				0.104

→ *The inhibition of* MMP1, -2, -3 *and* -9 *mRNA expression in NHEK was dose-dependent, compound-specific and correlated well with the GC classes. Moreover, it seemed to reflect the different atrophogenic potentials of GC of one class but with a different TIX. Thus, the criteria for a suitable test system are fulfilled. This test system is proposed to be used to determine the atrophogenic potential of GCs.*

4.3.3 3T3 Mouse Fibroblasts

4.3.3.1 Proliferation

After optimizing 3T3 cell system the maximum DEX effect on 3T3 fibroblast proliferation was detected by Alamar Blue fluorometry with 5000 cells / cm², treated for 3 days with a medium change and compound application every other day. Menadione was used as positive control and resulted in -81 ± 6 % (n=3) inhibition of proliferation relative to vehicle treatment. Application of 10 µ DEX led to -7 ± 7 % (n=5) change in proliferation. This was under the defined threshold of 2-fold regulation.

→ *There was no inhibition of proliferation by DEX treatment. Therefore, this test system was not further characterized.*

4.3.3.2 mRNA Expression

Collagens. The collagen mRNA expression was studied in DEX-treated 3T3 mouse fibroblasts after 24 hours. The mRNA expression of *COL1A1* and *COL3A1* was repressed of about -71 % and -69 %, respectively, whereas of *COL4A1* mRNA expression was induced of about +109 % by 1 µM DEX. *COL5A1* and *COL7A1* mRNA expression were not regulated by DEX (**Tab. 12**). The DEX-induced repression of *COL1A1* and *COL3A1* mRNA expression in 3T3 fibroblasts is clearly GR-mediated, because a parallel treatment of fibroblasts with DEX and the GR antagonist mifepristone (RU 486; **Fig. 4**) completely abolished the repression of collagen mRNA expression.

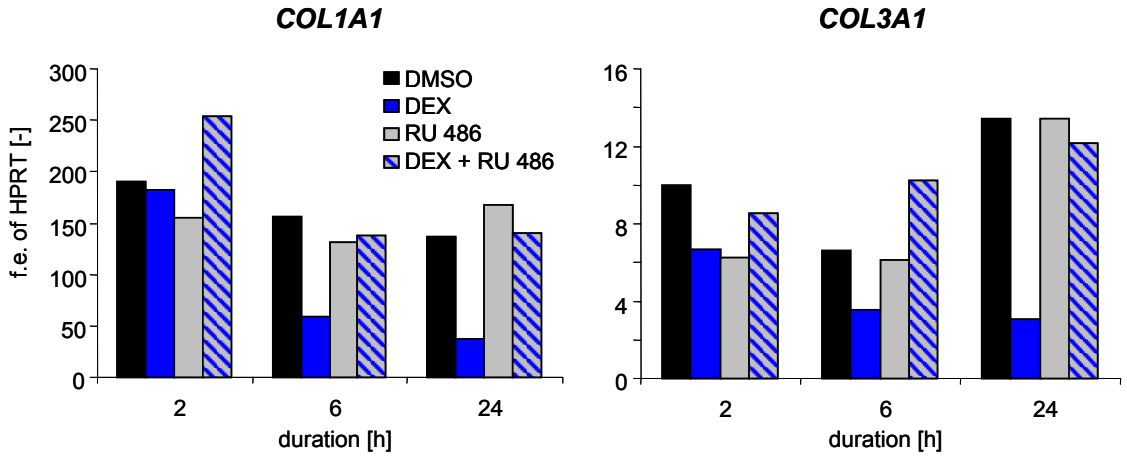

Fig. 4: Antagonizing DEX-induced *COL1A1* and *COL3A1* mRNA expression by treatment with RU 486 in 3T3 mouse fibroblasts. Cells were treated with 0.1 % DMSO and with or without 0.1 µM dexamethasone (DEX) and 1 µM RU 486 for 2, 6 and 24 hours. Collagen mRNA expression level is given as fold expression (f.e.) in relation to the house keeping gene HPRT. Results are representative for one out of three experiments.

MMPs. The expression of *MMP13* (rodent homolog of human MMP1), *MMP2* and *MMP3* mRNAs was analyzed in 3T3 cells treated with 1 µM DEX for 24 hours.

The mRNA of the rodent major collagenase MMP-13 was not detectable in 3T3 cells. The expression of *MMP2* mRNA was not regulated, while *MMP3* mRNA was strongly repressed of about -98 % after 1 µM DEX treatment compared to DMSO treatment (**Tab. 12**).

Prolyl-4-hydoxylase subunits. mRNA expression of the type I P4h subunits α1 and β was analyzed in 3T3 fibroblasts treated with 1 µM DEX for 24 hours. *P4HA1, P4HA2* and *P4HB* mRNA expression were not found to be regulated in 3T3 fibroblasts under the defined conditions (**Tab. 12**).

Tab. 12: DEX-dependent regulation of mRNA expression in 3T3 mouse fibroblasts. Cells were treated for 24 hours with 0.1 % DMSO and with or without 1 µM dexamethasone. Relative regulation compared to DMSO [%] is given as mean ± SD (n=3), DMSO control equates 0 %. n.d. = not detected, n.t. = not tested.

Gene	Change [%]
COL1A1	–71 ± 2
COL3A1	–69 ± 6
COL4A1	+110 ± 50
COL5A1	–20 ± 10
COL7A1	–30 ± 10
MMP1	n.d.
MMP2	–35 ± 4
MMP3	–98 ± 2
MMP9	n.t.
MMP13	n.d.
P4HA1	–27 ± 7
P4HA2	–18 ± 6
P4HB	–11 ± 8

COL1A1 and *COL3A1* mRNA expression were reproducibly inhibited more than 2-fold by GCs in 3T3 mouse fibroblasts. Thus, this test system will be further investigated.

Further Investigations with GC Panel

Dose-dependency. Treatment with increasing concentrations of CB resulted in an increased inhibition of *COL1A1* and *COL3A1* mRNA expression in 3T3 mouse fibroblasts. In the following, as the regulation pattern of *COL1A1* mRNA expression was similar to those of *COL3A1*, only *COL1A1* is described representatively (**Fig. 5**). Application of CB at concentrations ≤ 0.1 nM had no effects on *COL1A1* mRNA expression. The inhibitory CB-effect reached a maximum of -63 % at concentration ≥ 10 nM (**Fig. 5**).

Correlation with GC classification. The class I, III and IV GCs, HC, MF and CB displayed distinct potencies regarding the inhibition of *COL1A1* mRNA expression (IC_{50} = 92, 1.3 and 0.5 nM, respectively). The IC_{50} of these three GCs differed significantly from each other (**Tab. 13**). At equimolar concentrations (1 µM), the results were even more disparate; HC exhibited about -40 % decrease in *COL1A1* mRNA expression relative to control, while MF and CB exhibited both about -65 % decrease in *COL1A1* mRNA expression (**Fig. 5**). The repression activity correlated well with the classification system of topical GCs based on their potencies.

Correlation with TIX. The inhibitory effect of BMV on collagen mRNA expression in 3T3 cells was compared with MF-effects. Although of the same GC class, BMV is known to show a higher atrophy potential than MF in human skin. BMV displayed a potency of 1.3 nM with an efficacy of about -65 % for *COL1A1* mRNA expression (**Fig. 5**), whereas MF showed an IC_{50} of 2.9 nM. These differences were not significant (**Tab. 13**), however, it was possible to discriminate between these two GCs by trend.

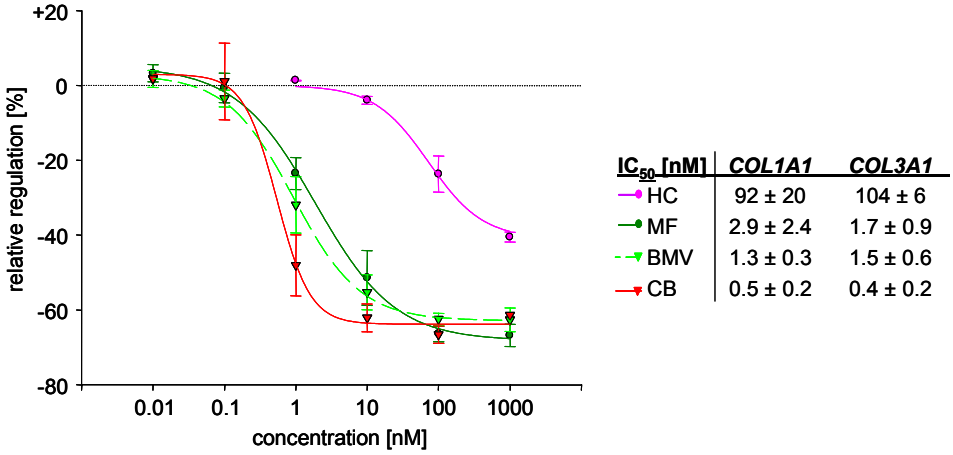

Fig. 5: Dose-dependent and compound-specific repression of collagen mRNA expression in 3T3 fibroblasts after GC treatment. After adhesion over night 3T3 cells were treated with ascending concentration of classical GCs for 24 hours and mRNA expression of *COL1A1* and *COL3A1* was measured by RT-PCR. Regulation of *COL1A1* mRNA expression is representative for *COL3A1* mRNA expression. The regulation relative to DMSO control is given in % and the resultant IC_{50} of GC-treated vs. DMSO-treated cells is given in the table as mean ± SD (n=5). Dotted line indicates DMSO control. HC – hydrocortisone, MF – mometasone furoate, BMV - betamethasone-17-valerate, CB – clobetasol-17-propionate.

Tab. 13: Results of statistical analysis of collagen mRNA expression in 3T3 fibroblasts. Cells were treated once for 24 hours with classical GCs at ascending concentrations (5 experiments). Collagen mRNA expression was analyzed by RT-PCR and resulted IC_{50} for every GC. Results of the paired t-Test to estimate variations of GC treatment among each other are given as p-values. (* ≤ 0.5, ** p ≤ 0.01, *** p ≤ 0.001)

COL1A1	MF	BMV	CB
HC	***	***	***
MF		0.176	*
BMV			0.073

COL3A1	MF	BMV	CB
HC	***	***	***
MF		0.184	*
BMV			*

→ *The mRNA expression of* COL1A1 *and* COL3A1 *in 3T3 mouse fibroblasts was dose-dependently repressed after GC treatment and correlated well with the GC classes. Additionally, differences in the atrophogenic potential of GCs from the same GC class but with a different TIX could be suggested. Thus, the test system met all criteria for a suitable test system that is predictive for GC-induced skin atrophy.*

4.3.4 Primary Dermal Rat Fibroblasts (rFib)

4.3.4.1 mRNA Expression

Collagens. As only *COL1A1* and *COL3A1* mRNA expression were found to be regulated in 3T3 fibroblast, these two collagens were analyzed in the following assays. In primary rat fibroblasts, no GC-dependent regulation of *COL1A1* and *COL3A1* mRNA expression was found after 24 hours of 1 µM DEX treatment (**Tab. 14**).

MMPs. In DEX-treated rFib, a regulation of *MMP2,-3* and *-13* mRNA expression was not detected (**Tab. 14**).

Prolyl-4-hydoxylase subunits. mRNA expression of the type I P4h subunits α1 and β was analyzed in rFib treated with 1 µM DEX for 24 hours (**Tab. 14**). None of the three subunits were found to be regulated more than 2-fold in rFib under the defined conditions.

→ *In rFib, the mRNA expression of the investigated read out parameter was not regulated under the defined conditions. Thus, test systems with rFib were not further characterized.*

Tab. 14: DEX-dependent regulation of mRNA expression in primary rat fibroblasts. Cells were treated for 24 hours with 0.1 % DMSO and with or without 1 µM dexamethasone. Relative regulation compared to DMSO [%] is given as mean ± SD (n=3), DMSO control equates 0 %. n.t. = not tested.

Gene	Change [%]
COL1A1	–12 ± 20
COL3A1	–10 ± 10
MMP2	–5 ± 5
MMP3	+19 ± 42
MMP9	n.t.
MMP13	–35 ± 18
P4HA1	–23 ± 10
P4HA2	+70 ± 22
P4HB	+26 ± 38

4.3.5 Normal Human Dermal Fibroblasts (NHDF)

4.3.5.1 Proliferation

Preliminary experiments with untreated NHDF resulted in a strong decrease of proliferation over time. For example, cells were seeded at a medium cell density of 5000 cells / cm² in fibroblast growth medium supplemented with 20 % CCS, the proliferation rate was detected with [^{3}H]-thymidine incorporation after 24, 48 and 72 hours and showed a decreased proliferation of -50 % after 48 hours and even -88 % after 72 hours relative to 24 hours of untreated cultivation. Proliferation experiments were repeated with other culture media, cell number, passage, serum amount and cells from other donors, and resulted in decreasing proliferation rates (data not shown).

→ *NHDF are not suitable at the investigated culture conditions to test anti-proliferative effects of compounds.*

4.3.5.2 mRNA Expression

Collagens. *COL1A1* and *COL3A1* mRNA expression were not found to be regulated in DEX-treated NHDF after 24 hours (**Tab. 15**). Experiments ending at other time points (4 and 48 hours) displayed also no regulation of these collagen mRNAs after 1 µM DEX treatment.

MMPs. In NHDF, *MMP1* and *-3* mRNA expression were repressed of about -66 % and -48 %, respectively after DEX treatment for 24 hours (**Tab. 15**). *MMP2* mRNA expression was not affected by DEX at the above mentioned time point. *MMP9* mRNA was not detected. Interestingly, the expression levels of *MMP1*, *-2* and *-3* mRNA in NHDF were much higher than in NHEK(data not shown).

Prolyl-4-hydoxylase subunits. *P4HA1*, *P4HA2* and *P4HB* mRNA expression were not found to be regulated more than 2-fold in NHDF treated with 1 µM DEX for 4 and 24 hours (**Tab. 15**).

Tab. 15: DEX-dependent regulation of mRNA expression in primary human fibroblasts. Cells were treated for 24 hours with 0.1 % DMSO and with or without 1 µM dexamethasone. Relative regulation compared to DMSO [%] is given as mean ± SD (n=3), DMSO control equates 0 %. n.t. = not tested.

Gene	Change [%]
COL1A1	–10 ± 20
COL3A1	–10 ± 10
MMP1	–66 ± 9
MMP2	+2 ± 7
MMP3	–48 ± 10
MMP9	n.d.
P4HA1	–13 ± 6
P4HA2	–35 ± 39
P4HB	–4 ± 25

→ *The detected inhibition of* COL1A1 *and* COL3A1 *mRNA expression in 3T3 fibroblasts was not detected in NHDF. Solely* MMP1 *mRNA expression was reproducibly inhibited GC-dependently more than 2-fold.*

4.4 Investigations of Test Systems Based on 3D Cell Cultures

In a further step, investigations on the full thickness skin equivalents AST-2000 and FTSM were performed. In these skin models, keratinocytes are arranged in multilayered cell structures and therefore, epidermal thickness can be determined by counting the single cell layers in histological sections. A reduced number of cell layers should indicate epidermal atrophy. As epidermal atrophy is an important part of skin atrophy, this parameter was investigated.

A mechanism of GC-induced epidermal atrophy is the inhibition of keratinocyte proliferation by GCs (Lange et al., 1997; Zöller et al., 2008). Ki-67 protein is a marker for cell proliferation (Onuma et al., 2001) as it is present during all active phases of cell division (G1, S, G2, and mitosis), but is absent from resting cells (G0). Thus, the number of proliferating cells in GC-treated skin equivalents were determined by Ki-67 staining of histological sections.

Results obtained in monolayer cell culture systems suggested that *COL1A1* and *COL3A1* as well as *MMP1*, *-2*, *-3* and *-9* might serve as convenient markers to predict the skin atrophy potential of test compounds. For that reason, it was of interest, whether GCs also affect these markers in the 3D skin models at the mRNA and at the protein level.

Firstly, the GC-dependent alteration of epidermal thickness, proliferation and collagen and MMP synthesis was investigated in screening experiments. Therefore, 0.1 µM CB was daily applied into the culture medium of AST-2000 and FTSM, respectively, and the read out parameters were screened for a regulation more than 2-fold. For a direct comparison of both skin models, a head-to-head comparison was performed.

After the screening experiments −similar to the monolayer test systems− the test systems were further characterized for their predictability of the known clinical effects of GC-induced skin atrophy: 1.) Dose-dependent effects of GCs were evaluated by application of GCs at two different concentrations. 2.) Correlation with the classification of topical GCs was evaluated by applying HC (class I), PC (class II), MF (class III) and CB (class IV) at equipotent concentrations. If both criteria were met, the test system was seen as suitable to determine the atrophogenic potential of GC.

4.4.1 Advanced Skin Test (AST-2000)

4.4.1.1 Epidermal Thickness

In pilot studies with untreated AST-2000 on day 0, this skin equivalent appeared as not convenient to determine epidermal thinning due to the following two reasons: 1.) The epidermal compartment consisted of only 3-6 keratinocyte layers after arrival from the manufacturer (**Fig. 6 A**). 2.) As the model is very fragile, the histological preparation resulted repeatedly in either detachment of the epidermis from the dermis in cryo-conserved samples or in unexpected compression of the epidermis in paraffin-embedded samples (**Fig. 6 B**).

→ *As an adequate histological preparation was not possible even with untreated AST-2000, histological analysis of this model in general were not further performed.*

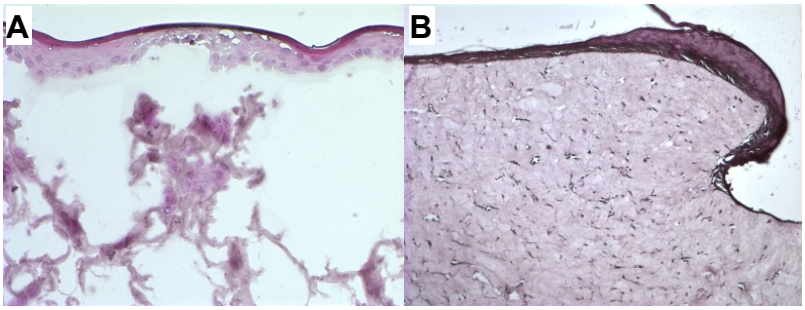

Fig. 6: Histological slides from untreated AST-2000 on day 0. A: Detachment of keratinocyte layers from the dermal compartment in cryo-conserved sections. **B**: Compression of the epidermis attached to the dermis in paraffin-embedded sections. H&E staining. Magnification: 10x.

4.4.1.2 mRNA / Protein Expression

Collagens. The *COL1A1* and *COL3A1* mRNA expression were determined in the dermal compartment. The secretion of C-terminal propeptide of collagen type I (CICP), that indicates the collagen *de novo* synthesis, was investigated in the supernatant.

In AST-2000 treated for 4 hours, 1, 3 and 12 days with the vehicle (0.01 % DMSO) displayed strong inhibitory effects on *COL1A1* mRNA expression and CICP secretion, while 0.1 µM CB had no additional effect on these parameters (exemplarily shown on day 12 **Fig. 7**).

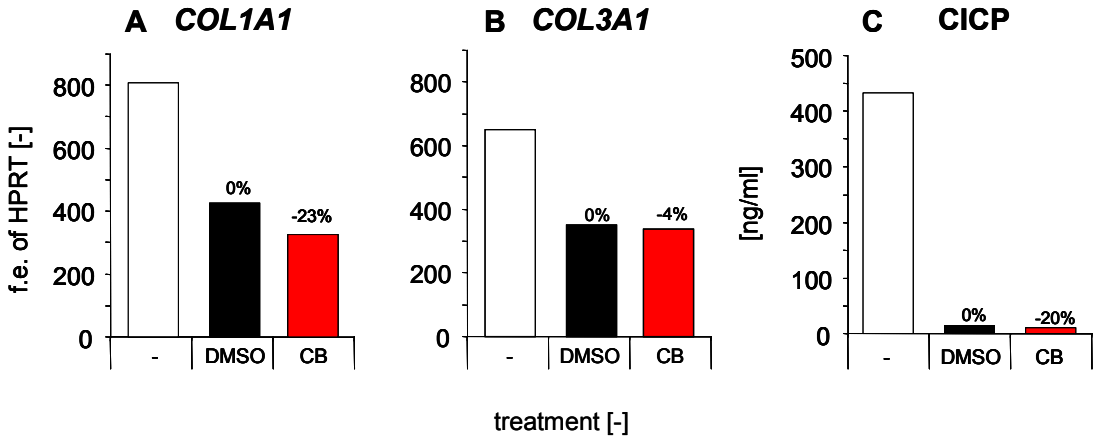

Fig. 7: Collagen synthesis in AST-2000 on day 12. Skin equivalents were treated daily with medium only (-), vehicle (0.01 % DMSO) or 0.1 µM clobetasol-17-propionate (CB). mRNA expression of *COL1A1* (**A**) and *COL3A1* (**B**) were measured in the dermal compartment, while type I C-terminal collagen propeptide (CICP) secretion (**C**) was detected in the medium as described in Material and Methods. Expression level of mRNA is given as fold expression (f. e.) relative to the house keeping gene HPRT. Single values of one experiment with AST-2000. Inhibition by compound treatment relative to control is given in %. Similar results were seen after 4 and 24 hours, 3 and 8 days of treatment.

MMPs. Vehicle- and CB-effects on MMP synthesis were investigated in AST-2000. *MMP1* and *-3* mRNA expression were determined in the epidermal and dermal compartment. Secretion of MMP-1 protein was determined in the supernatant.

The vehicle DMSO displayed strong inducing effects on expression of *MMP1* and *MMP3* mRNA in epidermal and dermal samples after 4 hours and 1, 3 and 12 days of treatment relative to medium-treated control. Furthermore, the CB-induced regulation of *MMP1* and *-3* mRNA expression in epidermis and dermis of AST-2000 was not reproducible (n=4). Even duplicates within one experiment showed strong variations in *MMP1* and *MMP3* mRNA expression (**Fig. 8 A-E**). At the protein level, strong DMSO-effects as well as intra-assay variations were also observed for MMP-1 (**Fig. 8 C**).

→ *With regard to the strong regulatory vehicle effects observed for collagen and MMP synthesis, these read out parameters were not further characterized in AST-2000.*

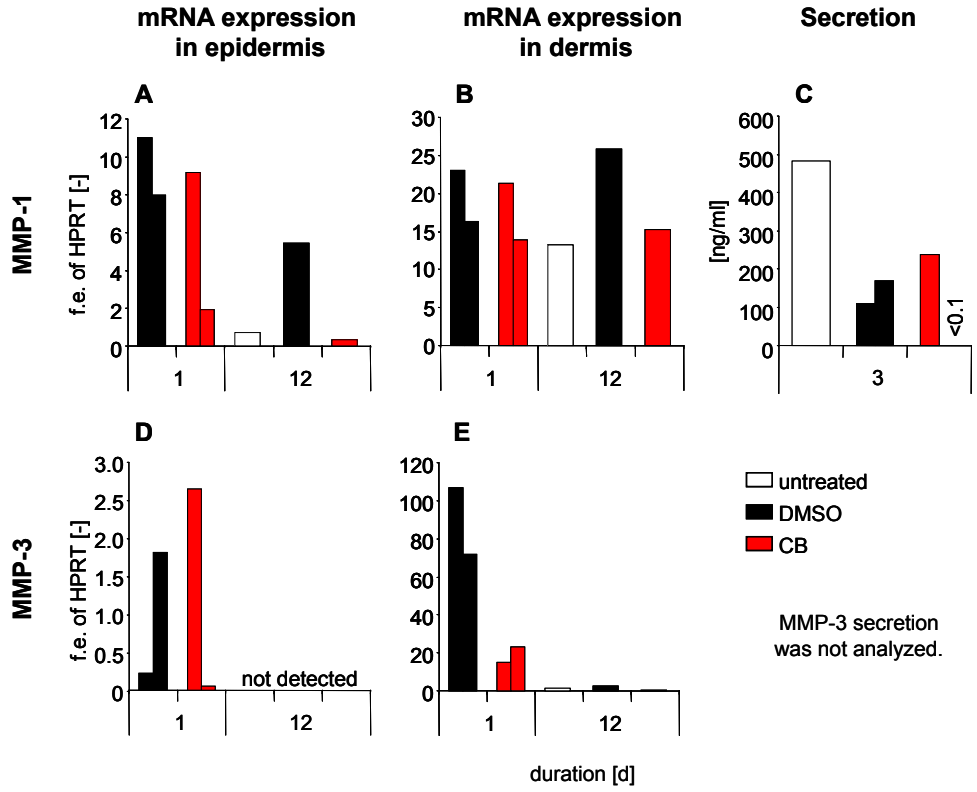

Fig. 8: Expression of MMP-1 and MMP-3 in AST-2000 after daily treatment with CB. AST-2000 was treated daily with medium only (-), vehicle (0.01 % DMSO) or 0.1 µM clobetasol-17-propionate (CB). mRNA expression of *MMP1* (**A, B**) and *MMP3* (**D,E**) was measured in the epidermal and dermal compartment after 1 (duplicates) and 12 days (single value) of treatment by RT-PCR as described in Material and Methods. Expression level of mRNA is given as fold expression (f. e.) relative to the house keeping gene HPRT. MMP-1 secretion into medium (**C**) was determined on day 3 by ELISA. One bar indicates the expression level of one sample.

4.4.2 Full-thickness Skin Model (FTSM)

4.4.2.1 Epidermal Thickness

Pilot investigations displayed FTSM as an appropriate model to detect epidermal thinning in general: 1.) The epidermal compartment of untreated FTSM consisted of 13-16 cell layers after arrival on day 0. 2.) The preparation of sections for histological examination was found to be much easier and feasible compared to the preparation of AST-2000.

Daily treatment of FTSM led to an increased epidermal atrophy on day 6 and day 12. The number of keratinocyte layers was reduced of about -32 % on day 6 and of about -75 % on day 12 by treatment with 0.1 µM CB (**Fig. 9**).

The epidermal thickness in FTSM was reduced more than 2-fold after a 12-day period of treatment with CB. Thus, this test system was further characterized for its suitability as skin atrophy model.

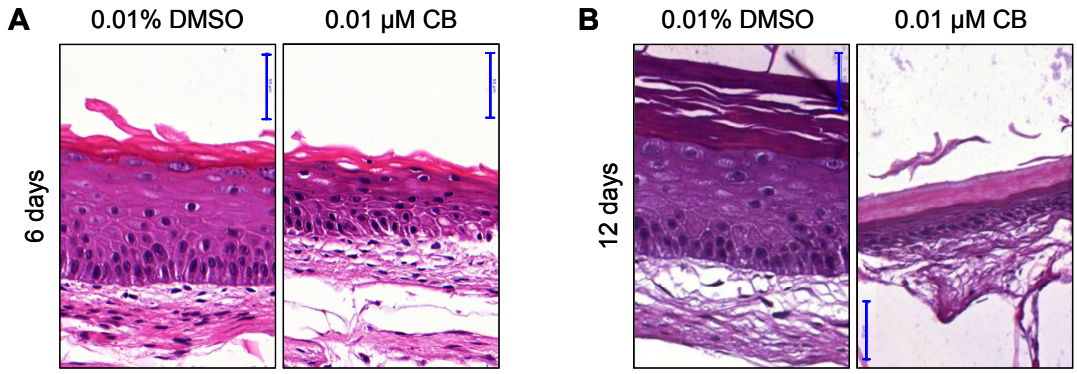

Fig. 9: Epidermal atrophy in CB-treated FTSM. Medium was changes daily and 0.1µM clobetasol-17-propionate (CB) added to the medium. The number of keratinocyte layers was counted on day 6 (**A**) and 12 (**B**). H&E stain of paraffin-embedded FTSM, blue scale = 50µm.

Further Investigations with GC Panel

Equi-efficiency. The regulation of read out parameters by different compounds in FTSM was investigated at anti-inflammatory equi-effective concentrations. These concentrations were defined in previous experiment with THP-1 cells (**Tab. 16**) and adapted to FTSM (see Material and Methods). To confirm, whether the chosen concentration were equi-effective in inhibition of pro-inflammatory cytokine secretion, the IL-1β, IL-6 and IL-8 secretion into medium of GC-treated FTSM was determined. IL-6 secretion, for example, was reduced about approximately -46 % by 1 µM HC, 0.7 µM PC, 0.005 µM MF and 0.01 µM CB compared to vehicle control (**Fig. 10**). Similar results were obtained for IL-1β and IL-8 secretion (data not shown). The GCs at the mentioned concentrations had similar effects on the cytokine secretion and thus, 1 µM HC, 0.7 µM PC, 0.005 µM MF and 0.01 µM CB are equi-effective with regard to anti-inflammatory effects. Thus, in FTSM, the atrophogenic effects of the GCs were determined at these concentrations.

Tab. 16: Anti-inflammatory activity of GCs in THP-1 cells. Cells were treated with GCs as described in Material and Methods. IL-8 concentration was determined in the supernatant by ELISA. The potency of the GCs is shown as IC_{50} [nM]. The efficacy [%] of the GCs is given in relation to the reference DEX and its maximum effect was set to 100 % inhibition of LPS-induced IL-8 secretion.

Glucocorticoid	IC_{50} [nM]	Efficacy [%]
hydrocortisone	7.4	94
prednicarbate	4.4	90
mometasone furoate	0.03	101
clobetasol-17-propionate	0.06	100

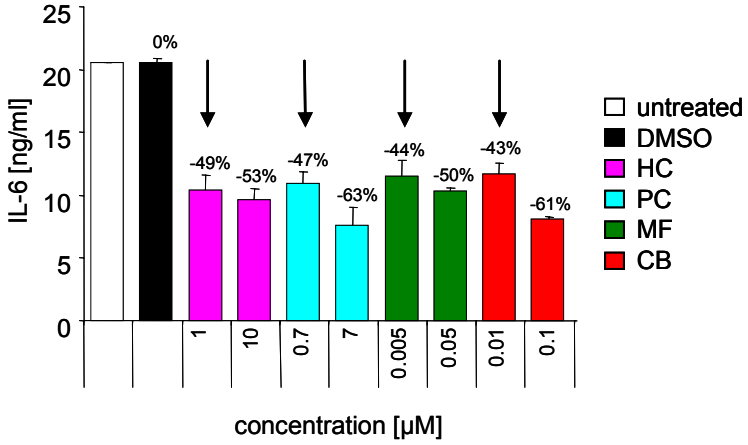

Fig. 10: Anti-inflammatory potential of GCs in FTSM. FTSM medium was changed daily and supplemented with GCs dissolved in 0.01 % DMSO. IL-6 secretion was measured in the supernatants after treatment for 3 days as described in Material and Methods. Mean ± SD, duplicates in one experiment. Arrows indicate equipotent concentrations of GCs. Inhibition by compound treatment relative to control is given in %. HC - hydrocortisone, PC - prednicarbate, MF - mometasone furoate, CB - clobetasol-17-propionate.

Dose-dependency. The atrophogenic effects of GCs on epidermal thickness were further characterized in FTSM. Treatment with 0.1 and 0.001 µM CB induced epidermal thinning in a dose-dependent manner (**Fig. 11**). The higher concentrated CB reduced the number of epidermal layers about -75 %, while the lower dosed CB reduced the layers about -64 % on day 12.

Correlation with GC classification. Application for 12 days of 1 µM HC, 0.7 µM PC, 0.005 µM MF and 0.01 µM CB reduced the number of keratinocyte layers of about -23 %, -31 %, -45 % and -64 %, respectively, relative to control (**Fig. 11 A+B**). Non-overlapping Fieller confidence intervals (see Material and Methods) indicated significant differences between GCs (**Fig. 11 C**).

→ *Epidermal atrophy in FTSM was dose-dependently and correlated with GC classes. Thus, the detection of epidermal thickness in FTSM seems to be a suitable test system to determine atrophogenic GCs effects.*

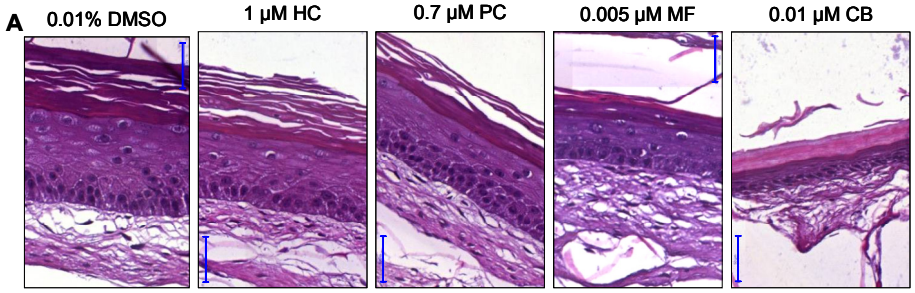

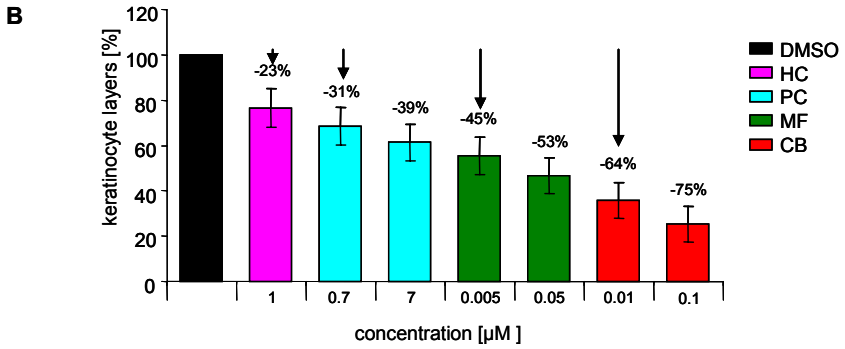

C

	1 µM HC	0.7 µM PC	0.005 µM MF	0.01 µM CB
0.01 % DMSO	*	*	*	*
1 µM HC			*	*
0.7 µM PC				*
0.005 µM MF				*

Fig. 11: GC-induced epidermal atrophy in FTSM on day 12. Increasing concentrations of GCs were daily added to growth medium. Medium was changed daily. H&E stained histological sections indicate effects of GCs on the epidermis (**A**). The number of keratinocyte layers was determined at 5 different areas on 3 non-consecutive sections. According to Fieller, statistical analysis of epidermal cell layers was performed (see Material and Methods) and resulted in mean inhibition ± upper and lower confidence level, n=2 (**B**). No overlap of the confidence intervals indicates significant differences shown by * between the treatment groups (**C**). Blue scale = 50µm, HC – hydrocortisone, PC – prednicarbate, MF – mometasone furoate, CB – clobetasol-17-propionate. Arrows indicate anti-inflammatory equipotent concentrations of GCs.

4.4.2.2 Proliferation

In FTSM, the amount of Ki-67 positive cells in the stratum basale was drastically reduced by GC treatment for 12 days. DMSO-treated epidermis displayed in average 16.3 ± 4.8 proliferating cells per 600 µm stratum basale (counted in 6 non-consecutive sections per sample, n=2), while treatment with 0.1 µM CB resulted in no proliferating keratinocytes in histological sections (data not shown). Consequently, as the proliferation was strongly reduced by CB, this parameter was further investigated.

Further Investigations with GC Panel

Correlation with GC classification. FTSM were treated daily with 1 µM HC (class I), 0.7 µM PC (class II) and 0.005 µM MF (class III). Treatment with HC, a mild GC, resulted in 6.7 ± 2.6 proliferating cells. That is 41 % less proliferating cells compared to vehicle treated control. Treatment with the more potent GCs PC and MF resulted in 0-1 proliferating cells (**Fig. 12**), which is an inhibition of about -100 %. The results confirm that epidermal atrophy might be partly caused by inhibited proliferation of keratinocytes. However, it was not possible to discriminate between effects of GCs of different GC classes.

→ *As no differentiation between the GC at the applied concentrations was possible, this determination of proliferating cells in GC-treated FTSM seems not convenient to predict atrophogenic potential of GCs.*

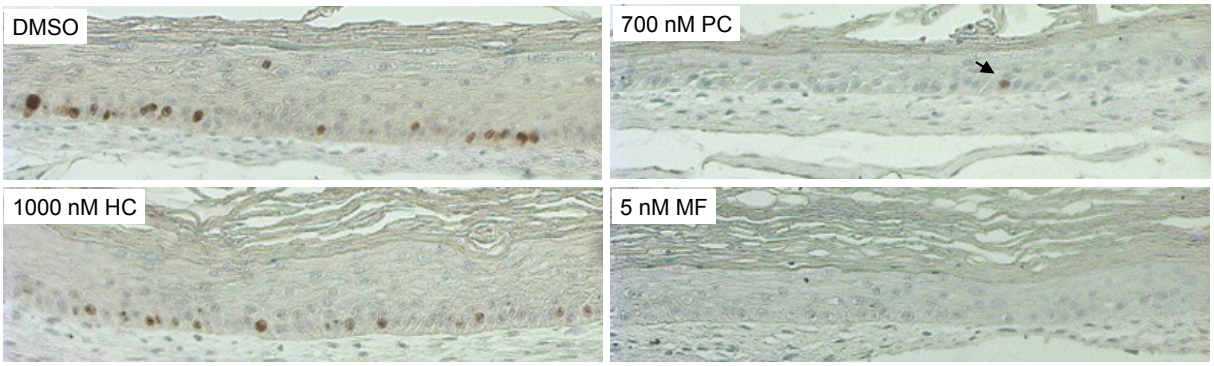

Fig. 12: GC-dependent reduction of Ki-67 positive cells in the stratum basale of FTSM. Skin models were treated daily with 0.01 % DMSO or GC for 12 days; afterwards samples were paraffin-embedded and sections were stained for Ki-67 positive cells. Samples treated with PC or MF showed only zero to one Ki-67 positive cell (arrow) in a whole section. Stained section of FTSM treated with MF is exemplarily shown for CB treatment. 20x magnification. HC – hydrocortisone, PC – prednicarbate, MF – mometasone furoate.

4.4.2.3 mRNA / Protein Expression

Collagens. *COL1A1* and *COL3A1* mRNA expression were reduced in FTSM treated with 0.1 µM CB for 3, 6 and 12 days. On day 12, the *COL1A1* and *COL3A1* mRNA expression were reduced of about -81 % and -80 %, respectively by 0.1 µM CB (**Fig. 7 D, E**). CICP secretion was only found to be reduced after a 12-day treatment period (**Fig. 7 F**).

As the screening criterion of a regulation more than 2-fold was fulfilled for collagen synthesis, *COL1A1* and *COL3A1* mRNA expression and CICP secretion were further characterized with a GC panel.

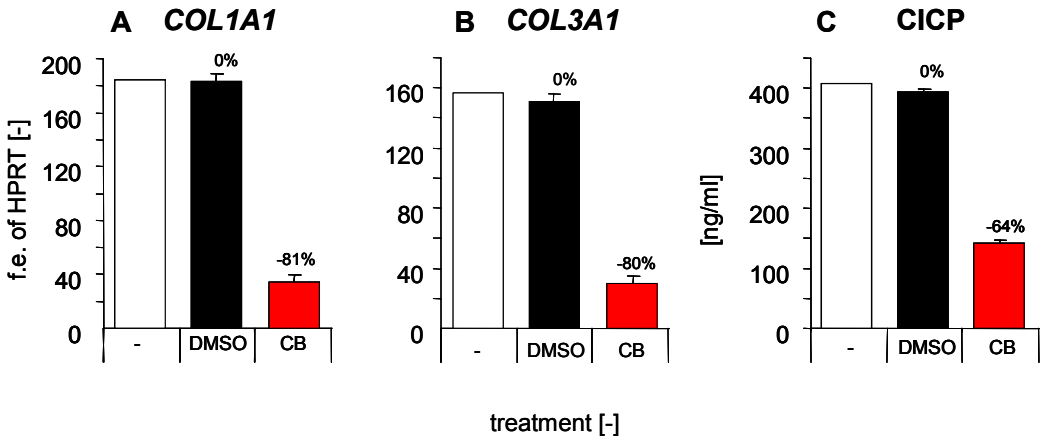

Fig. 13: Collagen synthesis in FTSM on day 12. Skin equivalents were treated daily with medium only (-), vehicle (0.01 % DMSO) or 0.1 µM clobetasol-17-propionate (CB). mRNA expression of *COL1A1* (**A**) and *COL3A1* (**B**) were measured in the dermal compartment, while type I C-terminal collagen propeptide (CICP) secretion (**C**) was detected in the medium as described in Material and Methods. Expression level of mRNA is given as fold expression (f. e.) relative to the house keeping gene *HPRT*. Mean ± SD of duplicates in one experiment with FTSM. Inhibition by compound treatment relative to control is given in %.

Further Investigations of Collagen Synthesis with GC Panel

Dose-dependency. Treatment with 0.1 and 0.01 µM CB inhibited *COL1A1* and *COL3A1* mRNA expression in dermal compartment of FTSM on day 12 dose-dependently. CB at the higher concentration reduced the mRNA expression of both collagens about -80 % relative to the vehicle, while the less concentrated CB reduced the expression levels about -64 % (**Fig. 14 A, B**). CICP secretion was tended to be dose-dependently regulated by CB.

Correlation with GC classification. FTSM were treated daily for 12 days with classical GCs at anti-inflammatorily equi-effective concentrations (1 µM HC, 0.7 µM PC, 0.005 µM MF, 0.01 µM CB, see chapter **4.4.2.1**). GC treatments inhibited compound-specifically all three parameters of collagen synthesis on day 12 (**Fig. 14**). *COL1A1* mRNA expression was inhibited by anti-inflammatory equi-effective doses of HC, PC, MF and CB relative to control of about -19 %, -33 %, -58 % and -64 %,

respectively. Similar results were obtained for the repression of *COL3A1*. These mRNA data were also confirmed at the protein level by determining CICP secretion. Thus, the detected effects of the standard GCs correlated well with their classification.

→ *The collagen synthesis in FTSM was dose-dependently repressed by GCs and correlated with the different GC classes. Therefore, this test system seems to be appropriate to determine the atrophogenic potentials of GCs.*

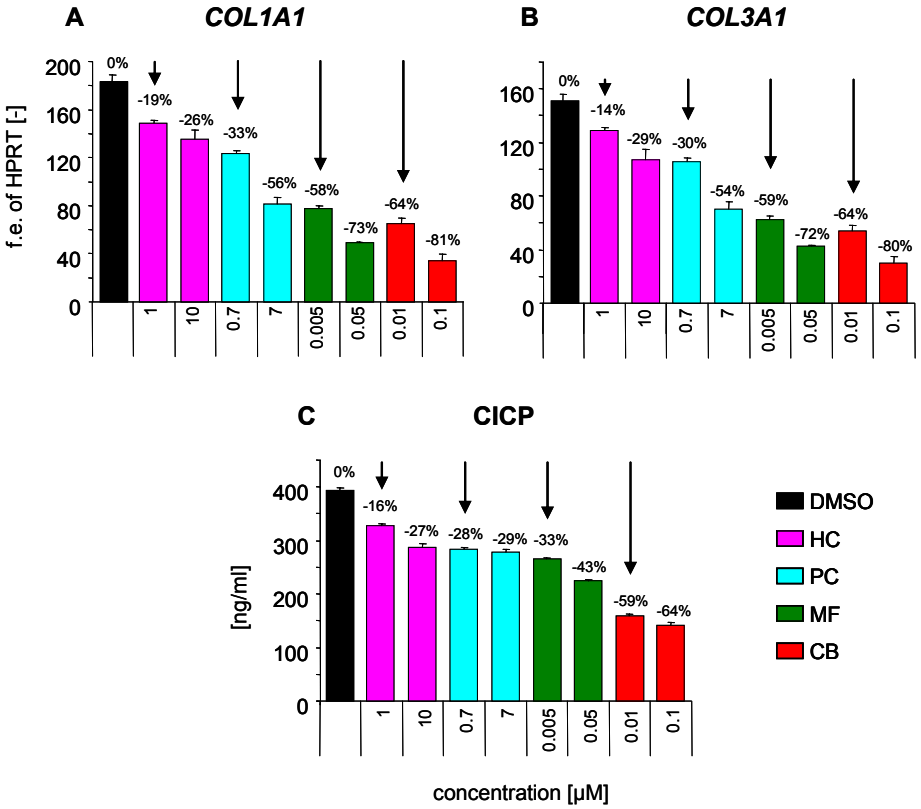

Fig. 14: Repression of collagen synthesis in GC-treated FTSM. Skin models were incubated with culture medium supplemented with GCs dissolved in 0.01 % DMSO. Medium was changed daily. Collagen synthesis was analyzed after 12 days of treatment. mRNA expression of *COL1A1* (**A**) and *COL3A1* (**B**) was detected in the dermal compartment by RT-PCR. Expression level of mRNA is given as fold expression (f. e.) relative to the house keeping gene *HPRT*. CICP secretion was determined in medium by ELISA (**C**). Mean ± SD, duplicates in one experiment with FTSM. Arrows indicate anti-inflammatory equi-effective concentrations of GCs tested. Inhibition by compound treatment relative to control is given in %. CICP – type I C-terminal collagen propeptide, HC – hydrocortisone, PC – prednicarbate, MF – mometasone furoate, CB – clobetasol-17-propionate.

MMPs. In screening experiments, CB-effects on MMP synthesis were also investigated in FTSM. *MMP1*, *-2*, *-3* and *-9* mRNA expression were determined in both epidermal and dermal compartments of the FTSM. Secretion of MMP-1, MMP-3 and MMP-9 protein was determined in the supernatant.

In FTSM, MMP-1 and MMP-3 synthesis was strongly repressed by CB (**Fig. 15**). *MMP1* and *MMP3* mRNA expression in the epidermal and dermal layer were inhibited time-dependently after GC treatment for 1, 3, 6 and 12 days (data exemplarily shown for day 1 and 12 in **Fig. 15 A, B, D, E**). The time-dependent reduction of epidermal mRNA expression of *MMP3* was so strong, that no *MMP3* mRNA was detectable on day 12 (**Fig. 15 D**). Comparable with the mRNA results, a reduction of MMP-1 and MMP-3 secretion of about -76 % and -66 %, respectively was detected after 3 days of CB treatment in FTSM (**Fig. 15 C, F**). In general, mRNA expression levels of MMPs were higher in the dermal than in the epidermal compartment.

MMP2 and *MMP9* mRNA expression were not regulated neither in the epidermal nor in the dermal compartment after 1, 3, 6, and 12 days of treatment with 0.1 µM CB. MMP-9 secretion was also not found to be regulated on day 3 (data not shown).

The screening criterion of a more than 2-fold regulation was met by MMP-1 and MMP-3 synthesis in CB-treated FTSM, thus, the test systems were further characterized with the GC selection.

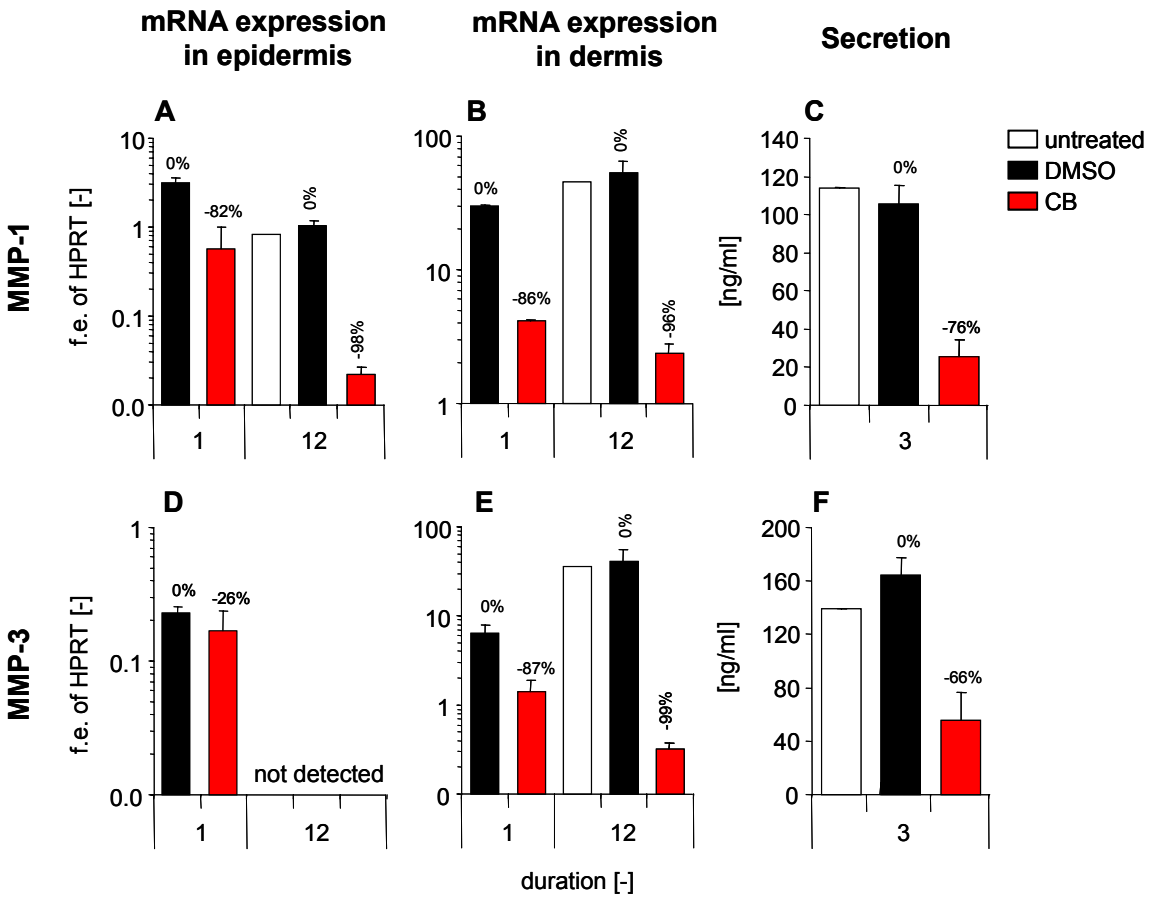

Fig. 15: Inhibition of MMP-1 and MMP-3 mRNA expression and secretion by CB in FTSM. Culture medium was changed daily and supplemented with 0.1 µM clobetasol-17-propionate (CB) dissolved in 0.01 % DMSO. mRNA expression of *MMP1* and *MMP3* was measured in the epidermal (**A, D**) and the dermal compartment (**B, E**) after 1 and 12 days of CB treatment by RT-PCR. Expression level of mRNA is given as fold expression (f. e.) relative to the house keeping gene *HPRT*. MMP-1 (**C**) and MMP-3 (**F**) secretion into the supernatant was measured on day 3 by MesoScale. Mean ± SD, duplicates of one experiment.

Further Investigations of MMP Synthesis with GC Panel

Dose-dependency. MMP-1 synthesis was strongly repressed after CB treatment compared to control. In the epidermal layer, *MMP1*mRNA expression was inhibited dose-dependently after a 12-day treatment with CB (**Fig. 16 A**). In contrast, *MMP1* mRNA expression in dermis was reduced to the maximum by CB at lower concentrations (**Fig. 16 C**). At the protein level, MMP-1 secretion was marginal dose-dependently reduced after a 3-day period of CB-treatment (**Fig. 16 E**).

Synthesis of MMP-3 was also repressed in FTSM after treatment with CB. The epidermal *MMP3* mRNA expression was undetectable in FTSM on day 12 as shown above (**Fig. 15, Fig. 16 B**). The dermal *MMP3* mRNA expression was reduced to the maximum by CB at lower concentrations and displayed no dose-dependent regulation (**Fig. 16 D**). However, a marginal dose-dependent repression by CB was observed for MMP-3 secretion on day 3 (**Fig. 16 F**).

Correlation with GC classification. MMP-1 synthesis was repressed in a compound-specific manner that corresponded to their atrophogenic potential. In the epidermal layer, *MMP1* mRNA expression was inhibited by HC, PC, MF and CB at anti-inflammatory equi-effective concentrations of about -7 %, -58 %, -83 % and -91 %, respectively, relative to control (**Fig. 16 A**). These results were confirmed at the protein level of MMP-1 (**Fig. 16 E**).

The secretion of MMP-3 was inhibited by different GCs corresponding to their atrophogenic potential. MF and CB, for instance, inhibited the MMP-3 secretion at equi-effective concentrations of about -45 % and -66 %, respectively, relative to control (**Fig. 16 F**).

→ MMP1 *mRNA expression in epidermis on day 12 as well as MMP-1 and MMP-3 secretion into medium on day 3 were dose-dependently repressed in GC-treated FTSM. Moreover, the data correlated with the different GC classes. Thus, the test systems are suitable to detect the atrophogenic potential of GCs.*

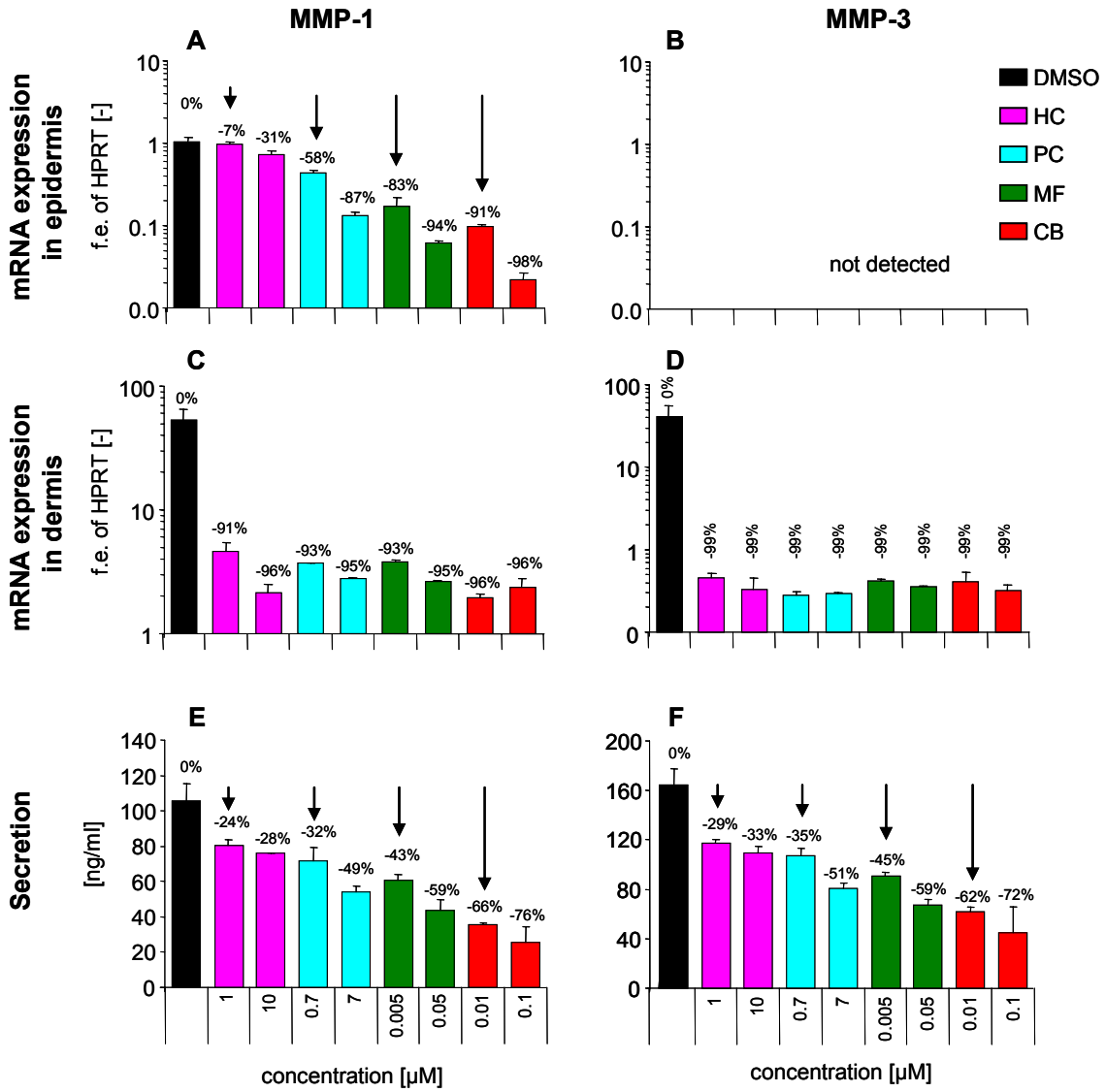

Fig. 16: Inhibition of MMP-1 and MMP-3 mRNA expression and secretion by GCs in FTSM. Culture medium was changed daily and supplemented with GR ligands dissolved in 0.01 % DMSO. On day 12, mRNA expression of *MMP1* and *MMP3* was determined in epidermal (**A, B**) and dermal compartment (**C, D**) by RT-PCR. Expression level of mRNA is given as fold expression (f. e.) relative to the house keeping gene *HPRT*. On day 3, MMP-1 (E) and MMP-3 (F) secretion into the supernatant was quantified by MesoScale. Mean ± SD, duplicates of one experiment. Arrows indicate anti-inflammatory equi-effective concentrations of GCs. HC – hydrocortisone, PC – prednicarbate, MF – mometasone furoate, CB – clobetasol-17-propionate.

→ *Summarizing the results obtained by analysis of mRNA and protein expression in FTSM, the expression of the following markers was dose-dependently repressed by GCs and with the GC classification: mRNA expression of* COL1A1 *and* COL3A1 *in dermis and* MMP1 *in epidermis, protein secretion of CICP, MMP-1, MMP-3 into medium. Therefore, this test systems seems to be appropriate to determine the atrophogenic potentials of GCs.*

4.5 Summary of the Results / Recommendation of Predictable Test Systems

Several *in vitro* test systems were investigated for their usability as atrophy models (**Tab. 17**). Investigations were performed in monolayer cell culture such as HaCaT cells, NHEK, 3T3 mouse fibroblasts, rFib and NHDF as well as in 3D skin equivalents such as AST-2000 and FTSM. In these rodent and human cell systems, the investigations were related to proliferation, the mRNA expression and partly the protein secretion and the epidermal thickness.

Pre-screening of all mentioned cellular systems were performed to identify the respective read out parameter that are repeatedly and clearly (2-fold) regulated by GC treatment using high concentrations of either DEX or CB only. The following test systems met these criteria: 1.) *MMP1, -2, -3* and *-9* mRNA expression in NHEK, 2.) *COL1A1* and *COL3A1* mRNA expression in 3T3 mouse fibroblasts, 3.) epidermal thickness as well as collagen and MMP synthesis in FTSM.

These three selected test systems with NHEK, 3T3 cells and FTSM were further characterized for their quality to serve as models to determine the atrophogenic potential of GCs. A suitable test system should comply with the known clinical effects of GC-induced skin atrophy and thus fulfill at least two of the following requirements: 1.) Dose-dependent regulation of read out parameters by reference GCs. 2.) Correlation with GC classification based on their potencies. 3.) Correlation with atrophogenic potential of GCs of one class but with a different TIX. Consequently, cells and skin equivalents were treated with ascending concentrations of at least four of the following compounds: HC (class I GC), PC (class II GC), MF (class III GC), BMV (class III GC) and CB (class IV GC). In NHEK and 3T3 test systems all requirements were met. The mRNA expression of MMP and collagen respectively were regulated in a dose-dependent and compound-specific manner by the applied GCs. In FTSM, the following read out parameters fulfilled the first two requirements: treatment with GCs at two concentrations resulted in a dose-dependent and compound-specific reduction of epidermal thickness, *COL1A1* and *COL3A1* mRNA expression in dermis and CICP secretion into medium as well as and *MMP1* mRNA expression in epidermis and MMP-1 and -3 secretion into medium.

Thus, the NHEK, 3T3 cell and FTSM test systems with NHEK, 3T3 cells and FTSM (**Tab. 17**) were considered as convenient for prediction of the atrophogenic potential of GC. The recommended cascade of the test systems (**Fig. 17**) to estimate the atrophogenic potential of GR ligands with hitherto unknown atrophogenicity is as follows:

1.) The two monolayer cell culture test systems will be used to test the inhibition of *MMP1*, *-2, -3* and *-9* mRNA expression in NHEK as well as the inhibition of *COL1A1* and *COL3A1* mRNA expression in 3T3 mouse fibroblasts by a novel GR ligands in comparison to reference GC. These test systems are easily to handle, fast growing and allow the throughput of higher number of compounds.

2.) The determination of the atrophogenicity of GR ligands relative to a reference GC in the more complex skin equivalent FTSM will be used in a further step. In that model, in addition to collagen

(dermis) and *MMP1* (epidermis) mRNA expression the reduction of keratinocyte cell layers and the CICP, MMP-1 and MMP-3 secretion into the medium can be used as parameter describing the atrophogenic potential of a compound. A few compounds can be screened in the current test system. However, beside the additional read out parameter there is a major advantage of a tissue simulating situation using these cellular systems.

In a final step, a limited number of favorable test compounds might be tested *in vivo* in *hr/hr* OFA rats. In this model, the atrophogenic potential is indicated by reduced skin thickness by GR ligands.

Tab. 17: Overview of investigated test systems as model for GC-induced skin atrophy.

	Suitable test systems	**Inappropriate test systems**
In vitro monolayer	**NHEK** → inhibited mRNA expression of *MMP1*, *MMP2*, *MMP3*, *MMP9*	**HaCaT cells** → proliferation → mRNA expression of *MMP2, MMP9*
		NHEK → proliferation
	3T3 fibroblasts → inhibited mRNA expression of *COL1A1*, *COL3A1*	**3T3 fibroblasts** → proliferation → mRNA expression of *COL4A1, COL5A1, COL7A1, MMP2, MMP3, MMP13, P4HA1, P4HA2, P4HB*
		rFib → mRNA expression of *COL1A1, COL3A1, MMP1, MMP2, MMP3, P4HA1, P4HA2, P4HB*
		NHDF → proliferation → mRNA expression of *COL1A1, COL3A1, MMP1, MMP2, MMP3, MMP9, P4HA1, P4HA2, P4HB*
In vitro 3D	**FTSM *** → reduced number of epidermal cell layers → inhibited mRNA expression of *COL1A1* and *COL3A1* in dermis, *MMP1* in epidermis → inhibited protein secretion of MMP-1, MMP-3, CICP into medium	**AST-2000** → epidermal thickness → mRNA expression of *COL1A1, COL3A1, MMP1, MMP2, MMP3* → protein secretion of CICP, MMP-1
		FTSM → proliferation

*further investigation and optimization necessary.

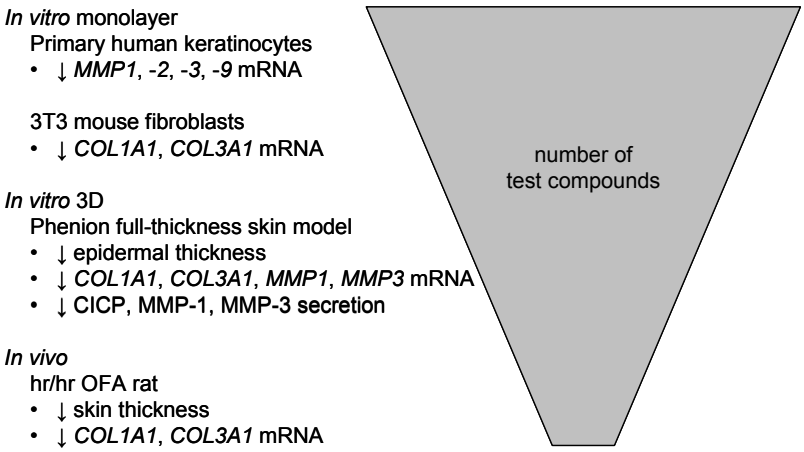

Fig. 17: Proposed screening cascade – throughput of novel test compounds in atrophy models.

4.6 First Application of the Recommended Test Systems in Drug Discovery

Based on the recommended *in vitro* test systems for GC-induced skin atrophy their feasibility was tested using a novel compound class of selective GR agonists (SEGRA). SEGRA compounds are hypothesized to display less atrophy but similar anti-inflammatory effects as classical GCs (Schäcke et al., 2007). A selected SEGRA compound was compared to the reference CB. To evaluate the hitherto unknown atrophogenic potential of the SEGRA compound, both GR ligands (SEGRA and CB) were applied to the recommended *in vitro* test systems with NHEK, 3T3 cells and FTSM. The resulting regulation of the read out parameters (MMP and collagen synthesis, epidermal thickness) was compared with the skin thinning potential of the compounds in the *hr/hr* rat skin atrophy model.

4.6.1 Anti-inflammatory Activity of GR Ligands

Prior determining atrophogenic properties, it was essential to compare anti-inflammatory potency of the novel SEGRA compound with the reference in FTSM and in *hr/hr* rat.

In FTSM, 0.1 µM SEGRA compound and 0.01 µM CB and additionally ten times less concentrations of each compound were applied and the GR ligand effects on the secretion of the pro-inflammatory cytokines IL-1β, IL-6 and IL-8 was detected in culture medium. IL-1β secretion was reduced about -68 % by 0.1 µM SEGRA and about -70 % by 0.01 µM CB compared to vehicle control (**Fig. 18**). The GR ligands at the mentioned concentrations inhibited equi-effectively the cytokine secretion. Similar results were obtained for IL-6 and IL-8 secretion. In FTSM, SEGRA displayed a ten times weaker potency but a similar efficacy compared to CB regarding the IL-1β, IL-6 and IL-8 secretion.

→ *In FTSM, the atrophogenic effects of SEGRA were compared with CB at equi-effective concentrations: 0.1 µM SEGRA vs. 0.01 µM CB.*

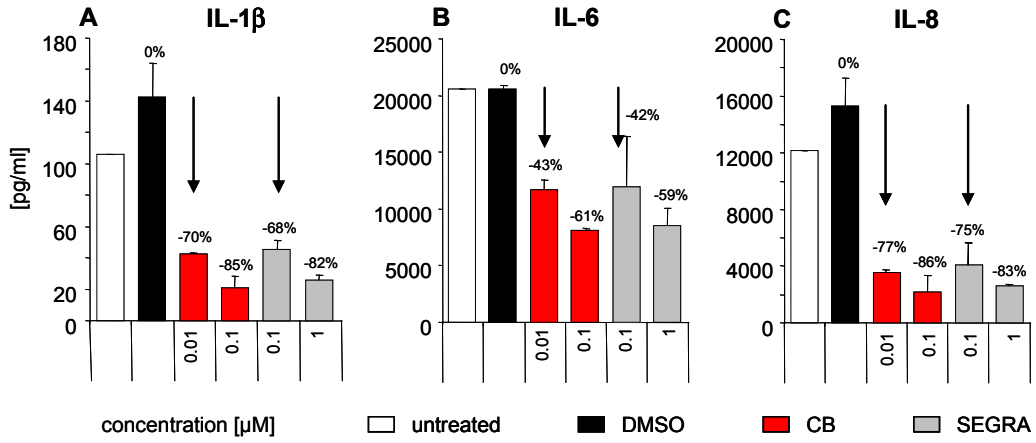

Fig. 18: Anti-inflammatory potential of GR ligands in FTSM. FTSM medium was changed daily and supplemented with GR ligands dissolved in 0.01 % DMSO. Equi-effective concentrations clobetasol-17-propionate (CB) and SEGRA were determined in THP-1 cells and adapted to FTSM (see Material and Methods). Additionally, a ten times lower concentration was used to test dose dependency. IL-1β (**A**), IL-6 (**B**) and IL-8 (**C**) secretion was measured in the supernatants after treatment for 3 days. Mean ± SD, duplicates in one experiment. Arrows indicate equipotent concentrations of compounds. Inhibition by compound treatment relative to vehicle control is given in %.

In Wistar rats, the anti-inflammatory equi-effective doses were also determined for SEGRA and CB. The inhibition of croton oil-induced ear edema formation resulted in an ED_{50} of 0.00049 % for SEGRA and 0.00034 % for CB (**Fig. 19**) with similar efficacy for both in a direct comparison.

→ *Doses of 0.01 % and 0.001 % were chosen to determine the atrophogenic effects of the two GR ligands in rodent* in vivo *atrophy model.*

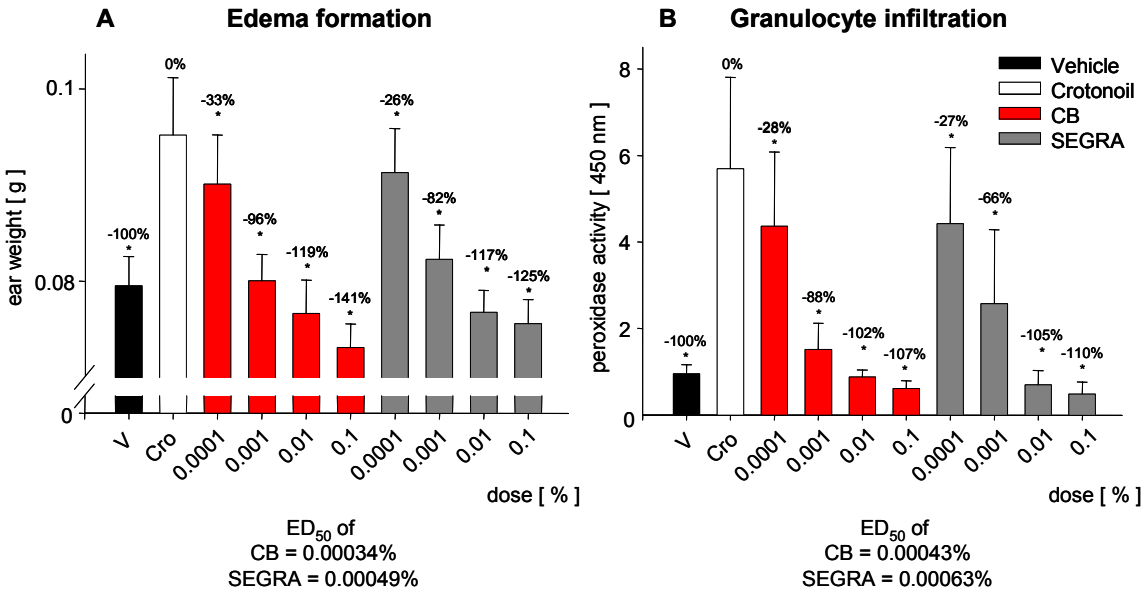

Fig. 19: Anti-inflammatory effects of SEGRA compared to CB in croton oil-induced inflammation of rat ear. Edema formation (**A**) and granulocyte infiltration (**B**) in rat ear. Animals were treated as described in Material and Methods. Weight of ear punch biopsies was determined as an overall read-out of inflammation. Peroxidase activity as parameter for granulocyte infiltration was analyzed in ear homogenates. The mean ± SD of ear weight and peroxidase activity is shown (n=10). A Mann Whitney test was used to estimate the variation of GR ligand treatment versus vehicle and croton oil control (*** $p \leq 0.001$,** $p \leq 0.01$; * $p \leq 0.05$). No statistically significant differences were found between the two compounds. Efficiencies [%] show inhibition compared with croton oil positive control. CB – clobetasol-17-propionate.

4.6.2 Atrophogenic Activity of GR Ligands

MMP mRNA Expression in NHEK

In the first *in vitro* model, compounds were applied to NHEK and mRNA expression of *MMP1*, *-2, -3* and *-9* was measured as an additional parameter to gage the atrophogenic profile of SEGRA. For inhibition of *MMP1* expression, SEGRA exhibited an IC_{50} of about 2 nM, while CB displayed an IC_{50} of about 1 nM (**Tab. 18**). The weaker potency of SEGRA relative to CB was confirmed for inhibition of *MMP2, -3* and *-9*. The ratio between the determined IC_{50} values showed, that SEGRA was 1.4 – 2.9-fold weaker than the reference GC in inhibition of MMP mRNA expression (**Tab. 18**). This difference was statistically significant for the inhibition of *MMP2* and *-3* mRNA expression.

Collagen mRNA Expression in 3T3 Fibroblasts

In the second *in vitro* model, GR ligands at increasing concentrations were applied to 3T3 fibroblasts and the *COL1A1* and *COL3A1* mRNA expression were measured. The SEGRA compound displayed an IC_{50} of about 1 nM, while CB showed an IC_{50} of 0.5 nM in inhibition of *COL1A1* expression (**Tab. 18**). Similar results were obtained for inhibition of *COL3A1* mRNA expression. SEGRA displayed a 2.3 – 2.6-fold significant weaker potency for inhibition of collagen mRNA expression than CB.

Tab. 18: Comparison of SEGRA and CB in NHEK and 3T3 fibroblasts test systems. Cells were treated for 24 hours with increasing concentrations of cobetasol-17-propionate (CB) or SEGRA compound. In NHEK, MMP mRNA expression was detected by RT-PCR. In 3T3 fibroblasts, the mRNA expression of collagen were determined. IC_{50} [nM] is shown as mean ± SD (n=5). The ratio between SEGRA and CB was calculated by dividing mean IC_{50}. p-values were calculated by using a paired t-test to estimate variations of IC_{50} of CB vs. SEGRA.

Inhibition of mRNA expression	**CB IC_{50} [nM]**	**SEGRA IC_{50} [nM]**	**Ratio** (SEGRA: CB)	**p-Value**
MMP1 in NHEK	0.7 ± 0.2	2.0 ± 1.5	2.9	0.063
MMP2 in NHEK	0.7 ± 0.6	1.6 ± 0.8	2.3	0.017
MMP3 in NHEK	0.3 ± 0.02	0.7 ± 0.1	2.0	<0.001
MMP9 in NHEK	0.6 ± 0.1	0.9 ± 0.1	1.4	0.063
COL1A1 in 3T3 fibroblasts	0.5 ± 0.2	1.1 ± 0.4	2.3	0.012
COL3A1 in 3T3 fibroblasts	0.4 ± 0.2	0.9 ± 0.3	2.6	0.010

Epidermal Thickness and Collagen and MMP Synthesis in FTSM

The third *in vitro* model (FTSM) was treated with anti-inflammatory equi-effective (0.01 µM CB, 0.1 µM SEGRA) and additionally ten times higher concentrations of GR ligands. The following read out parameters were determined: epidermal thickness on day 12, *MMP1* mRNA expression in epidermis on day 12, MMP-1 and MMP-3 protein secretion into medium on day 3, *COL1A1* and *COL3A1* mRNA expression in dermis and CICP secretion into medium on day 12.

The epidermal layers were reduced of about -54 % by 0.1 µM SEGRA compared to vehicle treated controls, while CB reduced the epidermal layers about -64 % at anti-inflammatory equi-effective concentration (**Fig. 20 A+B**). Thus, the SEGRA compound had 10 % weaker atrophogenic effects than CB at equi-effective concentration.

MMP1 mRNA expression was inhibited about -87 % by 0.1 µM SEGRA relative to control (**Fig. 20 C**). CB at equi-effective concentration inhibited the *MMP1* mRNA expression about -91 % relative to control. This slight advantage of SEGRA relative to CB at the mRNA level turned in a clear advantage at the protein level. MMP-1 secretion was reduced by SEGRA about -44 %, while CB reduced the MMP-1 secretion about -66 % (**Fig. 20 D**). Similar results were obtained for the inhibition of MMP-3 secretion (**Fig. 20 E**).

The mRNA expression of *COL1A1* and *COL3A1* was also reduced by both compounds. 0.1 µM SEGRA reduced the *COL1A1* mRNA expression about -55 % relative to vehicle control, whereas 0.01 µM CB led to an inhibition of -64 % (**Fig. 20 F**). At the protein level, the slight benefit of the SEGRA compound compared to CB became more distinct. CICP secretion was reduced by SEGRA about -45 %, while it was reduced by CB at equi-effective concentrations about -59 % (**Fig. 20 H**).

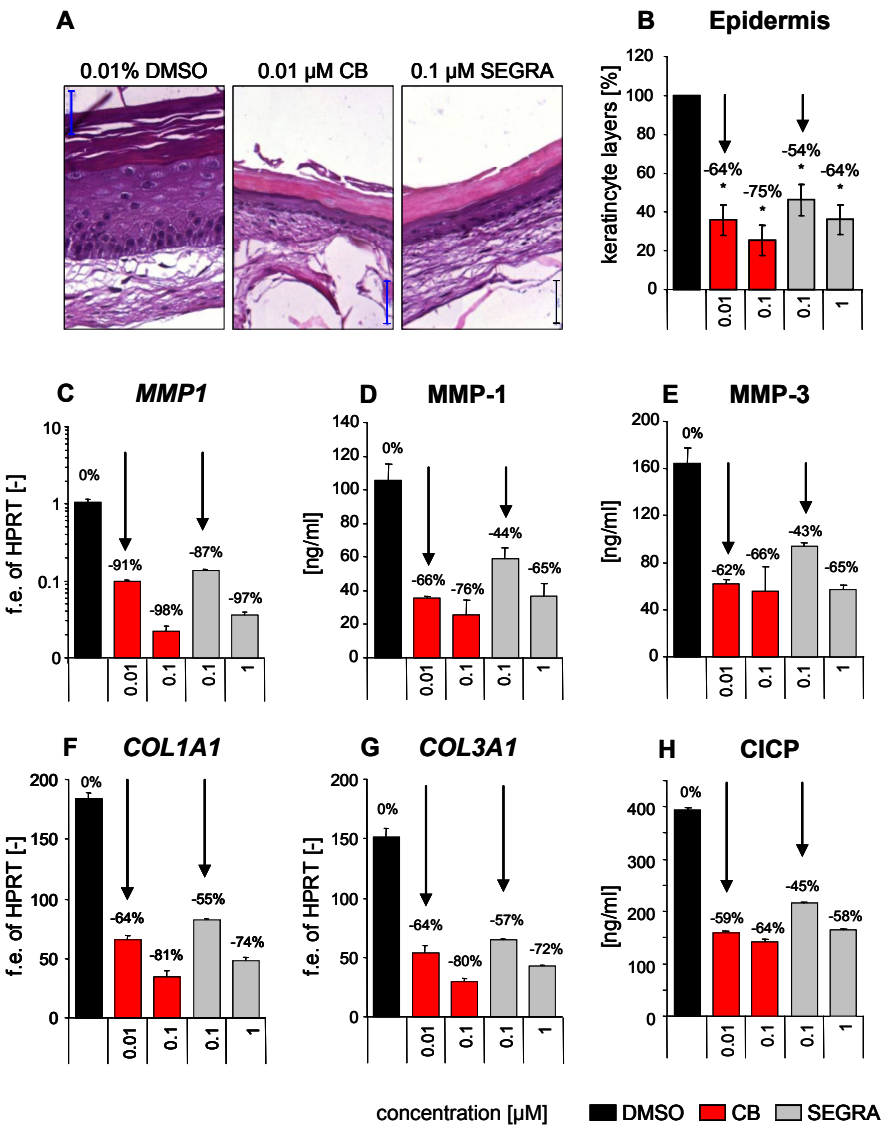

Fig. 20: SEGRA induces less skin atrophy in FTSM than CB at equi-effective concentration. Increasing concentrations of GR ligands were daily added to growth medium. Medium was changed daily. Histological sections (**A**) indicate atrophogenic effects of GCs on the epidermis. Epidermal thickness (**B**) was analyzed by counting keratinocyte layers after 12 days of GR ligand treatment. The number of keratinocyte layers was determined at 5 different areas on 3 non-consecutive sections. H&E stain, blue scale = 50µm. Statistical analysis of epidermal cell layers was performed after Fieller (see Material and Methods) and resulted in mean inhibition ± upper and lower confidence interval, n=2. Expression of *MMP1* mRNA in epidermal samples (**C**) was determined on day 12 by RT-PCR, while secretion of MMP-1 (**D**) and MMP-3 (**E**) into medium was determined on day 3 by MesoScale. mRNA expression of *COL1A1* (**F**) and *COL3A1* (**G**) was determined in dermal layer on day 12 by RT-PCR. Secretion of CICP on day 12 was measured by ELISA (**H**). For analysis of protein secretion mean ± SD of duplicates in one experiment is given. Arrows indicate anti-inflammatory equi-effective concentrations of GR ligands tested. Inhibition by compound treatment relative to control is given in %. CB – clobetasol-17-propionate.

→ *The SEGRA compound displayed a slightly weaker atrophogenic potential than CB in the three recommended in vitro test systems 1.)* MMP1, -2, -3 *and* -9 *mRNA expression in NHEK, 2.)* COL1A1 *and* COL3A1 *mRNA expression in 3T3 mouse fibroblasts and 3.) epidermal thickness as well as MMP and collagen synthesis in FTSM. These parameters were regulated with weaker effects by SEGRA than by CB at anti-inflammatory equi-effective concentrations.*

Skin Atrophy in hr/hr *Rat*

To test the predictability of the results of obtained from the three *in vitro* test systems for the rodent *in vivo* situation, the atrophogenicity of SEGRA in relation to CB was determined in *hr/hr* rat skin atrophy model. The croton-oil induced inflammation of Wistar rat ear displayed for 0.01 % CB and SEGRA an equal efficacy as shown above. For determination of skin atrophy, *hr/hr* rats were treated daily for 10 days with SEGRA and CB at these anti-inflammatory equi-effective and 10-times lower doses.

In *hr/hr* rats, both doses of SEGRA induced less skin atrophy than both doses of CB. At anti-inflammatory equi-effective doses (0.01 %), SEGRA resulted in a -23 % decrease in skin thickness relative to vehicle control, while CB resulted in a -33% decrease in skin thickness (**Fig. 21 A**). At ten-times lower concentrations (0.001 %), the difference was even more pronounced; SEGRA exhibited no significant decrease in skin thickness relative to vehicle control, while CB exhibited -20 % decrease in skin thickness.

These results were supported by collagen mRNA expression data. SEGRA was less efficient in repressing *COL1A1* and *COL3A1* mRNA expression than the reference compound CB (**Fig. 21 B, C**). The *COL3A1* mRNA expression e.g. was reduced of about -57 % by SEGRA, while CB reduced the expression of about -72 % at anti-inflammatory equi-effective doses.

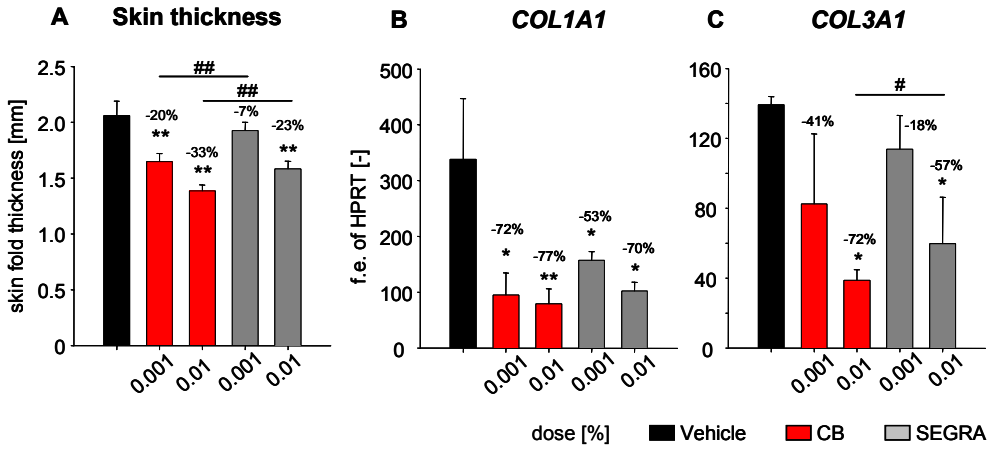

Fig. 21: SEGRA induces less skin atrophy than CB at anti-inflammatory equi-effective doses in *hr/hr* rats. After daily topical treatment for 10 days, skin fold thickness (**A**) was measured with a special gauge. Additionally, punch biopsies of skin were taken and used for mRNA expression analysis of *COL1A1* (**B**) and *COL3A1* (**C**). The mean ± SD of skin thickness and fold expression (f.e.) of *HPRT* respectively is given from 6 animals per group. A Mann Whitney test was used to estimate the variation of compound treatment and vehicle control (*** $p \leq 0.001$,** $p \leq 0.01$; * $p \leq 0.05$) and to calculate variations of compound treatments between each other (# $p \leq 0.05$, ## $p \leq 0.01$). CB – clobetasol-17-propionate.

Taken together, the atrophogenic potential of a SEGRA compound in relation to the atrophogenicity of the reference GC CB was determined in the recommended three *in vitro* test systems for GC-induced skin atrophy. The SEGRA compound displayed a slightly weaker atrophogenic potential compared to CB the three *in vitro* test systems based on NHEK, 3T3 fibroblasts and FTSM.

In a last step, the predictability of the three *in vitro* test systems for the rodent *in vivo* situation was investigated by determining the atrophogenicity of SEGRA compared to CB in *hr/hr* rats. *In vivo*, the SEGRA compound induced less skin thinning and less repression of *COL1A1* and *COL3A1* mRNA expression than CB at anti-inflammatory equi-effective doses. Thus, the *in vitro* predicted atrophogenic potential of the SEGRA compound was true for the *in vivo* situation.

In conclusion, the three *in vitro* test systems based on NHEK, 3T3 fibroblasts and FTSM are considered to be convenient models to determine the atrophogenic properties of GR ligands and to predicted the atrophogenicity for *in vivo*.

5 Discussion

The aim of the present study was the identification of *in vitro* test systems, which predict the atrophogenic potential of GR ligands *in vivo*. Different human and rodent *in vitro* monolayer cell culture systems (HaCaT cells, NHEK, 3T3 mouse fibroblasts, rFib, NHDF) and human *in vitro* 3D skin equivalents (AST-2000, FTSM) were selected as cellular assays. As read out parameters novel and known atrophy markers were investigated.

Pursuing a hypothesis-free approach of identifying novel atrophy markers, two microarray studies were performed with skin samples of GC-treated SKH1 mice and *hr/hr* rats. About 300 genes were found to be regulated by GCs in rodent skin. Genes that are known to be regulated by GCs served as marker genes to demonstrate, whether or not GC effects could be found in these probes. The 300 GC-regulated genes were clustered according to their potential functions. Eight genes with the highest regulation were selected for confirmatory investigations with RT-PCR. For four of eight genes, the regulation pattern in CB-treated mouse skin detected by microarray could be confirmed by RT-PCR. In a further step, it was investigated whether the expression of these four genes *COL11A1, FGFBP1, PRG4* and *TNMD* is GC-regulated in skin-derived human keratinocytes (NHEK) and human and rodent fibroblasts (NHDF, 3T3 cells) as well as in human full-thickness skin models (FTSM, AST-2000). However, it was not possible to confirm the GC effects on mRNA expression of *COL11A1* and *FGFBP1* in the subsequent *in vitro* experiments. For *TNMD*, no mRNA expression was found in either rodent or human *in vitro* models. GC effects on *PRG4* mRNA expression were verified in mouse 3T3 fibroblasts only. This gene was not found to be regulated or expressed in human cells. Species-specific differences in expression pattern of Prg4 might be involved in that effect. Synthesis of ECM components seems to be strongly dependent on the existence of an intact tissue. A number of differences in expression profiles of ECM proteins might be caused by the limitations of monolayer cell culture systems in comparison to the function of the respective cells in a tissue. Takahashi and colleagues demonstrated by for cartilage *in vitro* cultures, that 3D cultures show advantage over monolayer cell culture in possessing favorable mechanical properties. This advantage may result from the similarity of microenvironments in cell-to-matrix adhesion or cell-to-cell contacts with that of native cartilage (Takahashi et al., 2007). Taken together, eight novel molecules potentially participating in the induction of skin atrophy were identified by microarray analysis of GC-treated rodent skin. However, it was not possible to confirm the *in vivo* detected regulation of the novel molecules in different *in vitro* cell systems. Therefore, with the microarray approach under the given methodic settings no novel markers, that might be used in the investigated cellular assays were identified.

It may be conjectured that at earlier time points more genes involved in atrophy induction might be found to be regulated by GCs. It is known, that GCs may have rapid effects (0-12 hours) on gene expression (for review see Newton 2000). For skin atrophy, Lubach and colleagues demonstrated by

measuring the skin thickness every day, that a single topical application of CB may lead to a skin-thinning process lasting for 3 days (Lubach et al., 1995). In the present study, the gene expression profile in *hr/hr* rats treated for inter alia 6, 24, 48 and 96 hours with CB showed high intra-assay variability due to small sample number. Hence, further more comprehensive investigations with a higher sample number ($n \geq 6$) of rodent skin treated for e.g. 6, 12, 24 and 72 hours may lead to more potential atrophy markers.

Next, in a broad approach, a consistent analysis of pre-published or hypothesis-driven atrophy markers in different cross-species cellular systems was carried out to analyze their suitability as GC-induced skin atrophy model. In systematic pilot experiments, it was investigated, whether the effects of a high-concentrated GC on the marker were reproducible and more than 2-fold. Test systems based on HaCaT cells, NHDF, rFib and AST-2000 did not met the screening criteria regarding proliferation, collagen metabolism or epidermal thickness. However, the following three test systems fulfilled the criteria: A.) *MMP1*, *-2*, *-3* and *-9* mRNA expression in NHEK, B.) *COL1A1* and *COL3A1* mRNA expression in 3T3 mouse fibroblasts and C.) epidermal thickness as well as collagen and MMP synthesis in FTSM. They were further investigated with a panel of four to five classical GCs (e.g. HC a weak GC, CB a very potent GC), whether they comply with the known clinical effects of GC-induced skin atrophy. All mentioned read out parameters of the three test systems (A, B, C) were regulated in a dose-dependent manner after treatment with GCs and correlated well with the GC classification. Additionally, regarding the test systems based on monolayer cell culture (A, B), the regulation of the read out parameters correlated with the different atrophogenic potentials of two GCs from the same topical GC class but with a different TIX. Overall, the results obtained in these three *in vitro* test systems indeed give sufficient hints for the atrophogenic potential of known GCs and thus are considered as appropriate test systems for GC-induced skin atrophy. Their characteristics will be discussed in the following sections.

The two *in vitro* monolayer cell culture test systems (NHEK, 3T3 cells) were optimized to determine atrophogenic potential of classical GCs. NHEK are human primary cells and thus more challenging to handle as well as more time- and cost-intensive than the 3T3 mouse cell line. Murine 3T3 cells are a fast growing, frugal fibroblast cell line. The test systems with these human and rodent cells, respectively − MMP mRNA expression in NHEK and collagen mRNA expression in 3T3 mouse fibroblasts− generate well-reproducible data of a lots of compounds within 3 days (**Tab. 19**). The atrophogenic potential of approximately ten to 15 compounds with five to six concentrations each could be determined with these test systems. Thus, both test systems might be used for routine compound pre-screenings to determine atrophogenicity. Surprisingly, neither test systems with NHEK nor with 3T3 mouse fibroblasts have been published to be used as GC-induced skin atrophy models.

Although monolayer cell systems have many advantages and markers for GC-induced skin atrophy are predictably regulated for the *in vivo* situation, the non-physiological conditions are a major limitation

of these models: 1.) They show the characteristic of only one cell type and thus do not reflect the complex interactions of different cell types representative of organs like the skin. For example, collagen synthesis in human fibroblasts is described to be repressed by keratinocyte-derived cytokines (Harrison et al., 2006). Fibroblast growth factors also secreted by keratinocytes were able to partially overcome this repression and to increase collagen synthesis (Harrison et al., 2006). In the skin equivalent FTSM, the presence of keratinocytes revealed a beneficial effect on the metabolic activity of the fibroblasts (Mewes et al., 2007). As only few fibroblasts were seen in the collagen scaffold, the cell number and hence the amount of newly synthesized ECM proteins rapidly increased after adding the keratinocytes to the culture system (Mewes et al., 2007). 2.) In cells growing in monolayer cultures it is not possible to detect tissue thinning, the overall read out parameter for atrophy. 3.) The cells are growing in a large excess of growth medium and therefore, topical application of compounds is not possible. Likewise, it is impossible to test topical formulations in monolayer cell systems.

Tab. 19: Characteristics of test systems for GC-induced skin atrophy.

	Monolayer cell systems (NHEK, 3T3 cells)	**3D skin equivalent (FTSM)**	***In vivo* (hr/hr OFA, SKH1)**
Species	human, mouse	human	rat, mouse
Handling	easy	easy - moderate	moderate
Epidermal / skin thinning	not present	present	present
Interaction among different cell types	not present	present	present
Systemic side effects	not present	not present	present
Topical application	not possible	possible	possible
Testing of formulations	not possible	possible	possible
Time assumption	low	moderate – high	moderate – high
Assays duration	3 days	12 days	10 – 19 days
Data acquisition	~1 day	~14 days	~2 days
Work assumption	low	moderate - high	moderate - high
Compound assumption	minimal	moderate	moderate - high
Compound throughput	large	minimal - few	minimal
Costs	low	moderate - high	high

The establishment of *in vitro* models consisting of multilayer cells growth co-cultured with cells of another type was a big step forward to display the *in vivo* situation. Full-thickness skin equivalents are useful models for dermatological investigations as they consist of i.) human neonatal fibroblasts growing in a 3D matrix, ii.) a functional basal lamina and iii.) human neonatal keratinocytes differentiated in a real epidermis characterized by different strata. Besides stimuli of other cells, the properties of the matrix material of skin equivalents are important for the quality of the skin model (Mewes et al., 2007). The dermal compartment of the FTSM emerges by fibroblasts that are seeded into a special robust matrix material scaffold with spongy consistence (personal communication 2008 with Nadja Zöller, University of Frankfurt / Main). The matrix material is composed of bovine collagen type I only (Mewes et al., 2007). FTSM are cultured without any exogenous synthetic matrix materials (Mewes et al., 2007). Therefore, fibroblasts in FTSM secrete ECM compounds on their own and hence, behave more native than fibroblasts of skin models with exogenous synthetic supplements (personal communication 2008 with Dr. Klaus Schröder, Phenion). The AST-2000 matrix e.g. consists of rat collagen type I covered with fibronectin (personal communication 2008 with Dr. Bernd Becker, CellSystems). Although collagen type I is preserved across different species, human fibroblast might react differently on bovine and rat collagen type I. As exogenous fibronectin was added, AST-2000 appears slightly more artificial than FTSM. The grade of artificiality might influence the susceptibility of collagen synthesis to regulation. However, beside the complex fibroblast-keratinocyte and cell-matrix interaction, skin equivalents allow topical drug administration. Zöller and colleagues applied GC-containing creams onto the surface of the airlifted FTSM for the first time (Zöller et al., 2008).

In the present study, epidermal thickness as well as collagen and MMP synthesis in FTSM were characterized as reliable human test system for GC-induced skin atrophy. Handling, treatment duration and preparation of FTSM are more elaborate compared with monolayer cells, thus only a few compounds may be screened (**Tab. 19**). Certainly, handling, time and compound consumption should be optimized in further experiments. To decrease compound consumption, a medium change on every second or third day should be considered as opposed to everyday. Special inserts instead of metal supports plus filter paper should be tested for a simplified handling and decreased compound and culture medium consumption. Atrophogenicity of approximately six to eight compounds with two concentrations each could be determined with current system.

Taken together, the atrophogenic potential of novel GR ligands may be screened in the investigated test systems as follows:

First of all, the atrophogenic potential of a large number of compounds can be quickly and easily determined in the presented *in vitro* test systems using monolayer cultures (NHEK, 3T3 cells). In these two models, effects on MMP and collagen synthesis, respectively can be detected with good comparability with commercially available GCs.

Next, favorable compounds can be tested in the 3D *in vitro* test system FTSM. This allows screening of a few to a medium number of compounds for atrophogenicity. In this test system, epidermal thinning as well as inhibition of collagen and MMP synthesis can be determined within one model. FTSM closely reflects the human situation. Furthermore, FTSM screening narrows down the number of auspicious compounds and minimizes the number of previously selected compounds to be tested in rodents to analyze systemic side effects.

In a last approach, the relevance of the three well characterized *in vitro* test systems was investigated and their predictability for the rodent *in vivo* situation was demonstrated. The hairless rat is the best *in vivo* model available to determine atrophogenicity of uncharacterized SEGRA compounds (Schäcke et al., 2004). A major advantage of this *in vivo* model compared to the *in vitro* models, is the possibility to detect systemic side effects, like atrophy of thymus, spleen or adrenal glands (**Tab. 19**).

To demonstrate the relevance of the three *in vitro* test systems, the atrophogenic potential of a novel SEGRA compound with hitherto unknown atrophogenicity was determined *in vitro* and confirmed with the *hr/hr* rat model. All *in vitro* and *in vivo* test systems displayed comparable results: The SEGRA compound induced less skin atrophy than its reference compound CB at anti-inflammatory equi-effective concentrations. Thus, the appropriateness of the *in vitro* test systems for predictive detection of atrophogenicity in rodents was shown with the SEGRA compound.

In conclusion, the relevance of the three *in vitro* test systems was shown for the rodent *in vivo* situation. As a single *in vitro* test system only might not be absolutely reliable, a panel of three *in vitro* test systems is recommended to determine a GR ligand's atrophogenicity. Further investigations in the human *in vivo* situation are necessary to demonstrate clinical importance of the models. In comprehensive studies lots of known GCs and novel test compounds should be tested *in vitro* and in human *in vivo* models. The results should be compared with each other in correlation analyses. This studies might display, that a single *in vitro* test systems is absolutely reliable in prediction of the atrophogenic behavior of GR ligands for the human *in vivo* situation. Thus far, however, the use of the three *in vitro* test systems might 1.) minimize the number of animals needed for skin atrophy experiments, and 2.) supports the identification of novel drugs with weaker atrophogenicity and thus, minimizes the risk of compound failure in clinical development.

References

Abuharbeid, S.; Czubayko, F. and Aigner, A. (2006): The fibroblast growth factor-binding protein FGF-BP, Int J Biochem Cell Biol 38 [9], pp. 1463-8.

Ahn, S. K.; Bak, H. N.; Park, B. D.; Kim, Y. H.; Youm, J. K.; Choi, E. H.; Hong, S. P. and Lee, S. H. (2006): Effects of a multilamellar emulsion on glucocorticoid-induced epidermal atrophy and barrier impairment, J Dermatol 33 [2], pp. 80-90.

Autio, P.; Oikarinen, A.; Melkko, J.; Risteli, J. and Risteli, L. (1994): Systemic glucocorticoids decrease the synthesis of type I and type III collagen in human skin in vivo, whereas isotretinoin treatment has little effect, Br J Dermatol 131 [5], pp. 660-3.

Balbin, M.; Fueyo, A.; Knauper, V.; Lopez, J. M.; Alvarez, J.; Sanchez, L. M.; Quesada, V.; Bordallo, J.; Murphy, G. and Lopez-Otin, C. (2001): Identification and enzymatic characterization of two diverging murine counterparts of human interstitial collagenase (MMP-1) expressed at sites of embryo implantation, J Biol Chem 276 [13], pp. 10253-62.

Beato, M.; Chalepakis, G.; Schauer, M. and Slater, E. P. (1989): DNA regulatory elements for steroid hormones, J Steroid Biochem 32 [5], pp. 737-47.

Berthod, F.; Germain, L.; Guignard, R.; Lethias, C.; Garrone, R.; Damour, O.; van der Rest, M. and Auger, F. A. (1997): Differential expression of collagens XII and XIV in human skin and in reconstructed skin, J Invest Dermatol 108 [5], pp. 737-42.

Birkedal-Hansen, H.; Moore, W. G.; Bodden, M. K.; Windsor, L. J.; Birkedal-Hansen, B.; DeCarlo, A. and Engler, J. A. (1993): Matrix metalloproteinases: a review, Crit Rev Oral Biol Med 4 [2], pp. 197-250.

Booth, B. A.; Tan, E. M.; Oikarinen, A. and Uitto, J. (1982): Steroid-induced dermal atrophy: effects of glucocorticosteroids on collagen metabolism in human skin fibroblast cultures, Int J Dermatol 21 [6], pp. 333-7.

Brazzini, B. and Pimpinelli, N. (2002): New and established topical corticosteroids in dermatology: clinical pharmacology and therapeutic use, Am J Clin Dermatol 3 [1], pp. 47-58.

Cutroneo, K. R.; Rokowski, R. and Counts, D. F. (1981): Glucocorticoids and collagen synthesis: comparison of in vivo and cell culture studies, Coll Relat Res 1 [6], pp. 557-68.

Cutroneo, K. R.; Stassen, F. L. and Cardinale, G. J. (1975): Anti-inflammatory steroids and collagen metabolism: glucocorticoid-mediated decrease of prolyl hydroxylase, Mol Pharmacol 11 [1], pp. 44-51.

De Bosscher, K.; Vanden Berghe, W.; Vermeulen, L.; Plaisance, S.; Boone, E. and Haegeman, G. (2000): Glucocorticoids repress NF-kappaB-driven genes by disturbing the interaction of p65 with the basal transcription machinery, irrespective of coactivator levels in the cell, Proc Natl Acad Sci U S A 97 [8], pp. 3919-24.

De Paiva, C. S.; Pflugfelder, S. C. and Li, D. Q. (2006): Cell Size Correlates with Phenotype and Proliferative Capacity in Human Corneal Epithelial Cells, Stem Cells 24 [2], p. 368.

Delforno, C.; Holt, P. J. and Marks, R. (1978): Corticosteroid effect on epidermal cell size, Br J Dermatol 98 [6], pp. 619-23.

Deryugina, E. I. and Quigley, J. P. (2006): Matrix metalloproteinases and tumor metastasis, Cancer Metastasis Rev 25 [1], pp. 9-34.

Dixon, W. J. (1953): Processing Data for Outliers Biometrics 9 [1], pp. 74-89.

Dong, K. K.; Damaghi, N.; Picart, S. D.; Markova, N. G.; Obayashi, K.; Okano, Y.; Masaki, H.; Grether-Beck, S.; Krutmann, J.; Smiles, K. A. and Yarosh, D. B. (2008): UV-induced DNA damage initiates release of MMP-1 in human skin, Exp Dermatol.

Epstein, N.N.; Epstein, W.L. and Epstein, J.H. (1963): Atrophic striae in patients with inguinal intertrigo, Arch Dermatol 87, pp. 450-457.

Finley, E. M. and Kornfeld, S. (1994): Subcellular localization and targeting of cathepsin E, J Biol Chem 269 [49], pp. 31259-66.

Fischer, L.B. and Maibach, H.I. (1971): The effect of corticosteroids on human epidermal mitotic activity, Arch Dermatol 103, p. 39.

Frisch, S. M. and Ruley, H. E. (1987): Transcription from the stromelysin promoter is induced by interleukin-1 and repressed by dexamethasone, J Biol Chem 262 [34], pp. 16300-4.

Gans, E. H.; Sadiq, I.; Stoudemayer, T.; Stoudemayer, M. and Kligman, A. M. (2008): In vivo determination of the skin atrophy potential of the super-high-potency topical corticosteroid fluocinonide 0.1% cream

compared with clobetasol propionate 0.05% cream and foam, and a vehicle, J Drugs Dermatol 7 [1], pp. 28-32.

Garbe, C. and Wolf, G. (2005): Topische Therapie, Braun-Falco, O.; Plewig, G.; Wolff, H.H.; Burgdorf, W. and Landthaler, M., Dermatologie und Venerologie 5 pp. 1431-1461, Springer, Berlin.

Görmar, F. E.; Bernd, A. and Holzmann, H. (1990): [The effect of hydrocortisone aceponate on proliferation, total protein synthesis and collagen synthesis in human skin fibroblasts in vitro], Arzneimittelforschung 40 [2 Pt 1], pp. 192-6.

Gras, M. P.; Verrecchia, F.; Uitto, J. and Mauviel, A. (2001): Downregulation of human type VII collagen (COL7A1) promoter activity by dexamethasone. Identification of a glucocorticoid receptor binding region, Exp Dermatol 10 [1], pp. 28-34.

Hammer, S.; Sauer, B.; Spika, I.; Schraut, C.; Kleuser, B. and Schafer-Korting, M. (2004): Glucocorticoids mediate differential anti-apoptotic effects in human fibroblasts and keratinocytes via sphingosine-1-phosphate formation, J Cell Biochem 91 [4], pp. 840-51.

Harrison, C. A.; Gossiel, F.; Bullock, A. J.; Sun, T.; Blumsohn, A. and Mac Neil, S. (2006): Investigation of keratinocyte regulation of collagen I synthesis by dermal fibroblasts in a simple in vitro model, Br J Dermatol 154 [3], pp. 401-10.

Hein, R.; Korting, H. C. and Mehring, T. (1994): Differential effect of medium potent nonhalogenated double-ester-type and conventional glucocorticoids on proliferation and chemotaxis of fibroblasts in vitro, Skin Pharmacol 7 [5], pp. 300-6.

Heino, J. (1996): Biology of tumor cell invasion: interplay of cell adhesion and matrix degradation, Int J Cancer 65 [6], pp. 717-22.

Heisler, E.; Hoffmann, J. J.; Peters, P.; Ahr, H.-J. and Vohr, H.-W. (2002): Discrimination between local irritancy/cytotoxicity vs. immune reactions in vitro: 3D skin models as helpful tools in immunotoxicology., 33rd Annual Meeting of the German Society of Immunology.

Hench, P. S. ; Kendall, E. C.; Slocumb, C. H. and Polley, H. F. (1949): The effect of a hormone of the adrenal cortex and of pituitary adrenocorticotropic hormone on rheumatoid arthritis, Proc Staff Meet Mayo Clin 24, pp. 181-193.

Jay, G. D.; Britt, D. E. and Cha, C. J. (2000): Lubricin is a product of megakaryocyte stimulating factor gene expression by human synovial fibroblasts, J Rheumatol 27 [3], pp. 594-600.

Josse, G.; Rouvrais, C.; Mas, A.; Haftek, M.; Delalleau, A.; Ferraq, Y.; Ossant, F.; George, J.; Lagarde, J. M. and Schmitt, A. M. (2009): A multitechnique evaluation of topical corticosteroid treatment, Skin Research and Technology 15 [1], pp. 35-39.

Kähäri, V. M. and Saarialho-Kere, U. (1997): Matrix metalloproteinases in skin, Exp Dermatol 6 [5], pp. 199-213.

Kao, J. S.; Fluhr, J. W.; Man, M. Q.; Fowler, A. J.; Hachem, J. P.; Crumrine, D.; Ahn, S. K.; Brown, B. E.; Elias, P. M. and Feingold, K. R. (2003): Short-term glucocorticoid treatment compromises both permeability barrier homeostasis and stratum corneum integrity: inhibition of epidermal lipid synthesis accounts for functional abnormalities, J Invest Dermatol 120 [3], pp. 456-64.

Kimura, T. and Doi, K. (1999): Dorsal skin reactions of hairless dogs to topical treatment with corticosteroids, Toxicol Pathol 27 [5], pp. 528-35.

Kirby, J. D. and Munro, D. D. (1976): Steroid-induced atrophy in an animal and human model, Br J Dermatol 94 suppl 12, pp. 111-9.

Kolbe, L.; Kligman, A. M.; Schreiner, V. and Stoudemayer, T. (2001): Corticosteroid-induced atrophy and barrier impairment measured by non-invasive methods in human skin, Skin Res Technol 7 [2], pp. 73-7.

Korting, H. C.; Kerscher, M. J. and Schafer-Korting, M. (1992): Topical glucocorticoids with improved benefit/risk ratio: do they exist?, J Am Acad Dermatol 27 [1], pp. 87-92.

Krane, S. M. (1994): Clinical importance of metalloproteinases and their inhibitors, Ann N Y Acad Sci 732, pp. 1-10.

Kylmaniemi, M.; Oikarinen, A.; Oikarinen, K. and Salo, T. (1996): Effects of dexamethasone and cell proliferation on the expression of matrix metalloproteinases in human mucosal normal and malignant cells, J Dent Res 75 [3], pp. 919-26.

Lacraz, S.; Isler, P.; Vey, E.; Welgus, H. G. and Dayer, J. M. (1994): Direct contact between T lymphocytes and monocytes is a major pathway for induction of metalloproteinase expression, J Biol Chem 269 [35], pp. 22027-33.

Lange, K.; Gysler, A.; Bader, M.; Kleuser, B.; Korting, H. C. and Schafer-Korting, M. (1997): Prednicarbate versus conventional topical glucocorticoids: pharmacodynamic characterization in vitro, Pharm Res 14 [12], pp. 1744-9.

Lange, K.; Kleuser, B.; Gysler, A.; Bader, M.; Maia, C.; Scheidereit, C.; Korting, H. C. and Schafer-Korting, M. (2000): Cutaneous inflammation and proliferation in vitro: differential effects and mode of action of topical glucocorticoids, Skin Pharmacol Appl Skin Physiol 13 [2], pp. 93-103.

Laurence, E. B. and Christophers, E. (1976): Selective action of hydrocortisone on postmitotic epidermal cells in vivo, J Invest Dermatol 66 [4], pp. 222-9.

Lavker, R. M.; Dong, G.; Zheng, P. S. and Murphy, G. F. (1991): Hairless micropig skin. A novel model for studies of cutaneous biology, Am J Pathol 138 [3], pp. 687-97.

Lefstin, J. A. and Yamamoto, K. R. (1998): Allosteric effects of DNA on transcriptional regulators, Nature 392 [6679], pp. 885-8.

Lehmann, P.; Zheng, P.; Lavker, R. M. and Kligman, A. M. (1983): Corticosteroid atrophy in human skin. A study by light, scanning, and transmission electron microscopy, J Invest Dermatol 81 [2], pp. 169-76.

Lubach, D.; Rath, J. and Kietzmann, M. (1995): Skin atrophy induced by initial continuous topical application of clobetasol followed by intermittent application, Dermatology 190 [1], pp. 51-5.

Luger, T.; Loske, K.D.; Elsner, P.; Kapp, A.; Kerscher, M.; Korting, H.C.; Krutmann, J.; Nickner, R.; Röcken, M.; Ruzicka, T. and Schwarz, T. (2004): Topische Dermatotherapie mit Glukokortikoiden Therapeutischer Index, JDDG 2 [7], pp. 629-634.

Maibach, H. I. and Wester, R. C. (1992): Issues in measuring percutaneous absorption of topical corticosteroids, Int J Dermatol 31 Suppl 1, pp. 21-5.

Mallbris, L.; O'Brien, K. P.; Hulthen, A.; Sandstedt, B.; Cowland, J. B.; Borregaard, N. and Stahle-Backdahl, M. (2002): Neutrophil gelatinase-associated lipocalin is a marker for dysregulated keratinocyte differentiation in human skin, Exp Dermatol 11 [6], pp. 584-91.

Marks, R. (1976): Methods for the assessment of skin atrophogenicity of topical corticosteroids, Dermatologica 152 Suppl 1, pp. 117-26.

Marks, R.; Halprin, K.; Fukui, K. and Graff, D. (1971): Topically applied triamcinolone and macromolecular synthesis by human epidermis, J Invest Dermatol 56 [6], pp. 470-3.

Mendias, C. L.; Bakhurin, K. I. and Faulkner, J. A. (2008): Tendons of myostatin-deficient mice are small, brittle, and hypocellular, Proc Natl Acad Sci U S A 105 [1], pp. 388-93.

Mewes, K. R.; Raus, M.; Bernd, A.; Zöller, N. N.; Sattler, A. and Graf, R. (2007): Elastin expression in a newly developed full-thickness skin equivalent, Skin Pharmacol Physiol 20 [2], pp. 85-95.

Mills, C. M. and Marks, R. (1993): Side effects of topical glucocorticoids, Curr Probl Dermatol 21, pp. 122-31.

Mirshahpanah, P.; Döcke, W. D.; Merbold, U.; Asadullah, K.; Röse, L.; Schäcke, H. and Zollner, T. M. (2007): Superior nuclear receptor selectivity and therapeutic index of methylprednisolone aceponate versus mometasone furoate, Exp Dermatol 16 [9], pp. 753-61.

Nagase, H. and Woessner, J. F., Jr. (1999): Matrix metalloproteinases, J Biol Chem 274 [31], pp. 21491-4.

Newton, J. A.; Whitaker, J.; Sohail, S.; Young, M. M.; Harding, S. M. and Black, M. M. (1984): A comparison of pulsed ultrasound, radiography and micrometer screw gauge in the measurement of skin thickness, Curr Med Res Opin 9 [2], pp. 113-8.

Newton, R. (2000): Molecular mechanisms of glucocorticoid action: what is important?, Thorax 55 [7], pp. 603-13.

Niedner, R. (1996): Glukokortikosteroide in der Dermatologie: Kontrollierter Einsatz erforderlich, Dtsch Ärztebl 93 [44], pp. A-2868-72.

Nuutinen, P.; Autio, P.; Hurskainen, T. and Oikarinen, A. (2001): Glucocorticoid action on skin collagen: overview on clinical significance and consequences, J Eur Acad Dermatol Venereol 15 [4], pp. 361-2.

Nuutinen, P.; Riekki, R.; Parikka, M.; Salo, T.; Autio, P.; Risteli, J. and Oikarinen, A. (2003): Modulation of collagen synthesis and mRNA by continuous and intermittent use of topical hydrocortisone in human skin, Br J Dermatol 148 [1], pp. 39-45.

O'Brien, J.; Wilson, I.; Orton, T. and Pognan, F. (2000): Investigation of the Alamar Blue (resazurin) fluorescent dye for the assessment of mammalian cell cytotoxicity, Eur J Biochem 267 [17], pp. 5421-6.

Oakley, R.H. and Cidlowski, J.A. (2001): The glucocorticoid receptor: expression, function, and regulation of glucocorticoid responsiveness., Goulding, N.J. and Flower, R.J., Glucocorticoids pp. 55-80, Birkhäuser, Basel.

Oikarinen, A. and Autio, P. (1991): New aspects of the mechanism of corticosteroid-induced dermal atrophy, Clin Exp Dermatol 16 [6], pp. 416-9.

Oikarinen, A.; Haapasaari, K. M.; Sutinen, M. and Tasanen, K. (1998): The molecular basis of glucocorticoid-induced skin atrophy: topical glucocorticoid apparently decreases both collagen synthesis and the corresponding collagen mRNA level in human skin in vivo, Br J Dermatol 139 [6], pp. 1106-10.

Oikarinen, A. and Hannuksela, M. (1980): Effect of hydrocortisone-17-butyrate, hydrocortisone, and clobetasol-17-propionate on prolyl hydroxylase activity in human skin, Arch Dermatol Res 267 [1], pp. 79-82.

Oikarinen, A.; Salo, T.; Ala-Kokko, L. and Tryggvason, K. (1987): Dexamethasone modulates the metabolism of type IV collagen and fibronectin in human basement-membrane-forming fibrosarcoma (HT-1080) cells, Biochem J 245 [1], pp. 235-41.

Oishi, Y.; Fu, Z. W.; Ohnuki, Y.; Kato, H. and Noguchi, T. (2002): Molecular basis of the alteration in skin collagen metabolism in response to in vivo dexamethasone treatment: effects on the synthesis of collagen type I and III, collagenase, and tissue inhibitors of metalloproteinases, Br J Dermatol 147 [5], pp. 859-68.

Onuma, H.; Mastui, C. and Morohashi, M. (2001): Quantitative analysis of the proliferation of epidermal cells using a human skin organ culture system and the effect of DbcAMP using markers of proliferation (BrdU, Ki-67, PCNA), Arch Dermatol Res 293 [3], pp. 133-8.

Ponec, M.; de Haas, C.; Bachra, B. N. and Polano, M. K. (1977): Effects of glucocorticosteroids on primary human skin fibroblasts. I. Inhibition of the proliferation of cultured primary human skin and mouse L929 fibroblasts, Arch Dermatol Res 259 [2], pp. 117-23.

Ponec, M.; De Haas, C.; Bachra, B. N. and Polano, M. K. (1979a): Effects of glucocorticosteroids on cultured human skin fibroblasts. III. Transient inhibition of cell proliferation in the early growth stages and reduced susceptibility in later growth stages, Arch Dermatol Res 265 [2], pp. 219-27.

Ponec, M.; Kempenaar, J. A.; Van Der Meulen-Van Harskamp, G. A. and Bachra, B. N. (1979b): Effects of glucocorticosteroids on cultured human skin fibroblasts--IV. Specific decrease in the synthesis of collagen but no effect on its hydroxylation, Biochem Pharmacol 28 [18], pp. 2777-83.

Prockop, D. J.; Kivirikko, K. I.; Tuderman, L. and Guzman, N. A. (1979): The biosynthesis of collagen and its disorders (first of two parts), N Engl J Med 301 [1], pp. 13-23.

Raghow, R.; Gossage, D. and Kang, A. H. (1986): Pretranslational regulation of type I collagen, fibronectin, and a 50-kilodalton noncollagenous extracellular protein by dexamethasone in rat fibroblasts, J Biol Chem 261 [10], pp. 4677-84.

Russell, S. B.; Trupin, J. S.; Myers, J. C.; Broquist, A. H.; Smith, J. C.; Myles, M. E. and Russell, J. D. (1989): Differential glucocorticoid regulation of collagen mRNAs in human dermal fibroblasts. Keloid-derived and fetal fibroblasts are refractory to down-regulation, J Biol Chem 264 [23], pp. 13730-5.

Saarni, H. and Hopsu-Havu, V. K. (1978): The decrease of hyaluronate synthesis by anti-inflammatory steroids in vitro, Br J Dermatol 98 [4], pp. 445-9.

Sakai, D. D.; Helms, S.; Carlstedt-Duke, J.; Gustafsson, J. A.; Rottman, F. M. and Yamamoto, K. R. (1988): Hormone-mediated repression: a negative glucocorticoid response element from the bovine prolactin gene, Genes Dev 2 [9], pp. 1144-54.

Schäcke, H.; Berger, M.; Rehwinkel, H. and Asadullah, K. (2007): Selective glucocorticoid receptor agonists (SEGRAs): novel ligands with an improved therapeutic index, Mol Cell Endocrinol 275 [1-2], pp. 109-17.

Schäcke, H.; Docke, W. D. and Asadullah, K. (2002a): Mechanisms involved in the side effects of glucocorticoids, Pharmacol Ther 96 [1], pp. 23-43.

Schäcke, H.; Hennekes, H.; Schottelius, A.; Jaroch, S.; Lehmann, M.; Schmees, N.; Rehwinkel, H. and Asadullah, K. (2002b): SEGRAs: a novel class of anti-inflammatory compounds, Ernst Schering Res Found Workshop [40], pp. 357-71.

Schäcke, H. and Rehwinkel, H. (2004): Dissociated glucocorticoid receptor ligands, Curr Opin Investig Drugs 5 [5], pp. 524-8.

Schäcke, H.; Schottelius, A.; Döcke, W. D.; Strehlke, P.; Jaroch, S.; Schmees, N.; Rehwinkel, H.; Hennekes, H. and Asadullah, K. (2004): Dissociation of transactivation from transrepression by a selective glucocorticoid receptor agonist leads to separation of therapeutic effects from side effects, Proc Natl Acad Sci U S A 101 [1], pp. 227-32.

Schackert, C.; Korting, H. C. and Schäfer-Korting, M. (2000): Qualitative and Quantitative Assessment of the Benefit-Risk Ratio of Medium Potency Topical Corticosteroids In Vitro and In Vivo: Characterisation of Drugs with an Increased Benefit-Risk Ratio, BioDrugs 13 [4], pp. 267-77.

Schäfer-Korting, M.; Korting, H. C.; Kerscher, M. J. and Lenhard, S. (1993): Prednicarbate activity and benefit/risk ratio in relation to other topical glucocorticoids, Clin Pharmacol Ther 54 [4], pp. 448-56.

Schoepe, S.; Schäcke, H.; May, E. and Asadullah, K. (2006): Glucocorticoid therapy-induced skin atrophy, Exp Dermatol 15 [6], pp. 406-20.

Schüle, R.; Rangarajan, P.; Kliewer, S.; Ransone, L. J.; Bolado, J.; Yang, N.; Verma, I. M. and Evans, R. M. (1990): Functional antagonism between oncoprotein c-Jun and the glucocorticoid receptor, Cell 62 [6], pp. 1217-26.

Shapiro, S. D. (1998): Matrix metalloproteinase degradation of extracellular matrix: biological consequences, Curr Opin Cell Biol 10 [5], pp. 602-8.

Sheu, H. M.; Lee, J. Y.; Kuo, K. W. and Tsai, J. C. (1998): Permeability barrier abnormality of hairless mouse epidermis after topical corticosteroid: characterization of stratum corneum lipids by ruthenium tetroxide staining and high-performance thin-layer chromatography, J Dermatol 25 [5], pp. 281-9.

Sheu, H. M.; Tai, C. L.; Kuo, K. W.; Yu, H. S. and Chai, C. Y. (1991): Modulation of epidermal terminal differentiation in patients after long-term topical corticosteroids, J Dermatol 18 [8], pp. 454-64.

Sheu, H. M.; Yu, H. S. and Sheen, T. C. (1989): Histochemical and ultrastructural studies on cutaneous side effects due to topical corticosteroids. I. Changes in epidermis, Derm Sinica 7, pp. 143-153.

Shull, S. and Cutroneo, K. R. (1983): Glucocorticoids coordinately regulate procollagens type I and type III synthesis, J Biol Chem 258 [5], pp. 3364-9.

Smith, E. W.; Haigh, J. M. and Surber, C. (2002): Quantification of corticosteroid-induced skin vasoconstriction: visual ranking, chromameter measurement or digital imaging analysis, Dermatology 205 [1], pp. 3-10.

Smith, J. G., Jr.; Wehr, R. F. and Chalker, D. K. (1976): Corticosteroid-induced cutaneous atrophy and telangiectasia. Experimental production associated with weight loss in rats, Arch Dermatol 112 [8], pp. 1115-7.

Stein, M.; Bernd, A.; Ramirez-Bosca, A.; Kippenberger, S. and Holzmann, H. (1997): Measurement of anti-inflammatory effects of glucocorticoids on human keratinocytes in vitro. Comparison of normal human keratinocytes with the keratinocyte cell line HaCaT, Arzneimittelforschung 47 [11], pp. 1266-70.

Sterry, W. and Asadullah, K. (2002): Topical glucocorticoid therapy in dermatology, Ernst Schering Res Found Workshop [40], pp. 39-54.

Stromstedt, P. E.; Poellinger, L.; Gustafsson, J. A. and Carlstedt-Duke, J. (1991): The glucocorticoid receptor binds to a sequence overlapping the TATA box of the human osteocalcin promoter: a potential mechanism for negative regulation, Mol Cell Biol 11 [6], pp. 3379-83.

Takahashi, T.; Ogasawara, T.; Asawa, Y.; Mori, Y.; Uchinuma, E.; Takato, T. and Hoshi, K. (2007): Three-dimensional microenvironments retain chondrocyte phenotypes during proliferation culture, Tissue Eng 13 [7], pp. 1583-92.

Tuckermann, J. P.; Reichardt, H. M.; Arribas, R.; Richter, K. H.; Schutz, G. and Angel, P. (1999): The DNA binding-independent function of the glucocorticoid receptor mediates repression of AP-1-dependent genes in skin, J Cell Biol 147 [7], pp. 1365-70.

U, M.; Shen, L.; Oshida, T.; Miyauchi, J.; Yamada, M. and Miyashita, T. (2004): Identification of novel direct transcriptional targets of glucocorticoid receptor, Leukemia 18 [11], pp. 1850-6.

Vaalamo, M.; Mattila, L.; Johansson, N.; Kariniemi, A. L.; Karjalainen-Lindsberg, M. L.; Kahari, V. M. and Saarialho-Kere, U. (1997): Distinct populations of stromal cells express collagenase-3 (MMP-13) and collagenase-1 (MMP-1) in chronic ulcers but not in normally healing wounds, J Invest Dermatol 109 [1], pp. 96-101.

Vincenti, M. P. (2001): The matrix metalloproteinase (MMP) and tissue inhibitor of metalloproteinase (TIMP) genes. Transcriptional and posttranscriptional regulation, signal transduction and cell-type-specific expression, Methods Mol Biol 151, pp. 121-48.

Vincenti, M. P.; White, L. A.; Schroen, D. J.; Benbow, U. and Brinckerhoff, C. E. (1996): Regulating expression of the gene for matrix metalloproteinase-1 (collagenase): mechanisms that control enzyme activity, transcription, and mRNA stability, Crit Rev Eukaryot Gene Expr 6 [4], pp. 391-411.

Vuorio, E. and de Crombrugghe, B. (1990): The family of collagen genes, Annu Rev Biochem 59, pp. 837-72.

Wach, F.; Bosserhoff, A.; Kurzidym, U.; Nowok, K.; Landthaler, M. and Hein, R. (1998): Effects of mometasone furoate on human keratinocytes and fibroblasts in vitro, Skin Pharmacol Appl Skin Physiol 11 [1], pp. 43-51.

Westergren-Thorsson, G.; Antonsson, P.; Malmstrom, A.; Heinegard, D. and Oldberg, A. (1991): The synthesis of a family of structurally related proteoglycans in fibroblasts is differently regulated by TFG-beta, Matrix 11 [3], pp. 177-83.

Winter, G. D. and Wilson, L. (1976): The effect of clobetasone butyrate and other topical steroids on skin thickness of the domestic pig, Br J Dermatol 94 [5], pp. 545-50.

Woessner, J. F., Jr. (1994): The family of matrix metalloproteinases, Ann N Y Acad Sci 732, pp. 11-21.

Woodbury, R. and Kligman, A. M. (1992): The hairless mouse model for assaying the atrophogenicity of topical corticosteroids, Acta Derm Venereol 72 [6], pp. 403-6.

Xue, M.; Le, N. T. and Jackson, C. J. (2006): Targeting matrix metalloproteases to improve cutaneous wound healing, Expert Opin Ther Targets 10 [1], pp. 143-55.

Yates, K. E. and Glowacki, J. (2003): Altered expression of connective tissue genes in postnatal chondroinduced human dermal fibroblasts, Connect Tissue Res 44 [3-4], pp. 121-7.

Young, J. M.; Yoxall, B. E. and Wagner, B. M. (1977): Corticosteroid-induced dermal atrophy in the rat, J Invest Dermatol 69 [5], pp. 458-62.

Young, J. M.; Yoxall, B. E. and Wagner, B. M. (1978): Topical betamethasone 17-valerate is an anticorticosteroid in the rat. 1. Dermal atrophy, Br J Dermatol 99 [6], pp. 655-63.

Zendegui, J. G.; Inman, W. H. and Carpenter, G. (1988): Modulation of the mitogenic response of an epidermal growth factor-dependent keratinocyte cell line by dexamethasone, insulin, and transforming growth factor-beta, J Cell Physiol 136 [2], pp. 257-65.

Zerbe (1978): On Fieller's theorem and the general linear model, The Am Stat 32, pp. 103-105.

Zöller, N. N.; Kippenberger, S.; Thaci, D.; Mewes, K.; Spiegel, M.; Sattler, A.; Schultz, M.; Bereiter-Hahn, J.; Kaufmann, R. and Bernd, A. (2008): Evaluation of beneficial and adverse effects of glucocorticoids on a newly developed full-thickness skin model, Toxicol In Vitro 22 [3], pp. 747-59.

Appendix

Tab. 20: Fold regulation of mRNA expression of investigated genes in different assays. As described in Material and Methods experiments were performed and mRNA expression was measured by RT-PCR. Ratio between GC-treated : control is given as mean ± SD. Single samples of monolayer cells were treated for 24 hours with 1µM dexamethasone (DEX) (n=3). Skin equivalents were treated daily for 3 days and mRNA expression was determined in epidermal and dermal layers separately. Single samples of AST-2000 were treated with 1 µM DEX (n=3), triplicate samples of FTSM were treated with 10 µM clobetasol-17-propionate (CB) (n=1). Animals were treated daily topically with 0.01 % CB. Ten *hr/hr* rats per group were treated for 3 days (n=1). Four SKH1 mice per group were treated for 14 days (n=2). n.t. –not tested, n.d. –not detected, * –gene regulation was measured by microarray in one experiment.

Gene	*In vitro* monolayer					*In vitro* 3D skin equivalents				*In vivo*	
	3T3 cells	HaCaT cells	rFib	NHDF	NHEK	AST-2000 epidermis	AST-2000 dermis	FTSM epidermis	FTSM dermis	Rat	Mouse
COL1A1	0.29 ± 0.02	n.t.	0.88 ± 0.19	0.94 ± 0.24	n.t.	n.t.	1.86 ± 0.80	n.t.	0.64	0.26	0.41 ± 0.08
COL3A1	0.31 ± 0.06	n.t.	0.90 ± 0.10	0.86 ± 0.10	n.t.	n.t.	1.52 ± 0.36	n.t.	0.58	0.27	0.37 ± 0.13
COL4A1	2.09 ± 0.47	n.t.	n.t.	1.88 ± 0.02	n.t.	n.t.	n.t.	n.t.	n.t.	n.t.	1.09 ± 0.33
COL5A1	0.79 ± 0.13	n.t.	n.t.	n.t.	n.t.	n.t.	n.t.	n.t.	n.t.	n.t.	n.t.
COL7A1	0.73 ± 0.10	n.t.	n.t.	n.t.	n.t.	n.t.	n.t.	n.t.	n.t.	n.t.	n.t.
COL11A1	2.71 ± 1.47	n.t.	n.t.	23.5 ± 0.71	n.t.	n.t.	n.t.	n.t.	n.t.	n.t.	0.39 ± 0.14
COL14A1	1.15 ± 0.35	n.t.	n.t.	2.43 ± 1.99	n.t.	n.t.	n.t.	n.t.	n.t.	n.t.	0.97 ± 0.35
CTSE	n.d.	n.t.	n.t.	n.d.	n.t.	n.t.	n.t.	n.t.	n.t.	n.t.	0.98 ± 0.21
FGFBP1	n.t.	1.11 ± 0.12	n.t.	n.d.	0.53 ± 0.05	1.29 ± 0.35	n.t.	0.78	n.t.	1.43	1.70 ± 0.13
FMOD	0.27 ± 0.04	n.t.	0.88 ± 0.13	1.94 ± 0.57	n.t.	n.t.	1.14 ± 0.22	n.t.	0.78	1.02	0.93 ± 0.01
LCN2	n.t.	n.t.	n.t.	n.t.	0.59 ± 0.10	n.t.	n.t.	n.t.	n.t.	n.t.	1.22 ± 0.23
MMP1	n.d.	n.t.	n.d.	0.34 ± 0.09	0.24 ± 0.03	0.19 ± 0.14	0.20 ± 0.15	0.22	0.08	n.t.	n.t.
MMP2	0.65 ± 0.04	0.59 ± 0.07	0.95 ± 0.05	1.02 ± 0.07	0.34 ± 0.03	0.09 ± 0.05	1.05 ± 0.34	1.04	0.60	0.82	1.25*
MMP3	0.02 ± 0.02	n.t.	1.19 ± 0.42	0.52 ± 0.10	0.25 ± 0.08	0.11 ± 0.06	0.15 ± 0.09	0.05	0.01	6.95	0.59 ± 0.01
MMP9	n.t.	0.65 ± 0.14	n.t.	n.d.	0.35 ± 0.03	1.29 ± 1.05	n.t.	0.72	0.80	1.70	1.10*
MMP13	n.d.	n.t.	0.65 ± 0.18	n.t.	n.t.	n.t.	n.t.	n.t.	n.t.	n.d.	0.80 ± 0.31
P4HA1	0.73 ± 0.07	n.t.	0.77 ± 0.10	0.87 ± 0.06	n.t.	n.t.	1.03 ± 0.38	n.t.	0.88	1.00	1.05 ± 0.05
P4HA2	0.82 ± 0.06	n.t.	1.70 ± 0.22	0.65 ± 0.39	n.t.	n.t.	1.21 ± 0.48	n.t.	0.88	0.62	0.92 ± 0.18
P4HB	0.89 ± 0.08	n.t.	1.26 ± 0.38	0.96 ± 0.25	n.t	n.t	0.99 ± 0.17	n.t	1.09	1.38	1.42 ± 0.08
PRG4	36.0 ± 2.8	n.t.	n.t.	n.d.	n.t.	n.t.	n.d.	n.t.	n.d.	n.t.	3.24 ± 0.33
TNMD	n.d.	n.t.	n.t.	n.d.	n.d.	n.d.	n.d.	n.d.	n.d.	n.d.	0.06 ± 0.05

Protocol: Inhibition of MMP mRNA Expression in Primary Human Keratinocytes by Treatment with GR Ligands

Normal human epidermal keratinocytes (NHEK) from female adult donors are purchased from Promocell (Heidelberg, Germany). Cells of passages 2 – 7 are used for the experiments. Cells are **maintained** in serum-free keratinocyte growth medium kit 2 (Promocell) supplemented with penicillin (100 U/ml), streptomycin (100 mg/ml). The cells are grown in a moist atmosphere at 37°C and 7.5 % CO_2. To determine the effect of GCs on mRNA expression, cells are seeded in $1.63x10^5$ cells per 1.5 ml / well of a 12-well cell culture plates (Corning-Costar, Bodenheim, Germany). Test medium for NHEK has to be hydrocortisone-free. After 24 hours of adhesion cells were treated for 24 hours with 0.1 % DMSO with or without different GR agonists.

Total RNA is extracted using an ABI Prism 6100 Nucleic Acid PrepStation (Applied Biosystems, Darmstadt, Germany) according to the manufacturer's "RNA cell" protocol. All chemicals for the ABI 6100 are purchased from Applied Biosystems. Cells are lysed in 250 µl of 1x Nucleic Lyses Buffer, the yield is collected at a volume of 80 µl Elution solution and quantified using an Agilent 2100 BioAnalyzer (Applied Biosystems) and the RNA 6000 Nano Assay kit (Ambion Biotechnology, Cambridgeshire, UK). Total RNA can be stored at -80°C.

Total RNA is transcribed in complementary DNA (**cDNA**) using reverse transcriptase. Reverse transcription is performed using 250 ng of total RNA dissolved in 38.5 µl RNase-free water (Gibco, Eggenstein, Germany). The TaqMan® Reverse Transcription Reagents Kit (Applied Biosystems) is used according to the manufacturer's protocol. Afterwards 61.5 µl reaction mixture, containing 1× RT buffer, 5.5 mM $MgCl_2$, 2.5 µM random hexamer primers, 0.4 U/L RNase Inhibitor, 2 mM each NTP (dNTPs mixture) and 1.25 U/L MultiScribe™ reverse transcriptase (TaqMan® Reverse Transcription Reagents, Applied Biosystems), is added and samples incubated in a PCR System 9700 Thermocycler (Applied Biosystems) using the following cycling parameters: 25°C for 10 min, 48°C for 30 min, 95°C for 5 min, and 4°C hold. The originated cDNA product can be stored at -20°C.

The **quantitative RT-PCR** is performed using the ABI Prism® 7900HT sequence detection system (Applied Biosystems). PCRs contain 0.5 µl of cDNA template, 6.25 µl qPCR Mastermix Plus w/o UNG (Eurogentec, Cologne, Germany), 5.15 µl RNase-free water (Gibco) and 0.62 µl Assay-on-Demand™ (AoD) for *MMP1* (Hs00233958_m1), *MMP2* (Hs00234422_m1), *MMP3* (Hs00233962_m1), *MMP9* (Hs00234579_m1) and *HPRT* (Hs99999909_m1) as endogenous reference. The reactions are performed at 50°C for 2 minutes, 95°C for 10 minutes, and then 95°C for 15 seconds and 60°C for 1 minute for 40 cycles. Standard curves (log of template dilution versus Ct value) for each gene-specific primer set are used to determine relative mRNA content for each target gene. The value obtained from each gene-specific PCR is used to determine a relative starting template amount for each experimental group. Then fold regulation of GR ligand treated vs. DMSO-treated is calculated.

Protocol: Inhibition of *COL1A1* and *COL3A1* mRNA Expression in 3T3 Mouse Fibroblasts by Treatment with GR Ligands

3T3 mouse fibroblasts (ECACC, Taufkirchen) are **cultivated** in DMEM (Gibco, Eggenstein, Germany) supplemented with 10 % heatinactivated FCS (Gibco) in a moist atmosphere at 37°C and 7.5 % CO_2. To determine the effect of GCs on mRNA expression, cells are and seeded in $6.5x10^4$ cells / 1.5 ml test medium / well of a 12-well cell culture plates (Corning-Costar, Bodenheim, Germany). Test media for 3T3 is supplemented with 5 % charcoal-treated serum (CCS) instead of FCS. After a 24 hour time of adhesion, cells are treated for 24 h with 0.1 % DMSO with or without different GR agonists. DEX (1e-6 M – 1e-11 M) is used as reference.

At the end of the experiment, supernatants are aspirated and discarded, and 250 µl of 1x Nucleic Lyses Buffer (Applied Biosystems, Darmstadt, Germany) is added to the cells. Cells are lysed and transferred to the ABI Prism 6100 Nucleic Acid PrepStation (Applied Biosystems) by pipetting up and down. **Total RNA** is extracted following the "RNA cell" protocol after manufacturer's instructions. The yield is eluated in 80 µl Elution solution (Applied Biosystems) and quantified using an Agilent 2100 BioAnalyzer (Applied Biosystems) and the RNA 6000 Nano Assay kit (Ambion Biotechnology, Cambridgeshire, UK). Total RNA can be stored at -80°C.

Total RNA is transcribed in complementary DNA (**cDNA**) using reverse transcriptase. Reverse transcription is performed using 250 ng of total RNA dissolved in 38.5 µl RNase-free water (Gibco). The TaqMan® Reverse Transcription Reagents Kit (Applied Biosystems) is used according to the manufacturer's protocol. Afterwards 61.5 µl reaction mixture, containing 1× RT buffer, 5.5 mM $MgCl_2$, 2.5 µM random hexamer primers, 0.4 U/L RNase Inhibitor, 2 mM each NTP (dNTPs mixture) and 1.25 U/L MultiScribe™ reverse transcriptase (TaqMan® Reverse Transcription Reagents, Applied Biosystems), is added and samples are incubated in a PCR System 9700 Thermocycler (Applied Biosystems) using the following cycling parameters: 25°C for 10 min, 48°C for 30 min, 95°C for 5 min (inactivation), and 4°C hold. The originated cDNA product can be stored at -20°C.

The **quantitative RT-PCR** is performed in triplicates in 384-well plates using the ABI Prism® 7900HT sequence detection system (Applied Biosystems, Darmstadt). PCRs contain 0.5 µl of cDNA template, 6.25 µl qPCR Mastermix Plus w/o UNG (Eurogentec, Cologne, Germany), 5.15 µl RNase-free water (Gibco) and 0.62 µl Assay-on-Demand™ (AoD) for *COL1A1* (Mm00801666_g1), *COL3A1* (Mm00802331_m1) and *HPRT* (Mm00446968_m1) as endogenous reference. The reactions are performed at 50°C for 2 minutes, 95°C for 10 minutes, and then 95°C for 15 seconds and 60°C for 1 minute for 40 cycles. Standard curves (log of template dilution versus Ct value) for each gene-specific primer set are used to determine relative mRNA content for each target gene. The triplicate values obtained from each gene-specific PCR are used to determine a relative starting template amount for each experimental group. Then fold regulation of GR ligand treated vs. DMSO control treated is calculated.

Protocol: Skin Atrophy in Full-thickness Skin Models (FTSM)

After arrival, the 1 cm² FTSM (Phenion, Düsseldorf, Germany) are placed on filter papers on top of pre-placed metal support in 5 ml hydrocortinsone-free FTSM medium in a 6-well plate and later on adapted to **cell culture** conditions (37°C, 5 % CO_2, max. humidity). Test substances are dissolved in FTSM medium (final concentration 0.01 % DMSO with or without test compounds) and applied into medium. The conditioned medium is replaced daily by fresh and prewarmed medium. On day 3, **secreted IL-1β, IL-6 and IL-8** are determined in the supernatant by Human Proinflammatory II 4-Plex Kit for detection of IL-1β, IL-6, IL-8 and TNF-α (MesoScale Discovery, Gaithersburg, MD, USA) for analysis of anti-inflammatory potential of used GR ligands. Also on day 3, **secreted MMP-1 and MMP-3** are determined in the supernatant by MS6000 Human MMP 3-Plex Ultra-Sensitive Kit for detection of MMP-1, MMP-3 and MMP-9 (Meso Scale Discovery) for analysis of atrophogenic potential. On day 12, secretion of C-terminal propeptide of collagen type I (CICP) is analyzed by Metra CICP EIA Kit (Quidel, Marburg, Germany).

After exposure of test compounds for 12 d, epidermal thinning is determined by **histological** analysis. Therefore, FTSM are cut in halves, twice washed in PBS and fixed for 24 hours in 4 % formalin. Afterwards, samples are embedded in paraffin; paraffin must be curing at least 3 days. Six micrometer sections are transferred on object slides (Superfrost plus, Menzel, Wiesbaden, Germany) and dried at least 24 hours. Then, Hematoxylin-Eosin (HE) stain is performed. After deparaffinization in xylene and re-hydration in descending alcohol-solutions, nuclei are stained with the alcohol soluble hematoxylin (1:4 dilution in bidest. water) for 2.5 min, and rinsed in running drinking water. Thereafter staining in 1 % eosin (Dako, Hamburg, Germany) is performed over 40 s. After short washing in distilled water, the sections are covered with Faramount (watery medium, Dako) and cover slips and are analyzed 24 hours later at 10- to 20-fold extension under microscope (Zeiss Axioplan, Jena, Germany) with MetaVue program (Visitron, Puchheim, Germany). Keratinocyte layers are counted in 5 areas per section on three non-consecutive sections per sample. Epidermal thinning induced by GC treatment is also visible on day 6.

To determine the effect of GCs after on mRNA expression of MMP1, MMP3 in epidermal compartment and of Col1a1 and Col3a1 in dermal compartment, the epidermal layer has to be detached from the dermal layer by **thermolysin digestion**. For compartment separation FTSM are washed twice with PBS with Ca^{2+} and Mg^{2+}, incubated in thermolysin solution (0.5 mg / ml thermolysin in 33 mM KCl, 50 mM NaCl, 5 mM $CaCl_2$, 0.01 M HEPES) for 2 hours at 4°C, and forceps are used to detach the epidermis from the dermal part.

Total RNA is isolated from separated epidermis and dermis using the Qiagen RNeasy protocol to analyze the gene expression patterns with TaqMan®-RT-PCR. Initially, samples are placed in 300 µl RLT buffer including 1 % β-mercaptoethanol and homogenized using the Ultra-Turrax (IKA, Staufen, Germany) for 1-2 min. Samples are then processed using the Qiagen RNeasy protocol. Briefly, after

efficient homogenization, samples are centrifuged at 13000 rpm for 3 min. The supernatants are transferred into fresh tubes, 590 µl RNase-free water (Gibco) and 10 µl proteinase K (Qiagen, Hilden, Germany) are added, incubated at 55°C for 10 min and centrifuged at 13000 rpm for 30 sec. The supernatants are transferred into fresh tubes and half a volume of $ethanol_{abs}$ is added to the cleared lysate. The contents of each tube are then mixed and applied to an RNeasy minicolumn followed by a series of centrifugation steps and washes after manufacturer's protocol. In addition, the on-column DNase digestion is performed using the RNase-free DNase set (Qiagen). Epidermal RNA is finally eluted in 80 µl, dermal RNA is eluted in 100 µl of RNase-free water and quantified using the Agilent 2100 BioAnalyzer (Applied Biosystems, Darmstadt, Germany). Total RNA can be stored at -80°C.

Total RNA is transcribed in complementary DNA (**cDNA**) using reverse transcriptase. Reverse transcription is performed using 250 ng of total RNA dissolved in 38.5 µl RNase-free water (Gibco). The TaqMan® Reverse Transcription Reagents Kit (Applied Biosystems) is used according to the manufacturer's protocol. Afterwards 61.5 µl reaction mixture, containing 1× RT buffer, 5.5 mM $MgCl_2$, 2.5 µM random hexamer primers, 0.4 U/L RNase Inhibitor, 2 mM each NTP (dNTPs mixture) and 1.25 U/L MultiScribe™ reverse transcriptase (TaqMan® Reverse Transcription Reagents, Applied Biosystems), is added and samples incubated in a PCR System 9700 Thermocycler (Applied Biosystems) using the following cycling parameters: 25°C for 10 min, 48°C for 30 min, 95°C for 5 min (inactivation), and 4°C hold. The originated cDNA product can be stored at -20°C.

The **quantitative RT-PCR** is performed in triplicates in 384-well plates using the ABI Prism® 7900HT sequence detection system (Applied Biosystems). PCRs contain 0.5 µl of cDNA template, 6.25 µl qPCR Mastermix Plus w/o UNG (Eurogentec, Cologne, Germany), 5.15 µl RNase-free water (Gibco) and 0.62 µl Assay-on-Demand™ (AoD) for *COL1A1* (Hs00164004_m1), *COL3A1* (Hs00164103_m1), *MMP1* (Hs00233958_m1) and *HPRT* (Hs99999909_m1) as endogenous reference. The reactions are performed at 50°C for 2 minutes, 95°C for 10 minutes, and then 95°C for 15 seconds and 60°C for 1 minute for 40 cycles. Standard curves (log of template dilution versus Ct value) for each gene-specific primer set are used to determine relative mRNA content for each target gene. The triplicate / quadruplicate values obtained from each gene-specific PCR are used to determine a relative starting template amount for each experimental group. Then fold regulation of GR ligand treated vs. DMSO control treated is calculated.

It has to be mentioned, that this test system is not optimized for minimal time, work and compound consumption, i.e. the minimal experimental duration for induced dermal atrophy (inhibited CICP secretion) was not tested. For less compound consumption a medium change on every second or third day should be tested. Special inserts instead of metal supports plus filter paper should be tested for an easier handling and probably for a less compound and media consumption.

Abbreviation

3T3	mouse embryonic fibroblast cell line
AoD	Assay on Demand© from Applied Biosystems
AST-2000	advanced skin test from CellSystems
BMV	betamethasone-17-valerate
CB	clobetasol-17-propionate
CCS	charcoal-treated serum
cDNA	complementary deoxyribonucleic acid
CICP	type I C-terminal collagen propeptide
Col1a1	collagen type I, alpha 1
Col3a1	collagen type III, alpha 1
Col4a1	collagen type IV, alpha 1
Col5a1	collagen type V, alpha 1
Col7a1	collagen type VII, alpha 1
Col11a1	collagen type XI, alpha 1
Col14a1	collagen type XIV, alpha 1
CtsE	cathepsin E;
DEX	dexamethasone;
DMEM	Dulbecco's modified Eagles medium
DMSO	dimethylsulfoxide
DNA	deoxyribonucleic acid
ELISA	enzyme linked immunosorbent assay
f.e.	fold expression
FCS	fetal calf serum
FGFbp1	fibroblast growth factor binding protein 1
Fib	fibroblasts
Fmod	fibromodulin
FTSM	full-thickness skin model from Phenion®
GC	glucocorticoid
GR	glucocorticoid receptor
GRE	glucocorticoid response element
H&E	hematoxylin and eosin
HaCaT	immortalized human keratinocyte cell line
HC	hydrocortisone
HPRT	hypoxanthine-guanine phosphoribosyltransferase
IC_{50}	concentration with 50 % potency

IL	interleukin
Ker	keratinocytes
Lcn2	lipocalin 2
LPS	lipopolysaccharide
MF	mometasone furoate
MMP	Matrix Metalloproteinase
mRNA	messenger ribonucleic acid
NHDF	normal human dermal fibroblasts
NHEK	normal human epidermal keratinocytes
PC	prednicarbate
Prg4	proteoglycan 4
rFib	primary rat fibroblasts
RNA	ribonucleic acid
RT-PCR	real-time polymerase chain reaction
SEGRA	selective glucocorticoid receptor agonist
THP-1	human acute monocytic leukemia cell line
TNF-α	tumor necrosis factor alpha
Tnmd	tenomodulin
UV	ultraviolet

Danksagungen

Mein besonderer Dank gilt meinem Betreuer Prof. Dr. Khusru Asadullah für die Bereitstellung des interessanten Themas und die Sicherung der finanziellen Seite, für die Möglichkeit zu eigenständigem Arbeiten in der Arbeitsgruppe der CRBA Dermatology der Schering AG, für die jederzeit positive Einstellung und fachliche Unterstützung meiner Arbeit und nicht zuletzt für die Möglichkeit, Kongresse zu besuchen. Bei Dr. Ulrich Zügel bedanke ich mich ebenfalls für die Möglichkeit der Fortführung dieser Doktorarbeit in der Abteilung Common Mechanism Research von der Bayer Schering Pharma AG sowie deren weitere finanzielle Unterstützung.

Bei Prof. Dr. Hans-Dieter Volk bedanke ich mich, dass er mir ermöglicht hat, die Doktorarbeit an der Mathematisch-Naturwissenschaftlichen Fakultät der Humboldt-Universität zu Berlin einreichen zu können.

Mein großer Dank gilt Dr. Heike Schäcke für die kompetente wissenschaftliche Betreuung, ihre Geduld und Unterstützung während der Doktorarbeit.

Vielen Dank an alle Mitglieder der CRBA Dermatology der Schering AG für die hervorragende, kooperative und hilfsbereite Arbeitsatmosphäre, sowie für die exzellente technische und bürokratische Unterstützung, die zum Gelingen der Doktorarbeit beigetragen haben. Weiterhin bedanke ich mich bei Eginhard Matzke, Christian Okon und Detlef Opitz für die exzellente Durchführung und Hilfe bei den Tierexperimenten.

Bei den Mitarbeitern der Abteilung Target Research I Berlin bedanke ich mich für die Durchführung und Unterstützung der Genexpressionsstudien mit GeneChips.

Christian Wiegand, Doktorand der Firma Phenion in Düsseldorf, danke ich für das Erlernen des Umgangs mit den FTSM. Bei Dr. Martina Seifert, Arbeitsgruppen-Leiterin am Institut für Medizinische Immunologie der Charité Berlin, bedanke ich mich für die Unterstützung beim Erlernen der Isolation von Keratinocyten und Fibroblasten aus Rattenohren.

Ich möchte mich bei Dr. Wolf-Dietrich Döcke, Dr. Ekkehard May, Dr. Arne von Bonin und Dr. Lars Röse für ihre wissenschaftliche Unterstützung bedanken.

Bei Prof. Dr. August Bernd, Dr. Nadja Zöller sowie Vesselina Laubach bedanke ich mich für meinen Forschungsaufenthalt und für die herzliche Aufnahme und Unterstützung im Labor für Dermatologische und Klinische Biochemie der Universität Frankfurt.

Ferner möchte ich mich bedanken bei meinen Co-Autoren der Publikation „Glucocorticoid therapy-induced skin atrophy“ (Experimental Dermatology), aus der Auszüge für den Einleitungsabschnitt dieser Arbeit verwendet wurden.

Für das Korrekturlesen und gedankliche Unterstützung bedanke ich mich bei Dr. Tatjana Gust.

Meinen Eltern, Angelika und Rainer Schoepe, danke ich über alle Maße für die Ermöglichung meiner Ausbildung, ihren Glauben an mich und ihre außerordentliche Unterstützung.

Bei Eckhard Ehm bedanke ich mich für seine außerordentliche Geduld und Unterstützung, die zur Vollendung der Arbeit beigetragen haben.

Vielen Dank an meine Freunde Bettina Sickinger, Stephan Bissart, Christine Stock und allen anderen, die zu mir gehalten und mich unterstützt haben.

Eidesstattliche Erklärung

Hiermit versichere ich an Eides statt, die vorliegende Dissertation selbständig und nur unter Verwendung der angegebenen Hilfsmittel angefertigt zu haben. Ich besitze bisher keinen entsprechenden Doktorgrad und habe mich nicht anderwärts um den akademischen Grad "*Doctor rerum naturalium*" beworben. Ich erkläre die Kenntnisnahme der Promotionsordnung der Mathematisch-Naturwissentschaftlichen Fakultät I der Humboldt-Universität zu Berlin.

Berlin, den 4. März 2009

Stefanie Schoepe